Chapter 3

RESULTS

3.1 Preparation of ligands

2-(Phenylazo)pyridine (azpy) was prepared by modified literature method (Krause and Krause, 1980). Azpy was synthesized by coupling of 2-aminopyridine with nitrosobenzene. Other ligands (2-(4'-*N,N*-dimethylaminophenylazo)pyridine (dmazpy), 2-(4'-*N,N*-diethylaminophenylazo)pyridine (deazpy), 2-(phenylazo) pyrimidine (azpym) and 2-(4'-*N,N*-diethylaminophenylazo)pyrimidine (deazpym)), were synthesized by modification of synthesis of azpy ligand. The dmazpy and deazpy procedures were synthesized by coupling of 2-aminopyridine with *N,N*-dimethyl-1,4-nitrosoaniline or *N,N*-diethyl-1,4-nitrosoaniline, respectively. Azpym and deazpym ligands were synthesized by coupling of 2-aminopyridine with nitrosobenzene or *N,N*-diethyl-4-nitrosoaniline, respectively. The crude product was purified by column chromatography and the reactions were followed by equation (1) to (5).

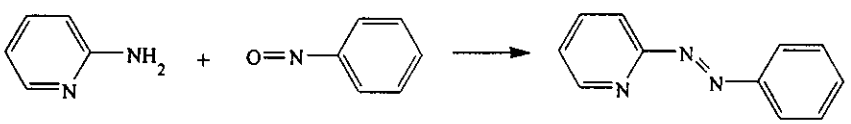

(1)

2-aminopyridine nitrosobenzene 2-(phenylazo)pyridine (azpy)

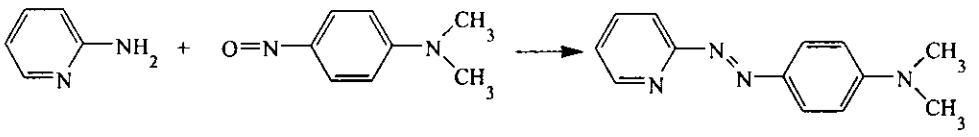

(2)

2-aminopyridine *N,N*-dimethyl-1,4-nitrosoaniline 2-(4'-*N,N*-dimethylaminophenylazo)pyridine (dmazpy)

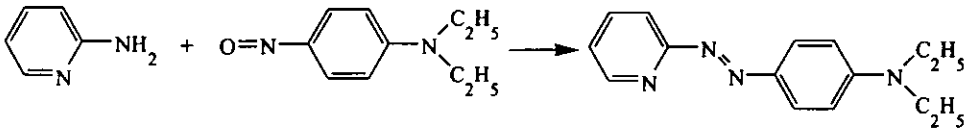

(3)

2-aminopyridine *N,N*-diethyl-1,4-nitrosoaniline 2-(4'-*N,N*-diethylaminophenylazo)pyridine (deazpy)

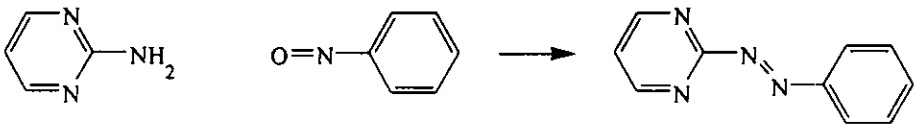

(4)

2-aminopyrimidine nitrosobenzene 2-(phenylazo)pyrimidine (azpym)

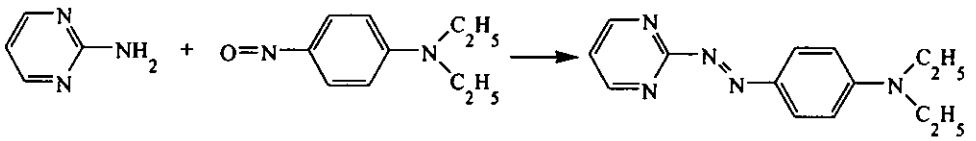

(5)

2-aminopyrimidine *N,N*-diethyl-1,4-nitrosoaniline 2-(4'-*N,N*-diethylaminophenylazo)pyrimidine (deazpym)

The yields of azpy, dmazpy, deazpy, azpym and deazpym ligands were low (5-30%) because there were many side reactions. Some of the physical properties of ligands are shown in Table1.

Table 1 The physical properties of ligands

Ligand	Physical properties		
	Appearance	Color	Melting point (°C)
azpy	Liquid	Orange	32-34[a]
dmazpy	Monoclinic	Red	104-105
deazpy	Orthorhombic	Red	109-110
azpym	Lquid	Orange	Liquid at room temperature
deazpym	Orthorhombic	Red	96-97

[a]Results from Krause and Krause (1980)

The solubility of 0.0015 g of each ligand was tested in 10 mL of various solvents (water, methanol, acetronitrile, acetone, ethanol, ethyl acetate, dichloromethane and hexane). Those ligands were very soluble in most solvents. However, they changed color into deep pink when they dissolved in water.

3.2 Characterization of ligands

The chemistries of azpy, dmazpy, deazpy, azpym and deazpym ligands were determined by using these techniques:

- Electrospray mass spectrometry
- Infrared spectroscopy
- UV-Visible absorption spectroscopy
- Nuclear magnetic Resonance spectroscopy
- Cyclic Voltammetry

- X-ray Diffractometer

3.2.1 Electrospray mass spectrometry

Mass spectroscopy is the principle technique to confirm molecular weigh of ligands. The results from electrospray mass spectrometry data of dmazpy, deazpy, azpym and deazpym ligands are shown in Table 2.

Table 2 Electrospray mass spectroscopic data of ligands

Ligand	m/z	Stoichiometry	Equivalent species	Rel. Abun.
dmazpy	227.1	$[dmazpy+H]^+$	$[M+H]^+$	100
deazpy	256.2	$[deazpy+2H]^+$	$[M+2H]^+$	35
	255.3	$[deazpy+H]^+$	$[M+H]^+$	100
azpym	184.9	$[azpym+H]^+$	$[M+H]^+$	100
deazpym	257.3	$[deazpym+2H]^+$	$[M+2H]^+$	28
	256.2	$[deazpym+H]^+$	$[M+H]^+$	100

M = Molecular weight (MW) of each ligand

MW of the dmazpy ligand = 226.28 g/mol

MW of the deazpy ligand = 254.34 g/mol

MW of the azpym ligand = 184.19 g/mol

MW of the deazpym ligand = 255.33 g/mol

From the data, the maximum peaks in an isotropic mass distribution showed molecular weight of each ligand. Therefore, electrospray mass spectrometry could confirm the ligand formula. The electrospray mass spectra for ligands are shown in Figure 3 to 6.

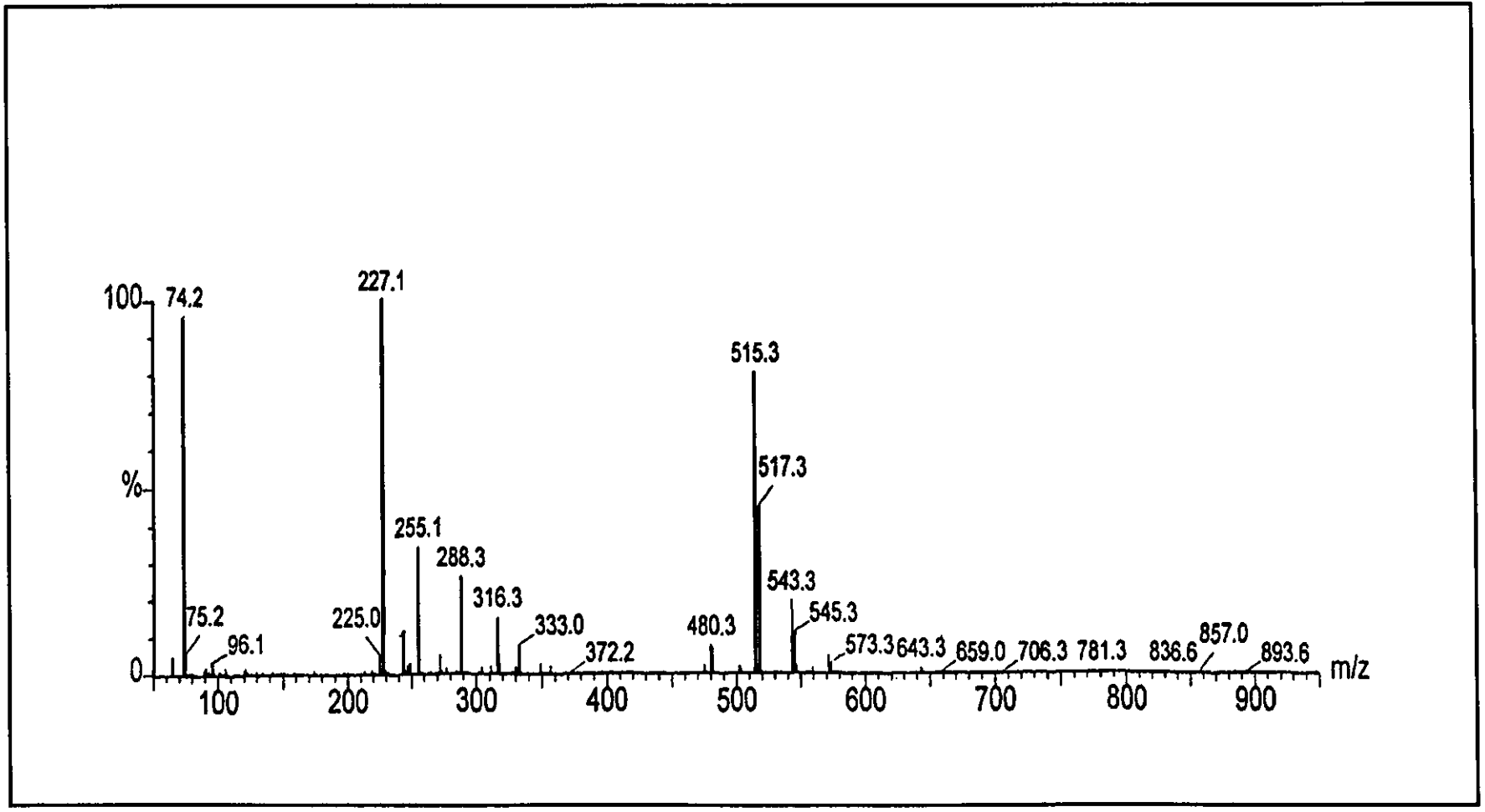

Figure 3 Electrospray mass spectrum of dmazpy.

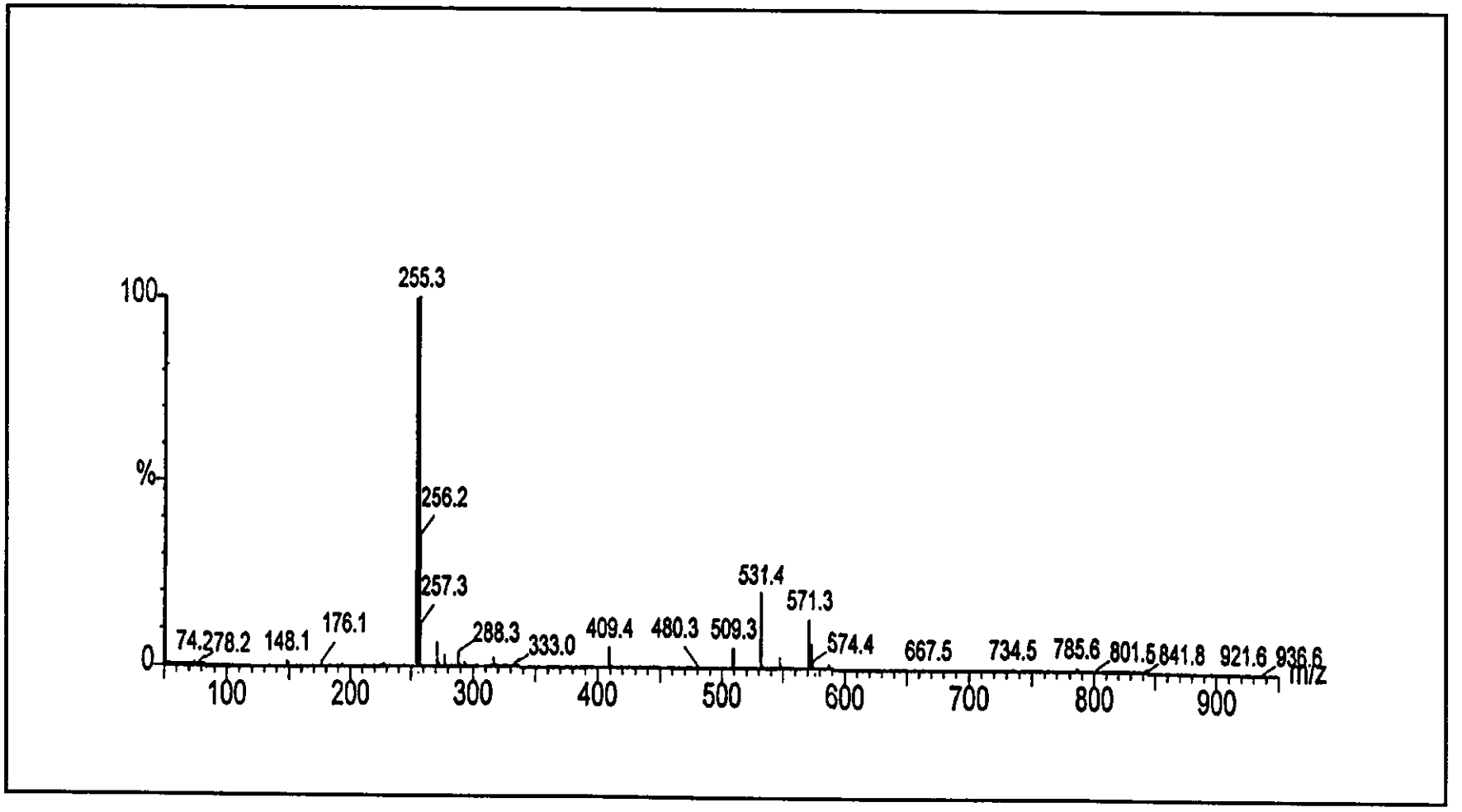

Figure 4 Electrospray mass spectrum of deazpy.

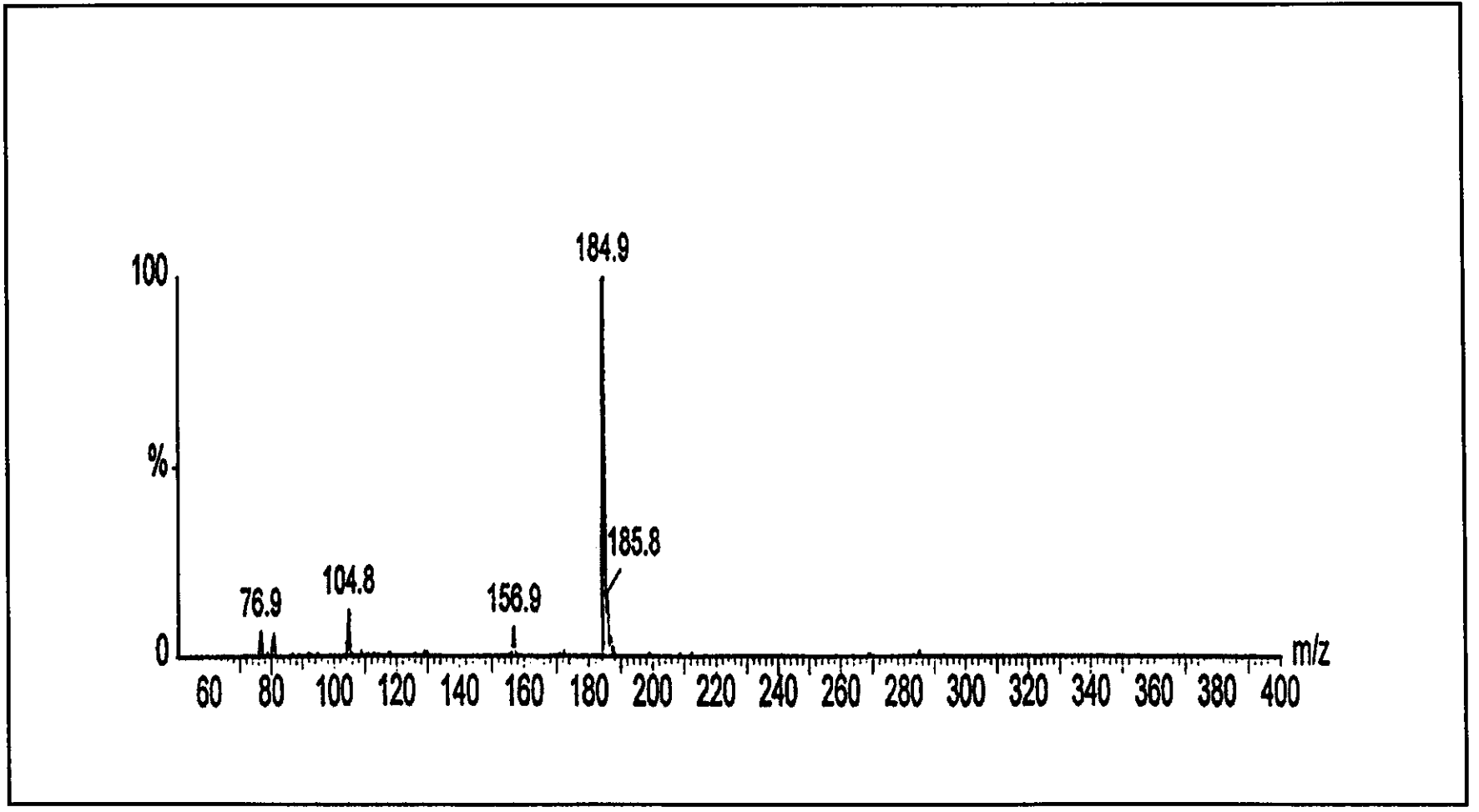

Figure 5 Electrospray mass spectrum of azpym.

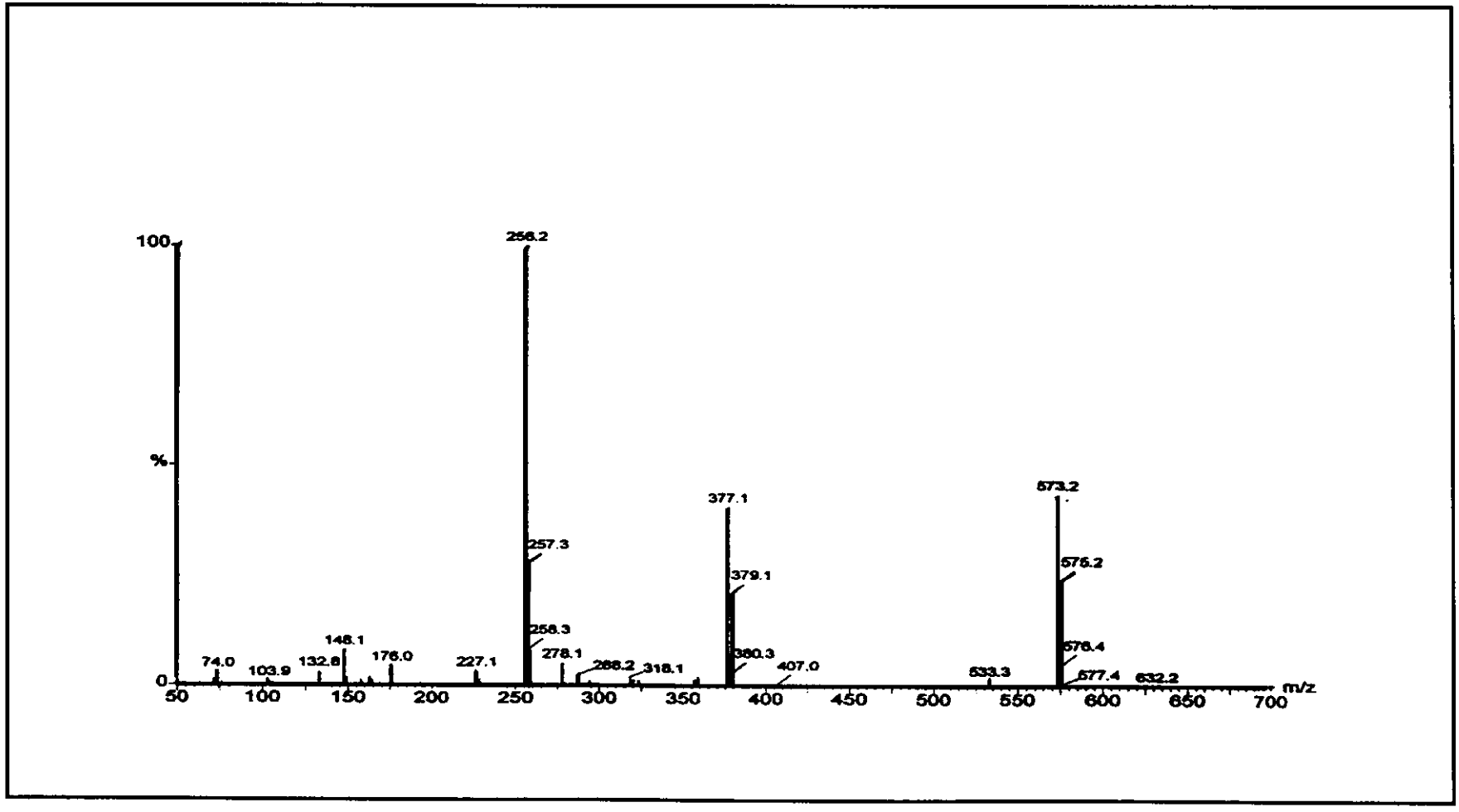

Figure 6 Electrospray mass spectrum of deazpym.

3.2.2 Infrared spectroscopy

Infrared spectroscopy is an important technique to identify the functional group in compounds. IR spectra of azpy, dmazpy, deazpy, azpym and deazpym ligands were recorded in the range 4000-370 cm^{-1} and shown in Figure 7 to 11, respectively. The interesting intense vibration frequencies of ligands were C=C, C=N, N=N (azo) stretching vibrations and C-H bending of para disubstituted benzene. The summary of infrared spectroscopic data is listed in Table 3.

Table 3 Infrared spectroscopic data of ligands

Vibration modes	Frequencies (cm^{-1})				
	azpy	dmazpy	deazpy	azpym	deazpym
C=N	1580(s)	1610(s)	1599(s)	1565(s)	1599(s)
C=C	1447(m)	1447(s)	1517(s)	1452(m)	1516(s)
N=N	1421(s)	1402(s)	1399(s)	1392(s)	1379(s)
C-H bending of para disubstituted benzene	-	823(s)	833(s)	-	838(s)

s = strong, m = medium

Infrared spectra of their ligands showed many intense vibrations in the 1,600-370 cm^{-1} range. The C=N and C=C stretching modes of dmazpy, deazpy, azpym and deazpym showed strong to medium absorption at the frequencies similar to those of azpy. Krause and Krause showed the C=N and C=C stretching modes of azpy ligand. It appeared at 1584, 1578, 1498 and 1495 cm^{-1} (Krause and Krause, 1980).

The most important peak was the N=N stretching which was used to compare the π-acid property in azo compounds. The N=N stretching of azpy, dmazpy, deazpy, azpym and deazpym showed the intense peak at 1421(s), 1402(s), 1399(s), 1392(s), and 1397(s) cm^{-1}, respectively. The N=N stretching of azpy appeared at higher frequencies than dmazpy and deazpy. Because the N=N bond order of azpy was stronger than dmazpy and deazpy. This may be due to effect of substituent ($-NR_2$) as electron donating group. Similarly, azpym had the N=N stretching higher frequencies than deazpym. than deazpym.

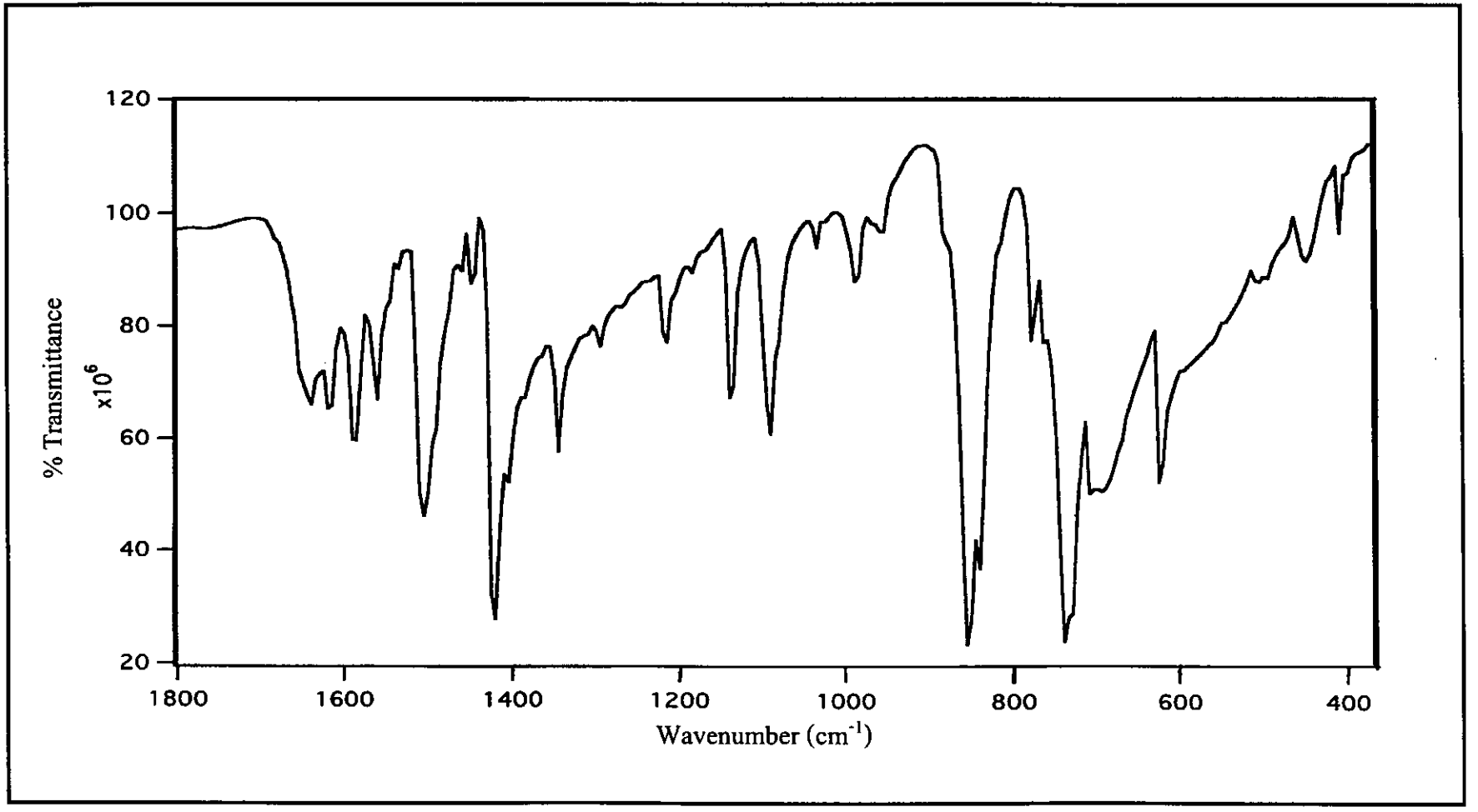

Figure 7 IR spectrum of azpy.

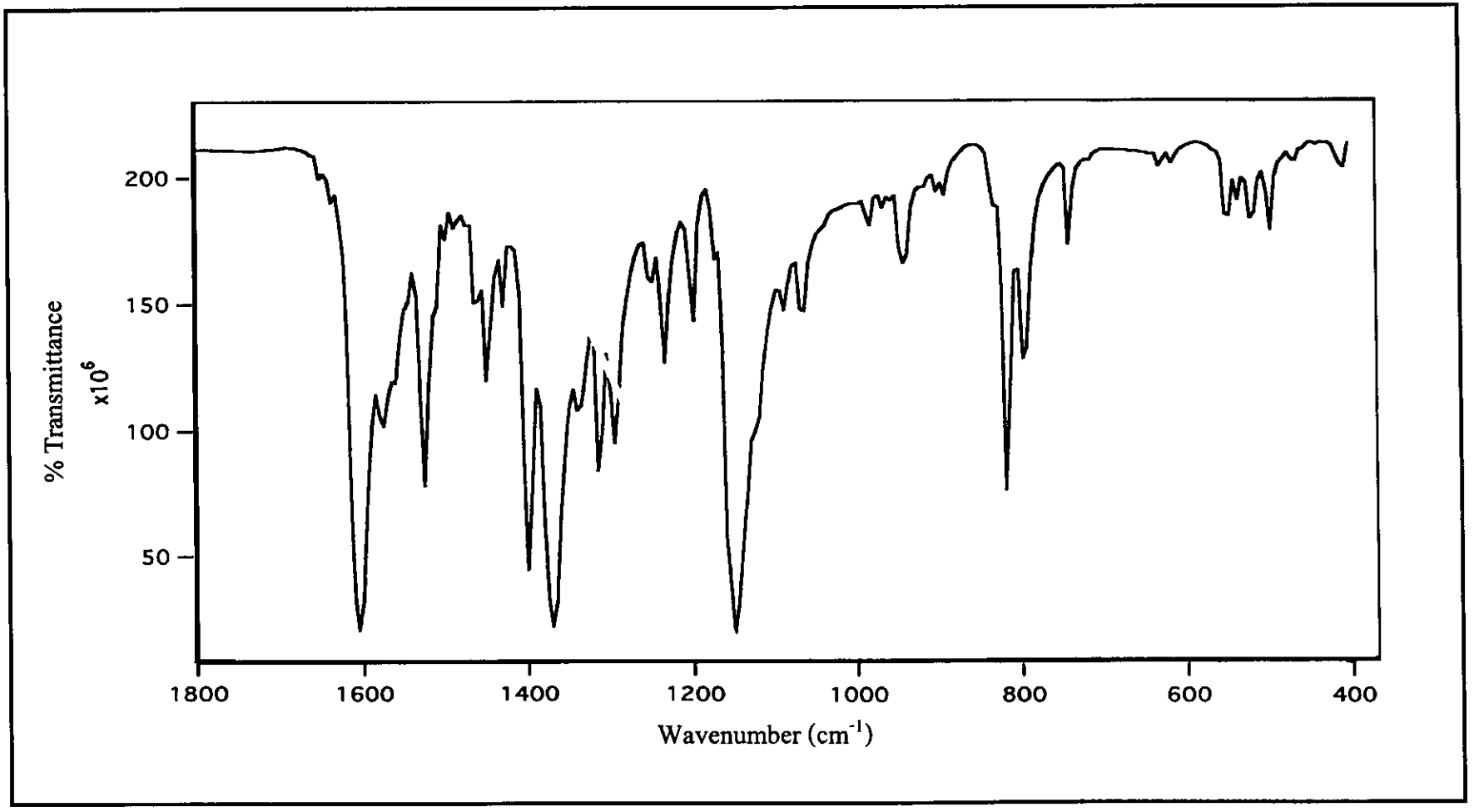

Figure 8 IR spectrum of dmazpy.

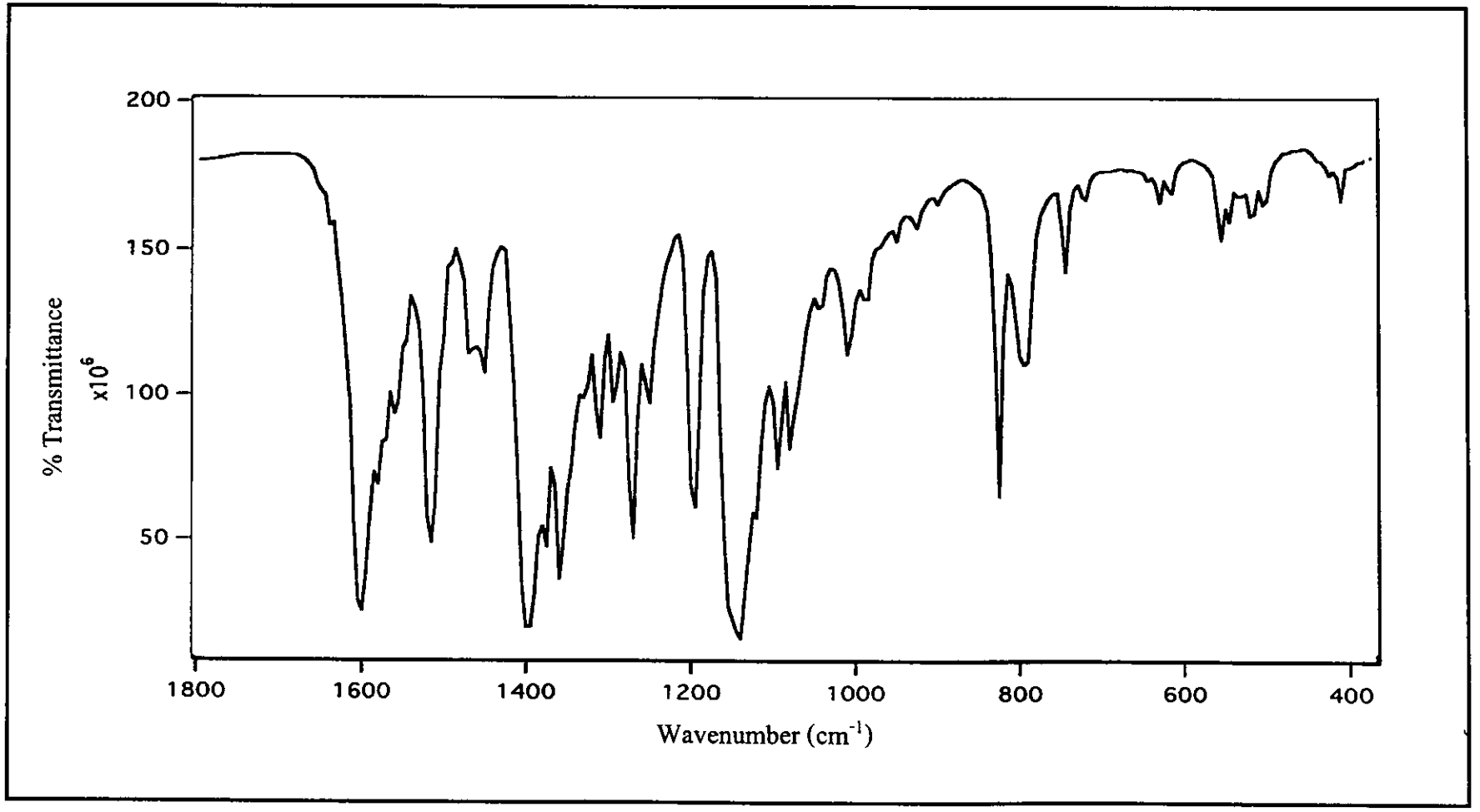

Figure 9 IR spectrum of deazpy.

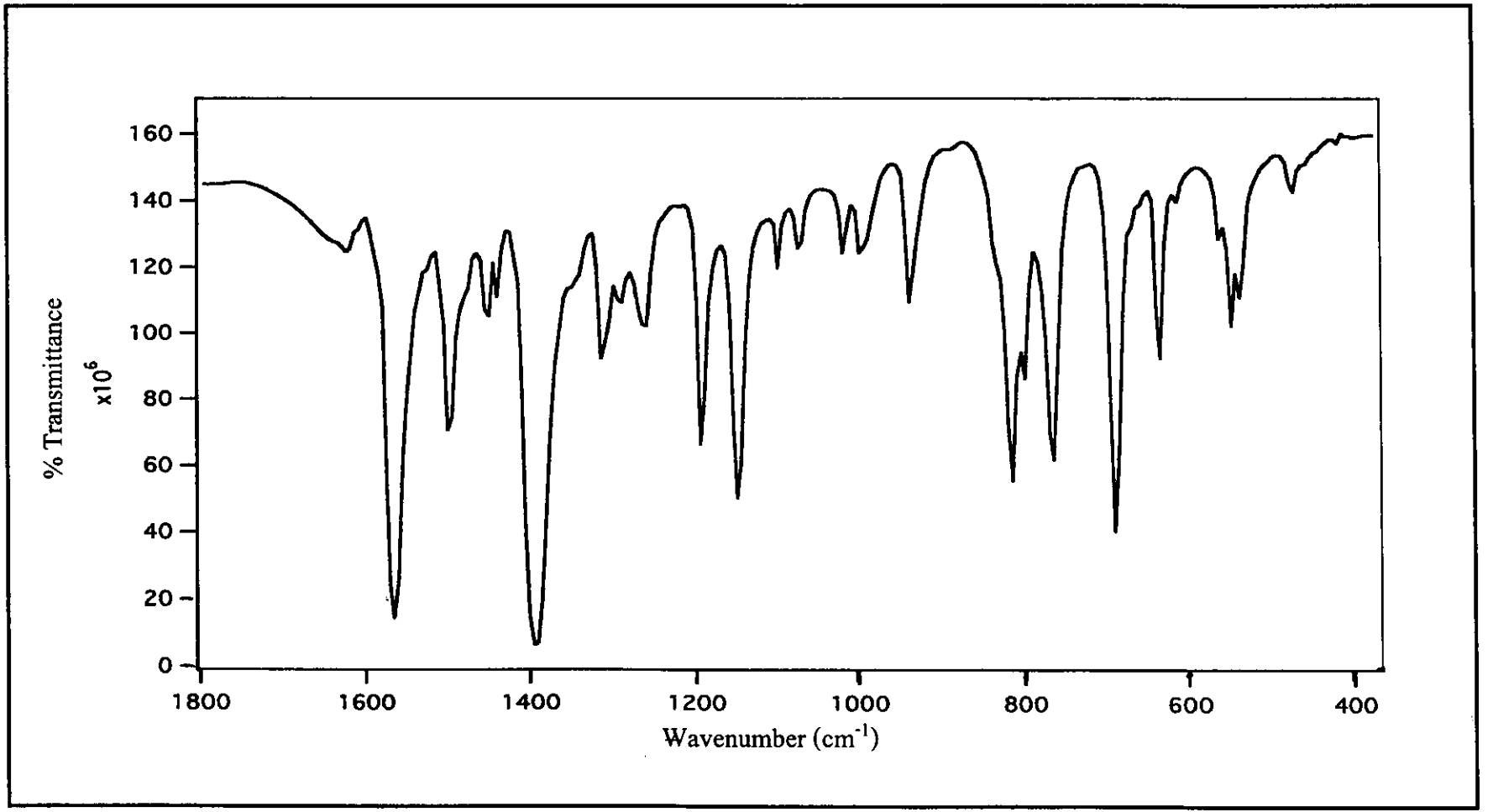

Figure 10 IR spectrum of azpym.

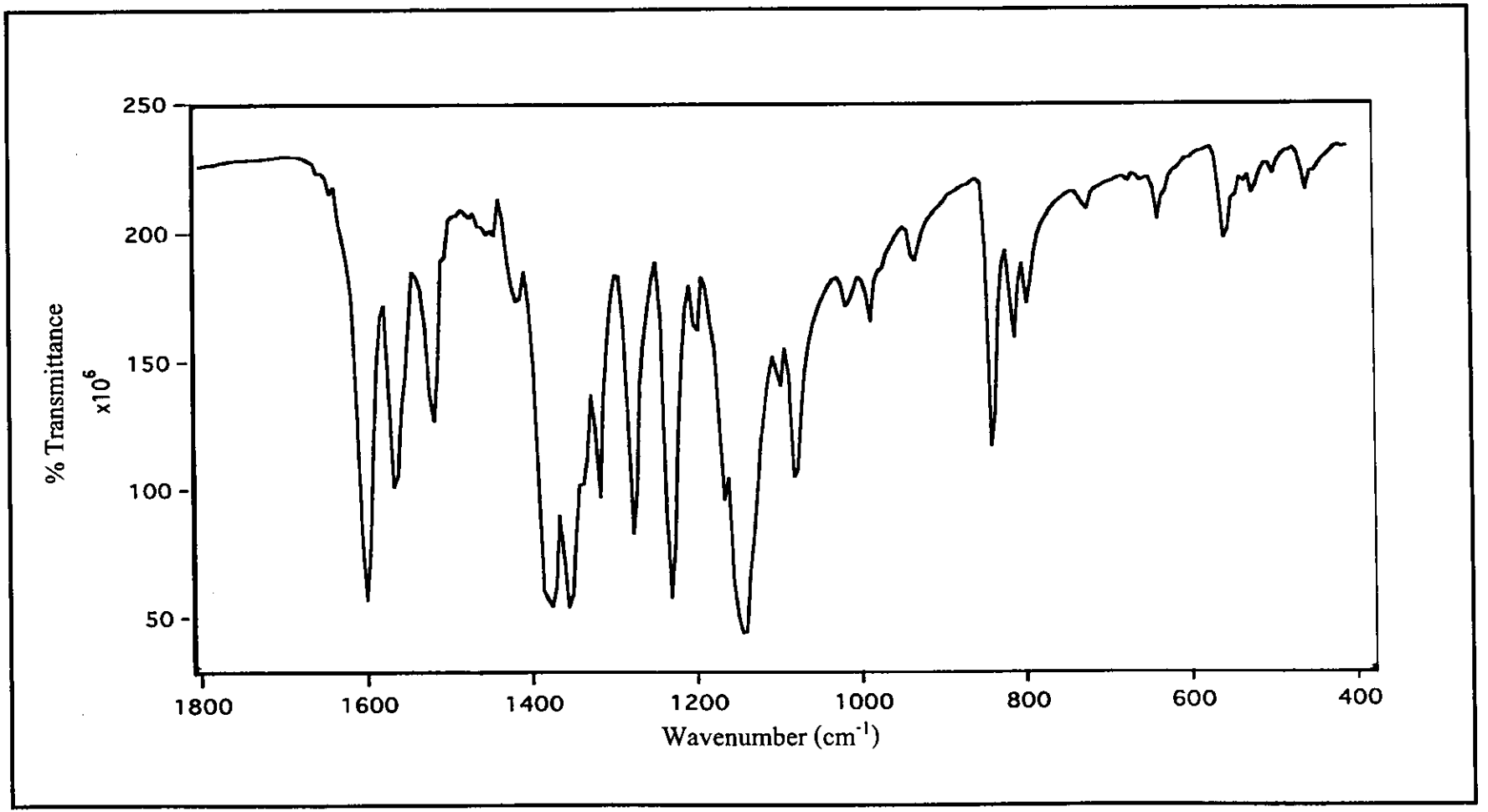

Figure 11 IR spectrum of deazpym.

3.2.3 UV-Visible absorption spectroscopy

UV-Visible absorption spectroscopy is the technique used for study the electronic transitions of the ligands. The UV-Visible absorption spectra data of phen, azpy, dmazpy, deazpy, azpym and deazpym exhibited absorption in the range 200-800 nm in CH_3CN, EtOH, DMF, DMSO and CH_2Cl_2 solvent . In addition, the absorption spectra of all ligands in CH_3CN solution are shown in Figure 12 and 17. The spectroscopic data is summarized in Table 4.

Table 4 UV-Visible absorption spectroscopic data of ligands

Ligands	λ_{max} nm,(εX10^{-4} $M^{-1}cm^{-1}$)				
	DMSO	CH_3CN	CH_3COCH_3	EtOH	CH_2Cl_2
phen	-	230 (6.6) 264 (3.9)	-	226 (8.3) 264 (4.2)	266 (5.7)
azpy	319 (1.8) 450 (0.05)	314 (1.8) 448 (0.04)	446 (0.5)	318 (1.7) 442 (0.1)	318 (1.8) 448 (0.05)
dmazpy	269 (1.0) 437 (2.5)	267 (1.2) 423 (3.7)	422 (2.7)	274 (1.4) 430 (3.4)	270 (1.1) 426 (3.4)
deazpy	271 (1.0) 444 (2.5)	271 (1.0) 431 (3.4)	430 (2.6)	276 (1.2) 440 (4.7)	273 (1.0) 436 (3.5)
azpym	303 (1.3) 438 (0.05)	298 (1.6) 439 (0.04)	439 (0.4)	304 (1.6) 440 (0.04)	304 (1.7) 447 (0.04)
deazpym	273 (1.2) 442 (3.0)	269 (1.1) 431 (2.9)	426 (2.8)	277 (1.8) 460 (3.1)	277 (1.8) 460 (3.1)

The absorption spectra of azpy, dmazpy, deazpy, azpym and deazpym ligands in this series of solvents showed intense bands at 225-330 nm (ε~ 9,000-20,000 $M^{-1}cm^{-1}$) in UV region which referred to $\pi \rightarrow \pi^*$ (1) transition. In visible region, the bands at 420-460 nm (ε~ 24,000-38,000 $M^{-1}cm^{-1}$) were assigned to $\pi \rightarrow \pi^*$ (2) transition for dmazpy, deazpy and deazpym. In contrast, azpy and azpym ligands showed absorption bands (ε~ 400-600 $M^{-1}cm^{-1}$) in visible region which referred to $n \rightarrow \pi^*$ transitions. Dmazpy, deazpy and deazpym had $\pi \rightarrow \pi^*$ transitions at the lowest energies, whereas azpy and azpym were $n \rightarrow \pi^*$ transitions. The phen ligand had only two $\pi \rightarrow \pi^*$ transitions in the UV region.

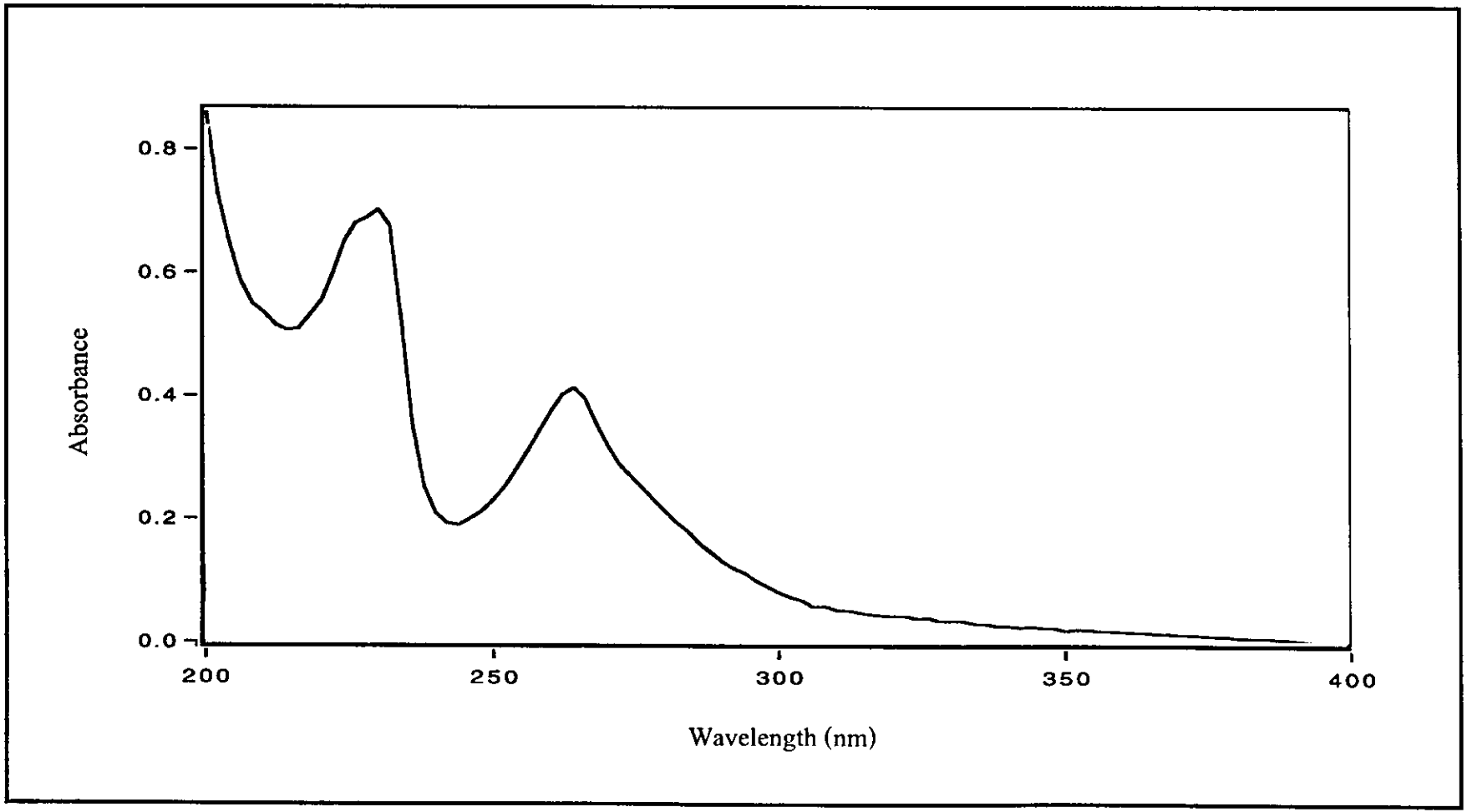

Figure 12 UV-Visible absorption spectrum of phen in CH_3CN.

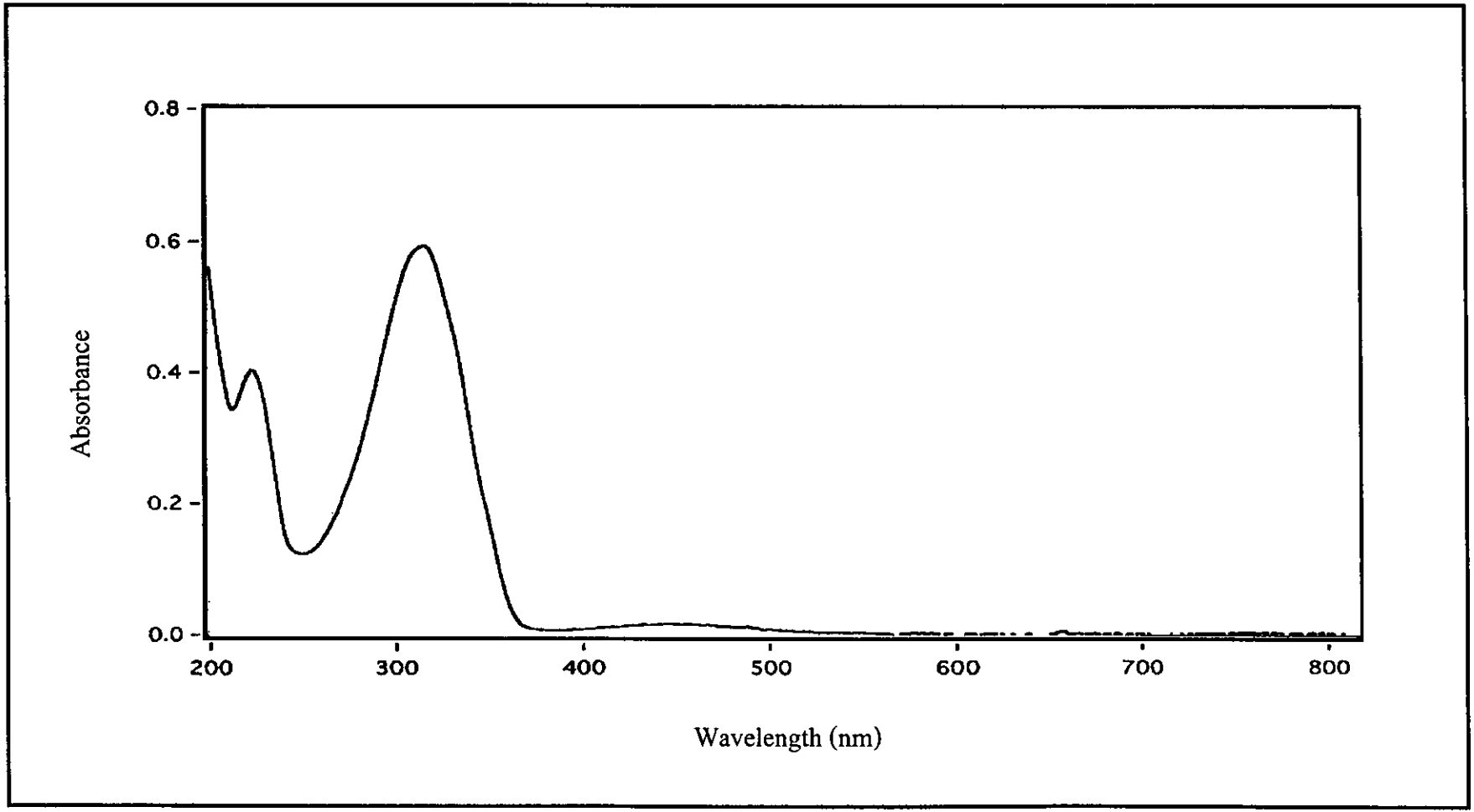

Figure 13 UV-Visible absorption spectrum of azpy in CH_3CN.

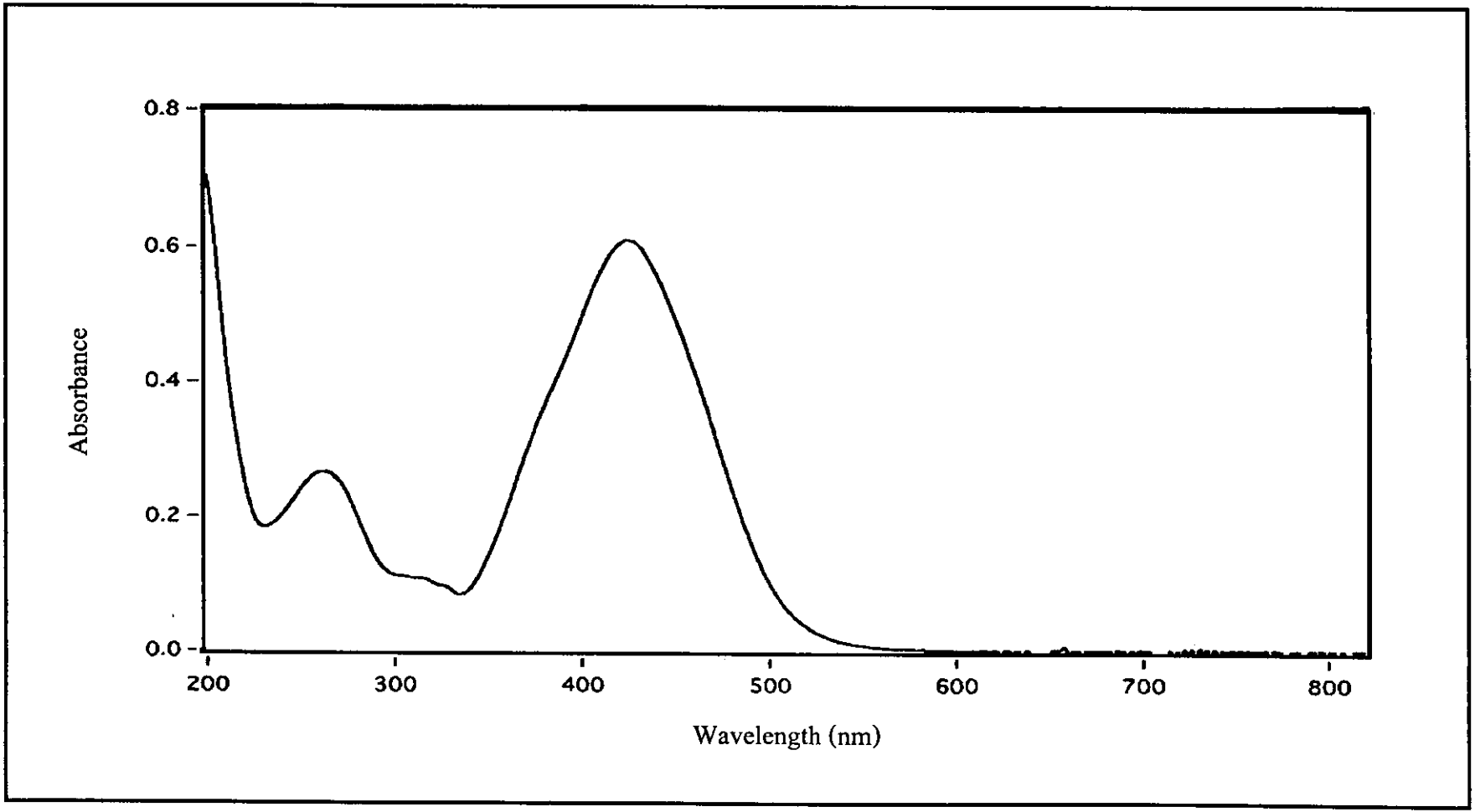

Figure 14 UV-Visible absorption spectrum of dmazpy in CH_3CN.

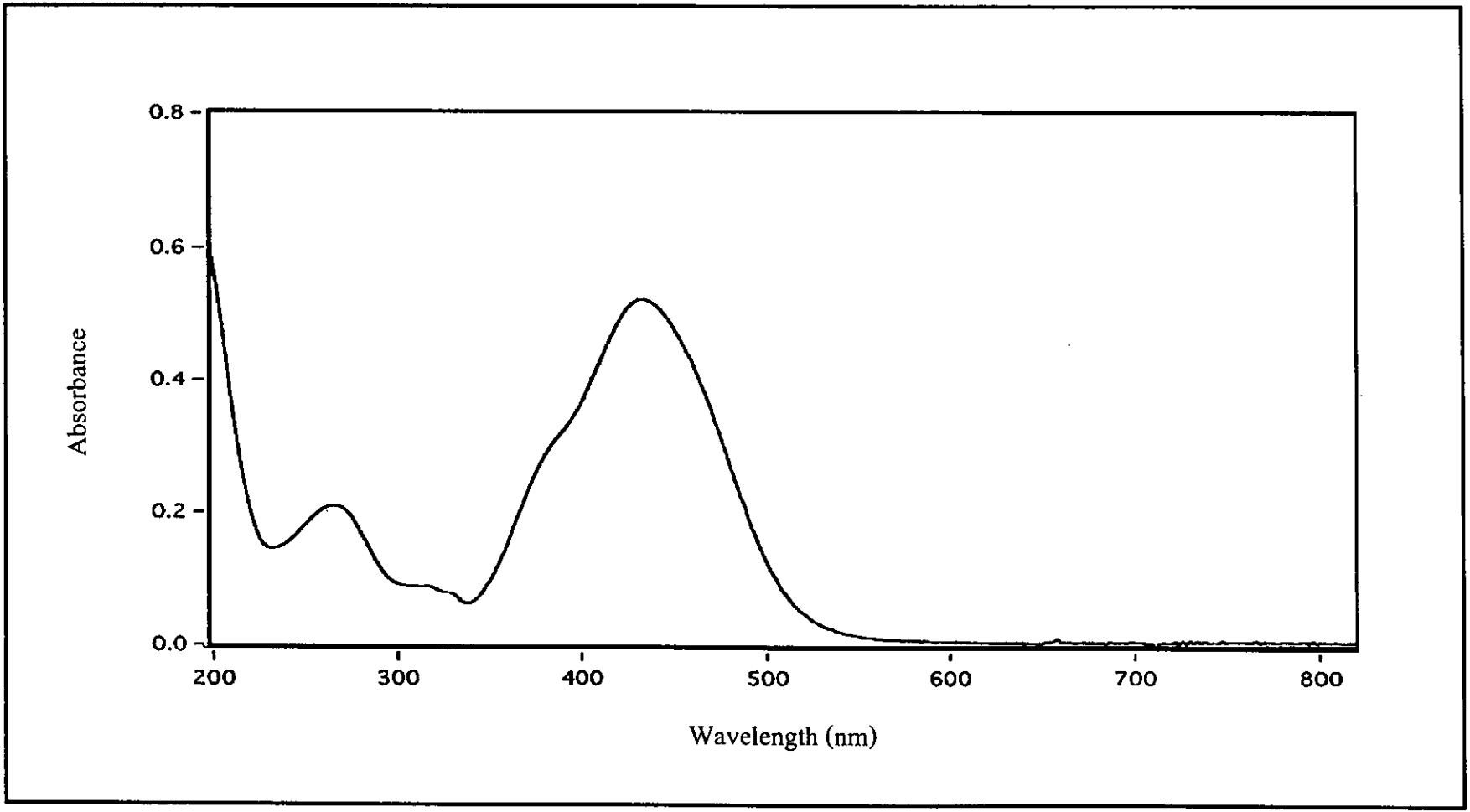

Figure 15 UV-Visible absorption spectrum of deazpy in CH_3CN.

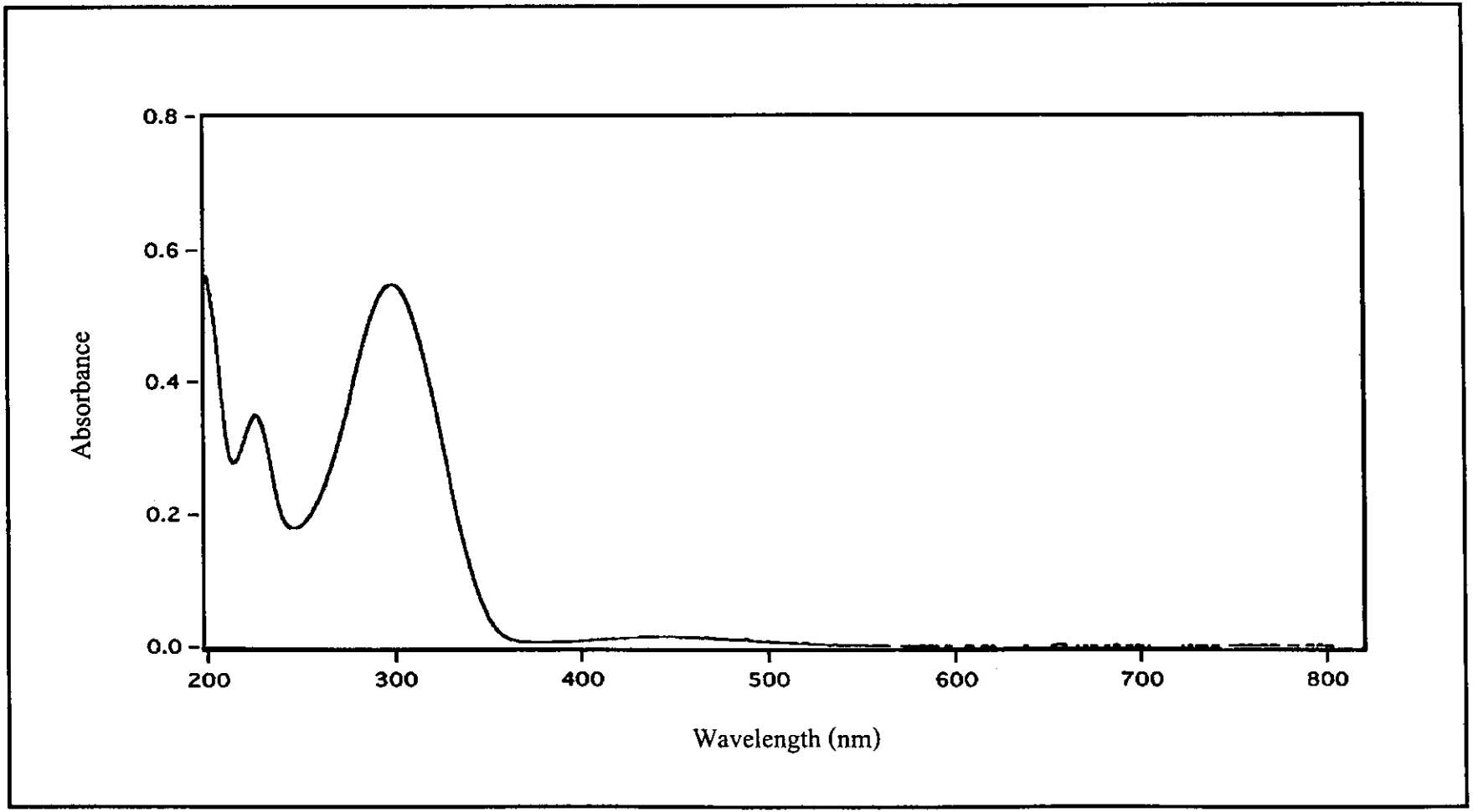

Figure 16 UV-Visible absorption spectrum of azpym in CH_3CN.

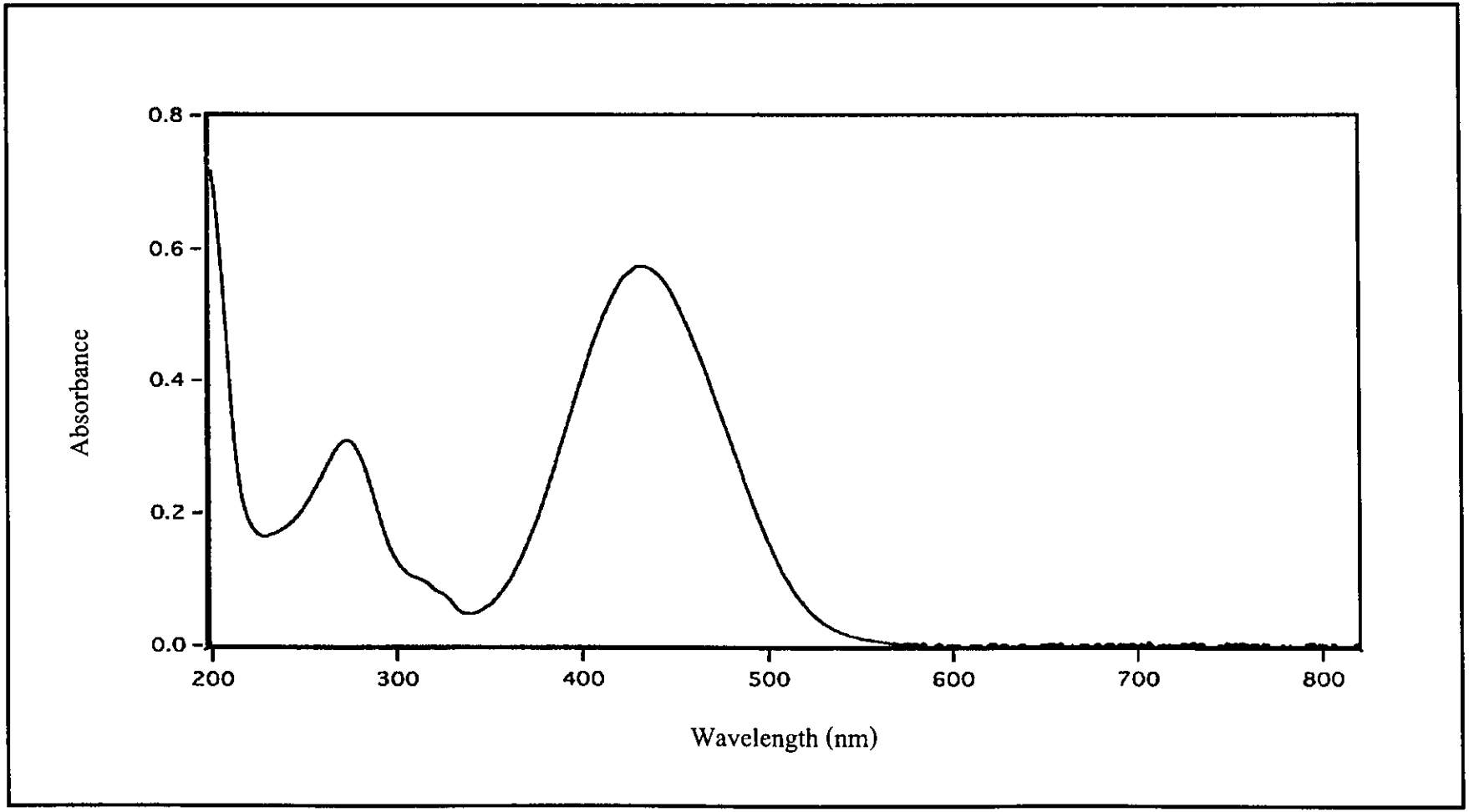

Figure 17 UV-Visible absorption spectrum of deazpym in CH_3CN.

3.2.4 Nuclear magnetic resonance spectroscopy

Nuclear magnetic resonance (NMR) spectroscopy is important technique to determine molecular structure. The ^{1}H NMR spectra of ligands are recorded in acetone -d_6. Tetramethylsilane (TMS, $(CH_3)_4Si$) is used as an internal reference. The chemical shift (δ) is expressed in parts per million (ppm) downfield from TMS and J-coupling is expressed in hertz (Hz). The ^{1}H NMR spectrum of phen, azpy, dmazpy, deazpy, azpym and deazpym are displayed in Figure 18 to 23, respectively. The spectral data are given in Table 5 to 10 for all ligands.

Table 5 ^{1}H NMR spectroscopic data of phen

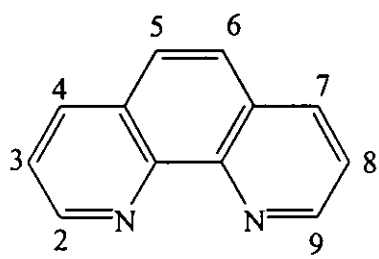

H-position	δ (ppm)	J-coupling (Hz)	Amount of H
2	9.12 (dd)	5.0, 2.0	2
4	8.45 (dd)	8.0, 2.0	2
5	7.97 (s)	-	2
3	7.76 (dd)	8.0, 4.5	2

s = singlet and dd = doublet of doublet

The phen ligand had four equivalent protons on molecule. The ^{1}H NMR data of phen appeared four signals.

The H2 was next to the nitrogen atom (inductive effect). Therefore, the chemical shift of H2 occurred at low field than other protons. The signals were doublet of doublet peaks and splitted by H3 (J = 5.0 Hz) and H4 (J = 2.0 Hz) at 9.12 ppm. The H3 was located between H2 and H4 and coupled with J = 4.5 and 8.0 Hz, respectively. It appeared doublet of doublet peaks at 7.76 ppm (the highest field). The H4 had the chemical shift value at 8.45 ppm by coupled with proton H3 (J = 8.0 Hz) and H2(2.0 Hz). It appeared doublet of doublet peaks. The H5 signal was singlet at 7.97 ppm.

Table 6 ^{1}H NMR spectroscopic data of azpy

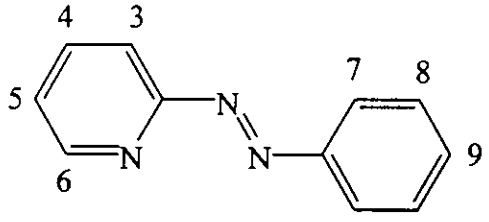

H-position	δ (ppm)	J-coupling (Hz)	Amount of H
6	8.75 (ddd)	5.0, 2.0, 1.0	1
4	8.04 (ddd)	7.0, 7.0, 2.0	1
7	8.02 (dd)	5.5, 2.0	2
3	8.77 (ddd)	8.0, 1.0, 0.5	1
8,9	7.64 (m)	-	3
5	7.57 (ddd)	7.5, 5.0, 1.0	1

d = doublet, m = multiplet, dd = doublet of doublet and

ddd = doublet of doublet of doublet

In case of azpy ligand, the H3 was located next to proton H4 and effected by nitrogen of azo function and resonance in molecule. The signal occurred at low field more than proton H5 but high field than H4 and H6. It showed as doublet of doublet of doublet peaks with J-coupling 8.0 (H4), 1.0 (H5), 0.5 (H6) Hz at 8.77 ppm. The H4 signals appeared doublet of doublet of doublet peaks at 8.04 ppm. It coupled with H3 (J = 7.0 Hz), H5 (J = 7.0 Hz) and H6 (J = 2.0 Hz). The H5 was located next to H6 and gave resonance effect. The signals appeared at a highest field (7.57 ppm) and coupled with H6 (J = 5.0 Hz), H4 (J = 7.5 Hz) and H3 (J = 1.0 Hz). The H6 was on pyridine located next to pyridine nitrogen atom and appeared at most low field. The signals were splitted by H5 (J = 5.0 Hz), H4 (J = 2.0 Hz) and H3 (J = 1.0 Hz) and peaks appeared as doublet of doublet of doublet. The H7 were two equivalent protons on phenyl ring located closed to azo nitrogen. The H7 interacted with proton H8 and H9. The signal showed as doublet of doublet peaks with J-coupling 5.5 (H8), 2.0 (H9) Hz at 8.02 ppm. The H8 and H9 showed very similar chemical shifts. Because the H9 had lowest density of electron (resonance effect), the singnals of H8 and H9 appeared mulitiplet peaks at 7.64.

Table 7 ^{1}H NMR spectroscopic data of dmazpy

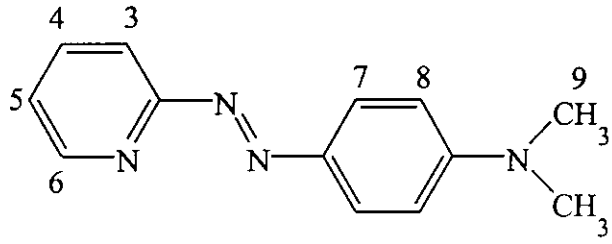

H-position	δ (ppm)	J-coupling (Hz)	Amount of H
6	8.66 (ddd)	5.0, 2.0, 1.0	1
4	7.94 (ddd)	8.0, 7.0, 2.0	1
7	7.93 (d)	9.0	2
3	7.70 (ddd)	8.0, 1.0, 1.0	1
5	7.41 (ddd)	7.0, 5.0, 1.5	1
8	6.89 (d)	9.0	2
9	2.90 (s)	-	6

d = doublet, s = singlet and ddd = doublet of doublet of doublet

The protons on pyridine ring of dmazpy ligands were similar to azpy ligand. Due to the substituent group, it appeared at high field than protons of azpy. The protons on phenyl ring, H7 and H8 were two equivalent protons. The H8 located closed to substituent group. Then H8 appeared at high field than H7 at 6.89 (H8) and 7.93 (H7) ppm. The signal of H9 showed as singlet peak at 2.90 ppm.

Table 8 ^{1}H NMR spectroscopic data of deazpy

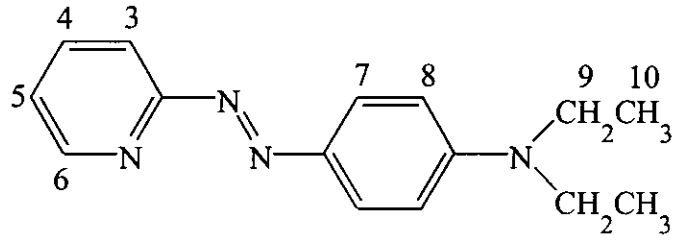

H-position	δ (ppm)	J-coupling (Hz)	Amount of H
6	8.65 (ddd)	5.0, 2.0, 1.0	1
4	7.93 (ddd)	8.0, 7.0, 2.0	1
7	7.92 (d)	9.0	2
3	7.69 (ddd)	8.0, 1.0, 1.0	1
5	7.39 (ddd)	7.5, 5.0, 1.0	1
8	6.88 (d)	9.0	2
9	3.56 (q)	7.0	4
10	1.25 (t)	7.0	6

d = doublet, q = quartet, t = triplet and ddd = doublet of doublet of doublet

Deazpy ligand had $-C_2H_5$ group on phenyl ring then protons of deazpy appeared at higher than dmazpy and azpy. Protons of substituent group, H9 showed quartet peakes at 3.56 ppm (J = 7.0 Hz) and H10 showed triplet peaks at 1.25 ppm (J = 7.0 Hz).

Table 9 ^{1}H NMR spectroscopic data of azpym

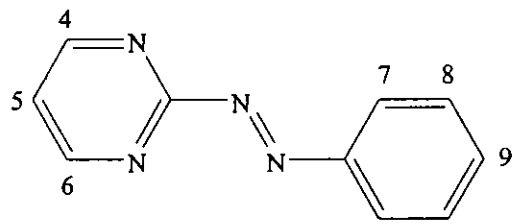

H-position	δ (ppm)	J-coupling (Hz)	Amount of H
4, 6	9.00 (d)	5.0	2
7	8.05 (dd)	8.0, 1.5	2
9	7.66 (dd)	5.0, 0.5	1
8	7.66 (dd)	5.0	2
5	7.61 (t)	5.0	1

d = doublet, t = triplet and dd = doublet of doublet

In case of azpym ligand, the H4 and H6 were equivalent protons on pyrimidine ring and appeared at most low field (9.00 ppm). The signals were splitted by H5 (J = 5.0 Hz). The H5 appeared triplet peaks at highest field (7.61 ppm) by coupled with H4 and H6. The H7 were two equivalent protons on phenyl ring located close to azo nitrogen. It interacted with H8 and H9 and gave doublet of doublet peaks with J-coupling 8.0 (H8) and 1.5 (H9) Hz. The H8 were two equivalent protons located next to H7. The signals were also doublet of doublet peaks and splitted by H7 (J =8.0 Hz) and H9 (J = 1.5 Hz). The last proton, H9 gave signals doublet of doublet peaks at 7.66 ppm by coupling with H8 (J = 5.0 Hz) and H7 (J = 1.0 Hz).

Table 10 ^{1}H NMR spectroscopic data of deazpym ligand

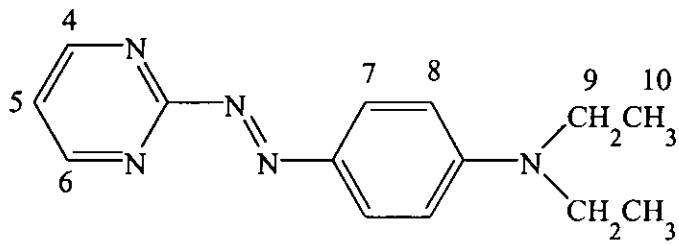

H-position	δ (ppm)	J-coupling (Hz)	Amount of H
4, 6	8.92 (d)	4.5	1
7	7.96 (d)	9.0	1
5	7.46 (t)	5.0	1
8	6.89 (d)	9.5	2
9	3.57 (q)	7.0	4
10	1.25 (t)	7.0	6

d = doublet, q = quartet, s = singlet and t = triplet

The last ligand was deazpym. The result of ^{1}H NMR was similar to azpym but this ligand had -C_2H_5 on phenyl ring. Therefore, the positions of protons on phenyl ring of deazpym are different from azpym ligand. The H7 and H8 were two equivalent protons. Each proton showed douplet peak at 7.96 and 6.89 ppm, respectively. The H9 were methylene protons. The signal appeared as quartet peaks of 4 protons. It coupled with H10 (J = 5.0 Hz). The H10 were methyl proton. Those protons were located next to H9 and occurred at 1.25 ppm by coupled with H9 (J =7.0 Hz).

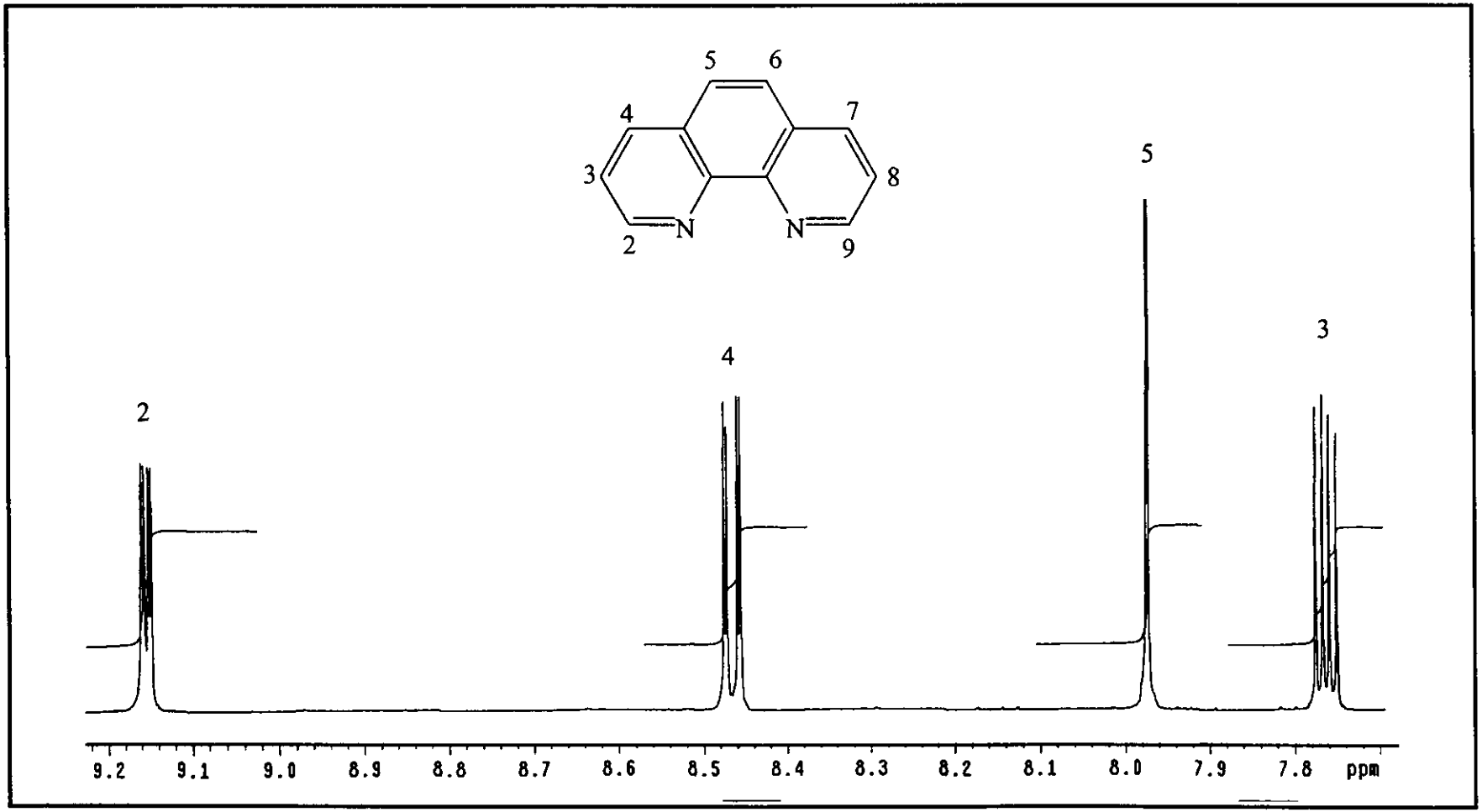

Figure 18 ^{1}H NMR spectrum of phen in acetone-d_6.

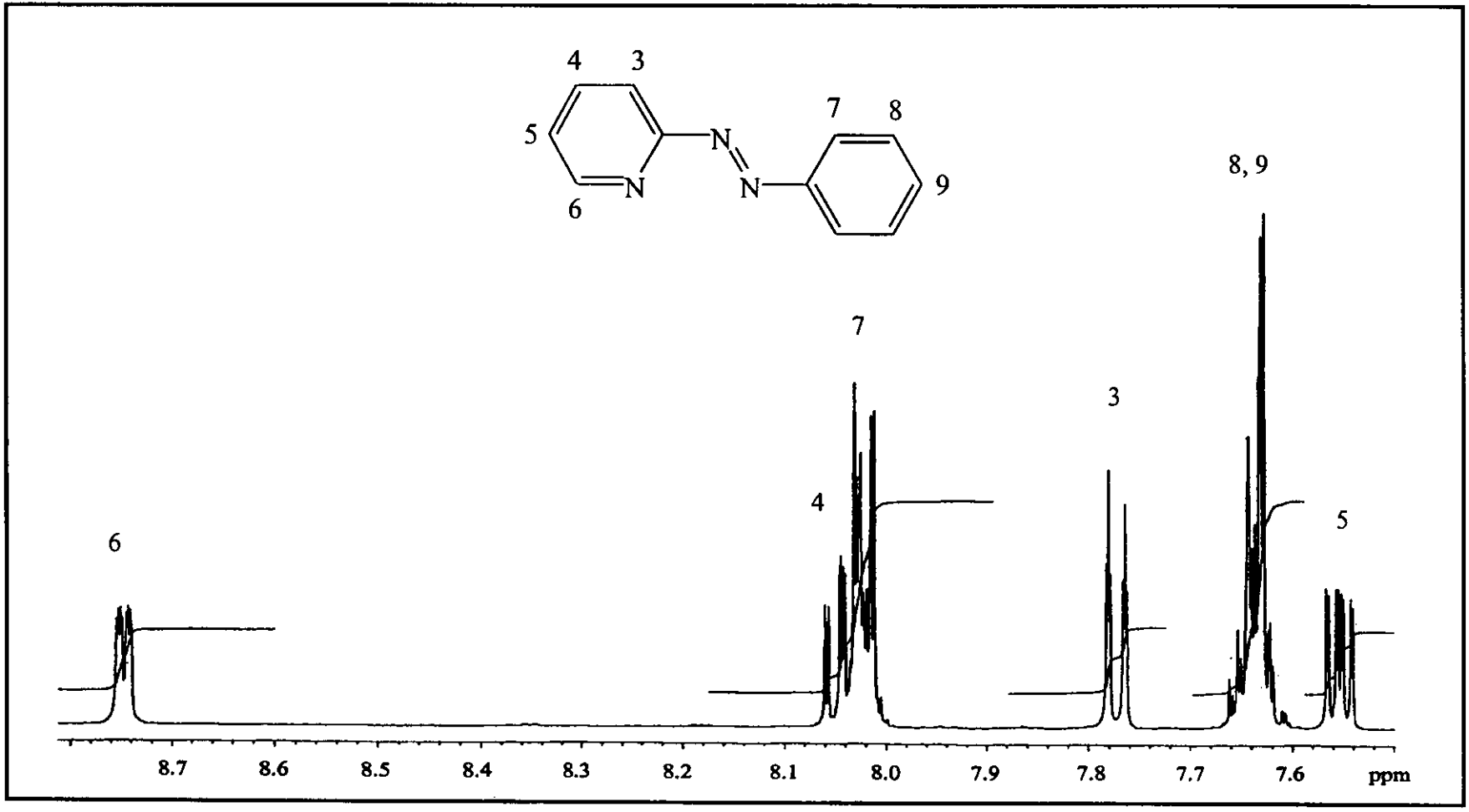

Figure 19 ^{1}H NMR spectrum of azpy in acetone-d_6

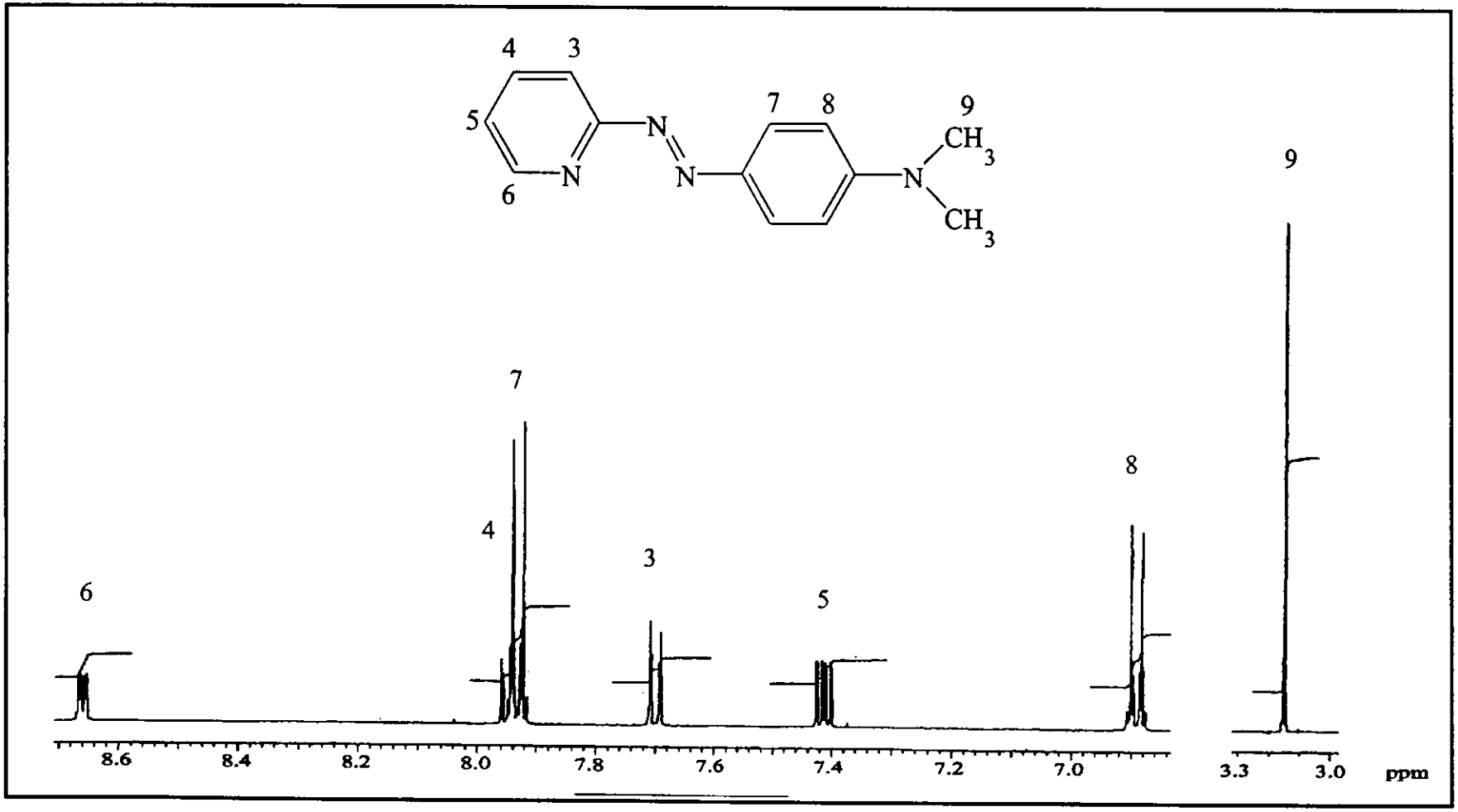

Figure 20 ^{1}H NMR spectrum of dmazpy in acetone-d_6

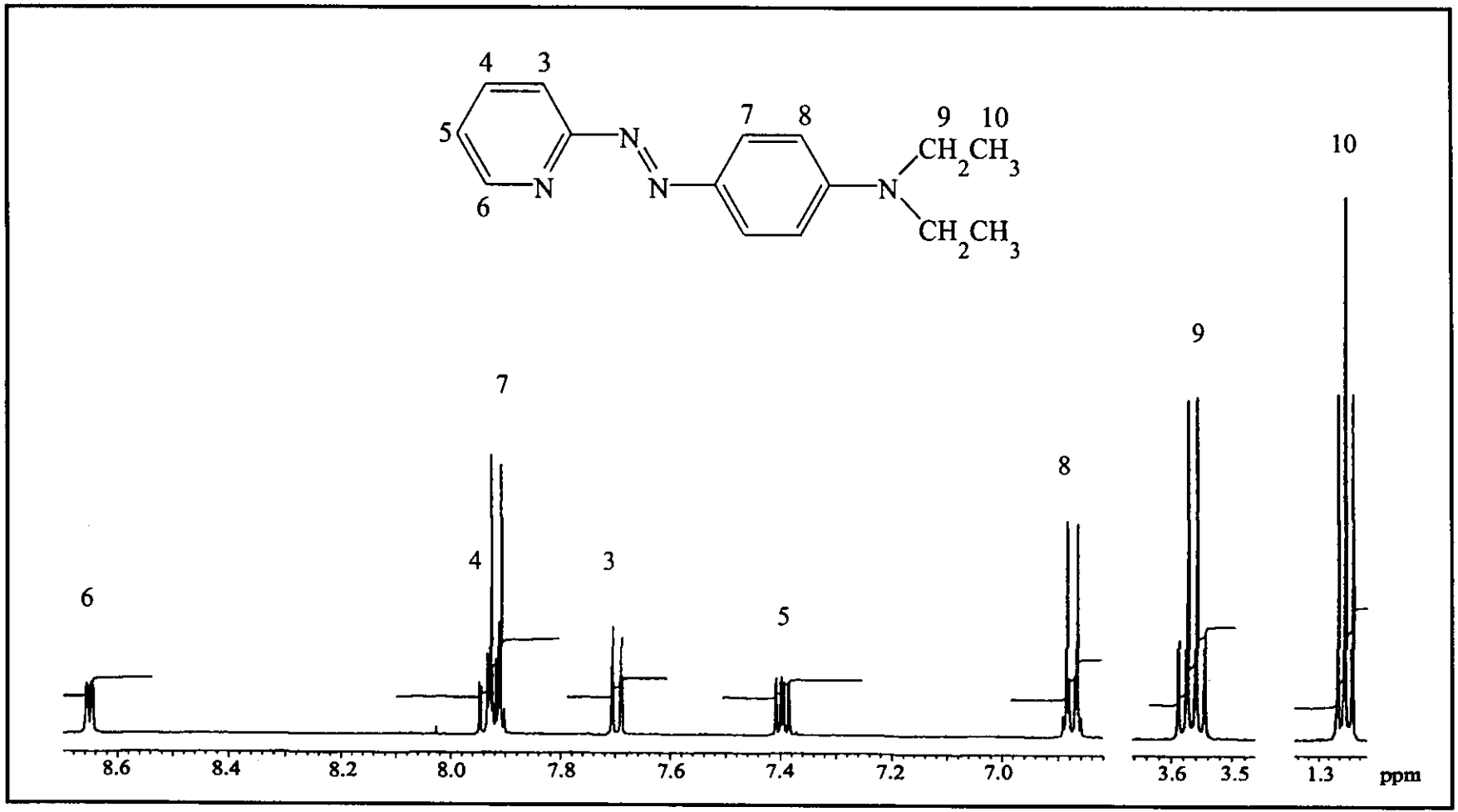

Figure 21 ^{1}H NMR spectrum of deazpy in acetone-d_6

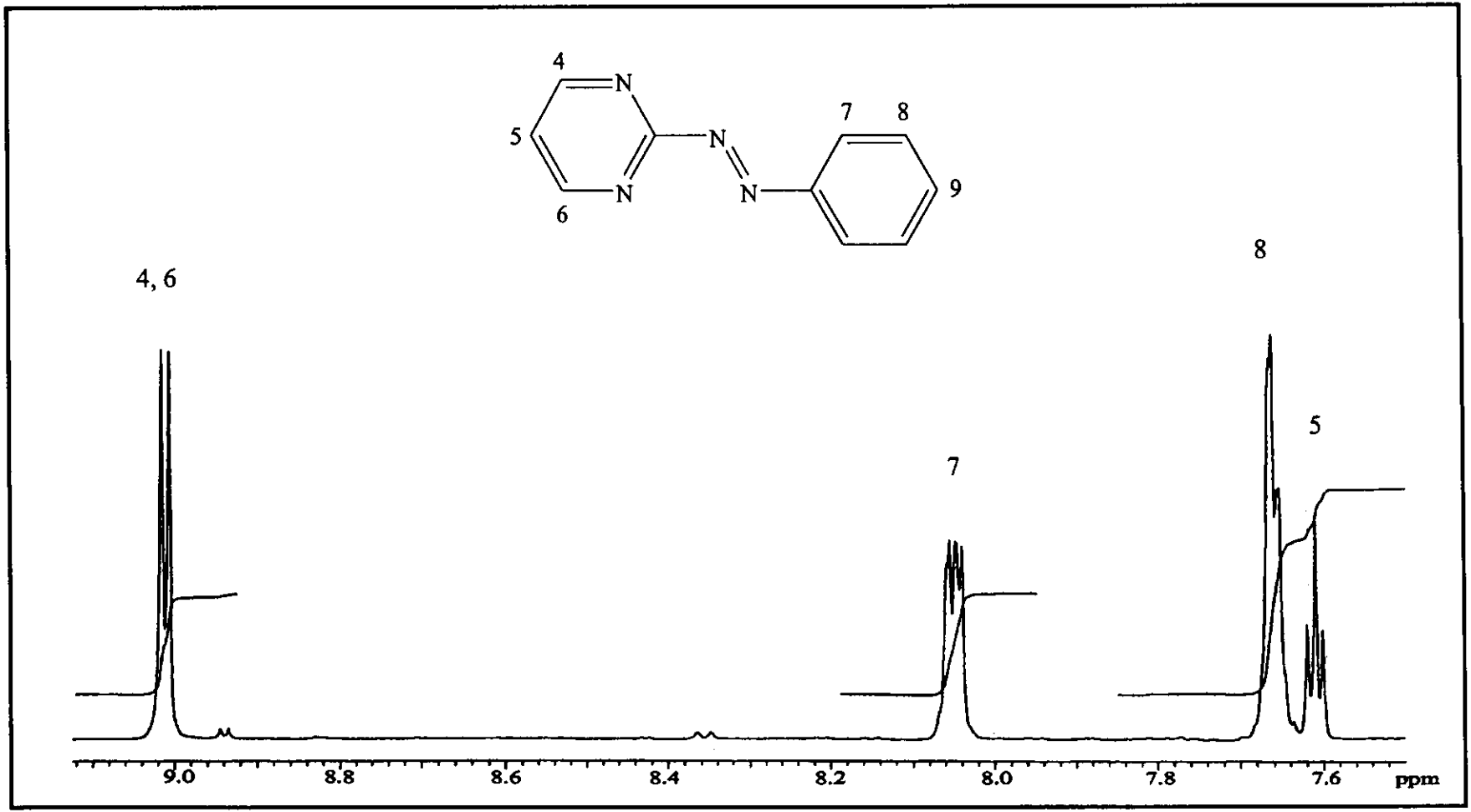

Figure 22 ^{1}H NMR spectrum of azpym in acetone-d_6.

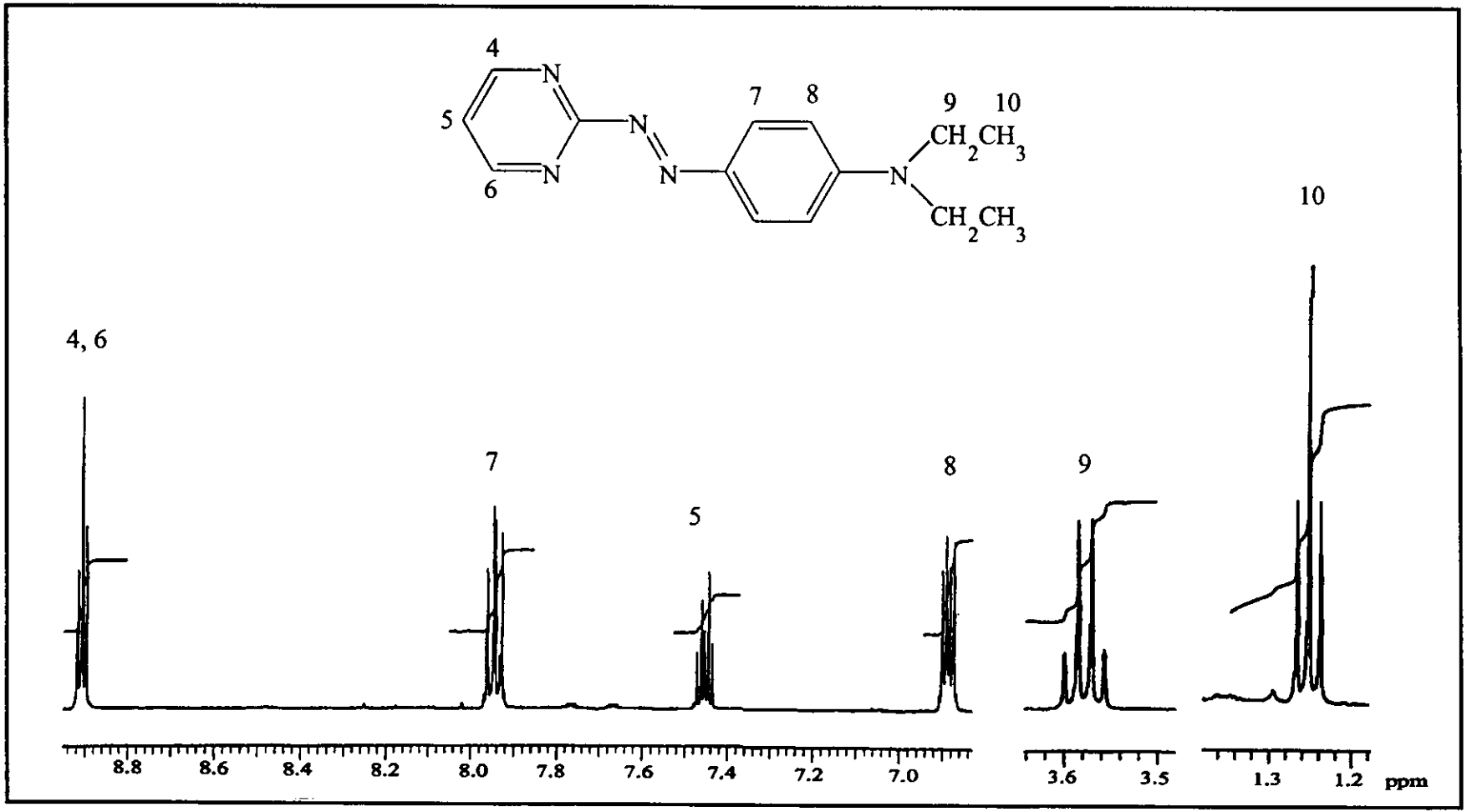

Figure 23 ^{1}H NMR spectrum of deazpym in acetone-d_6.

3.2.5 Cyclic voltammetry

The cyclic voltammetry is an important technique to study the electrochemistry of the azpy, dmazpy, deazpy, azpym and deazpym ligands. The cyclic voltammograms of these ligands should be considered first. Because of the similarity of the structures of ligands, it was important to compare the cyclic voltammograms of complexes. The potentials were reported with referrence to the ferrocene couple ($E_{1/2}$ = 0 V, ΔE_p = 65 mV). The $E_{1/2}$ value was calculated from the average of the anodic and cathodic peak potentials ($E_{1/2} = (E_{pa} + E_{pc})/2$) at scan rate of 50 mVs^{-1} and the ΔE_p value was calculated from the difference of both peaks. The cyclic voltammograms of complexes displayed metal oxidation in oxidation range and ligand reduction in reduction range. In addition, the ligands having substituent group displayed electrochemistry both in oxidation and reduction range. In this experiment, the different scan rates were used to check the couple or the redox reaction. The couple gave equal anodic and cathodic currents were referred to reversible couple. The unequal currents were referred to the unequally transfer of the electron in the reduction and oxidation. This led to irreversible couple. If different scan rate were applied to the unequal currents, these currents gave equal anodic and cathodic currents. This led to quasi-reversible couple. The cyclic voltammograms of ligands are shown in Figure 24 to 28.

Azpy dmazpy, deazpy, deazpym and azpym ligands had E_{pa} and E_{pc} in reduction range. But dmazpy, deazpy and deazpym showed E_{pa} and $E_{1/2}$ of substituent group in oxidation range. The results from cyclic voltammetry are displayed in Table11.

Table 11 Cyclic voltammetric data of azpy, dmazpy, deazpy, azpym and deazpym ligand in 0.1 M TBAH acetonitrile at scan rate 50 mV/s. (ferrocene as an internal standard, $\Delta E_p = 65$ mV).

Ligands	Oxidation		Reduction	
	E_{pa}, V	$E_{1/2}$, V (ΔE_p,mV)	E_{pa}, V	E_{pc}, V
azpy	-	-	-1.47	-1.61
dmazpy	+0.57	+0.81(93)	-1.42	-1.79
deazpy	+0.55	+0.83(70)	-1.42	-1.79
azpym	-	-	-1.05	-1.32
deazpym	+0.60	+0.89(88)	-1.29	-1.66

E_{pa} = anodic peak and E_{pc} = cathodic peak

Reduction range

The cyclic voltammetric data of these ligands were studied in the range 0.0 to 2.0 V and gave two irreversible couples. E_{pc} of azpy occurred closed to 0.0 V than other ligands.

Oxidation range

In the potential 0.0 to +1.3 V, the cyclic voltammograms of azpy and azpym ligands showed no signals in this range. The dmazpy, deazpy and deazpym ligands showed irreversible couple and quasi-reversible couples.

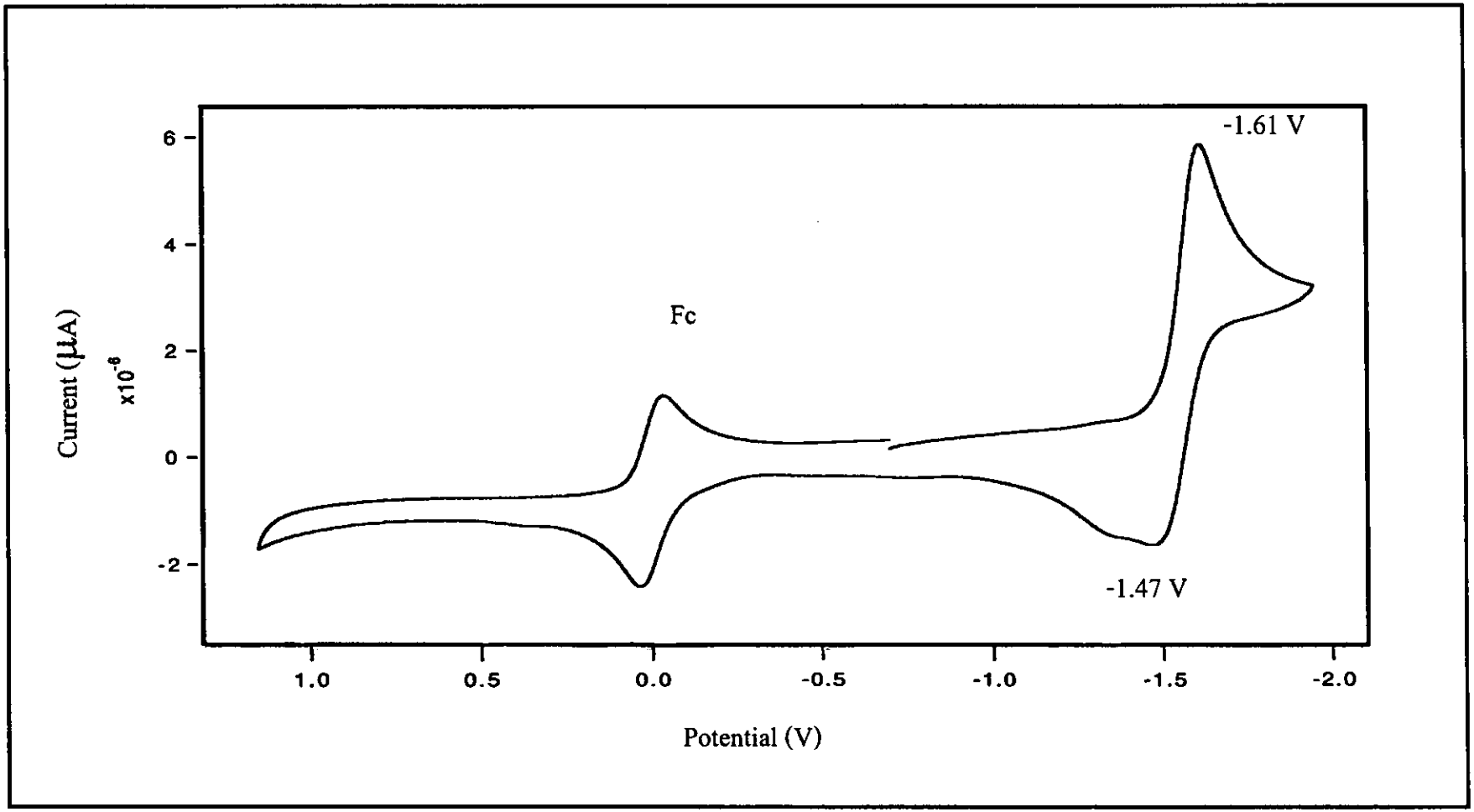

Figure 24 Cyclic voltammogram of azpy in 0.1 M TBAH CH_3CN at scan rate 50 mV/s.

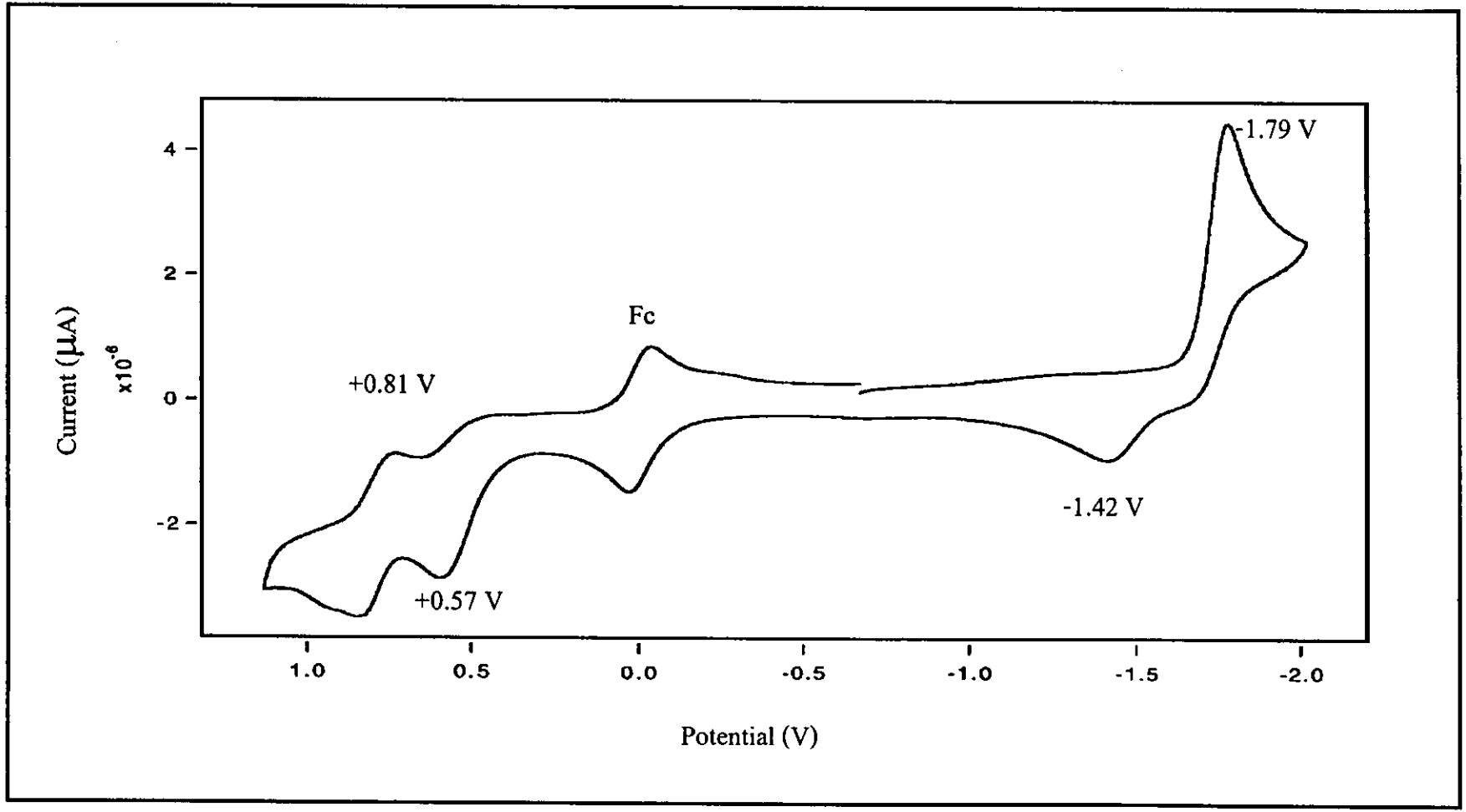

Figure 25 Cyclic voltammogram of dmazpy in 0.1 M TBAH CH_3CN at scan rate 50 mV/s.

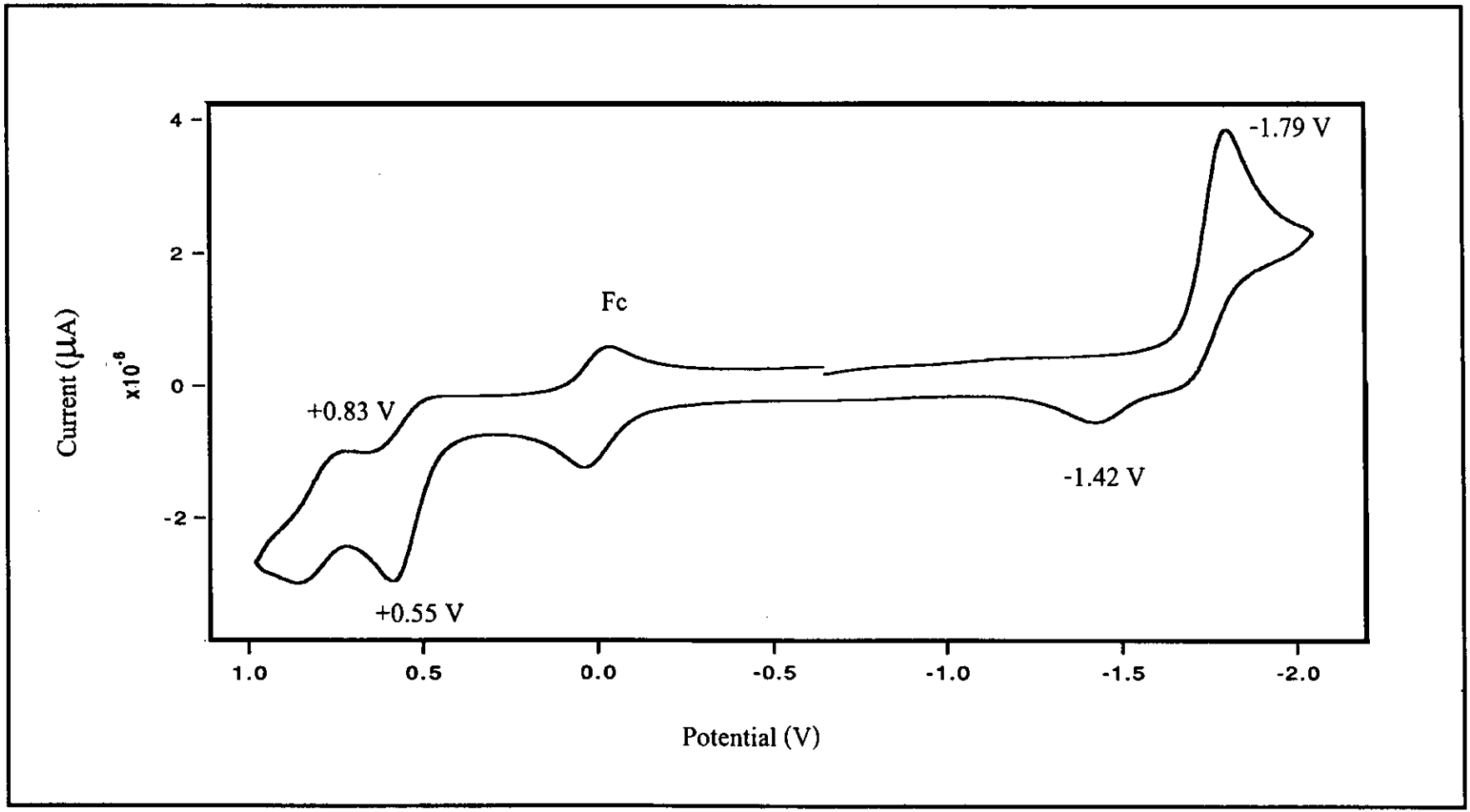

Figure 26 Cyclic voltammogram of deazpy in 0.1 M TBAH CH_3CN at scan rate 50 mV/s.

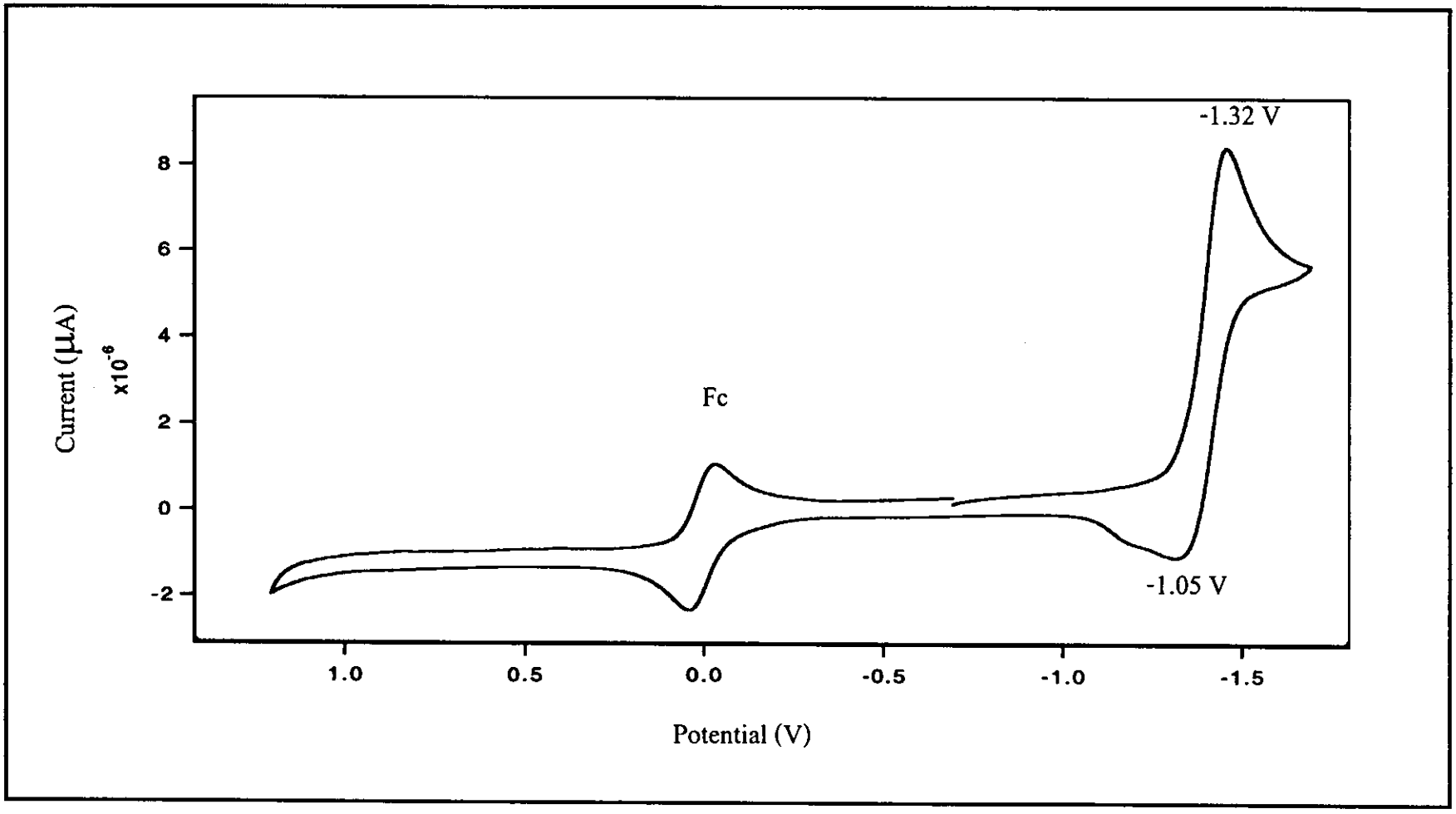

Figure 27 Cyclic voltammogram of azpym in 0.1 M TBAH CH_3CN at scan rate 50 mV/s.

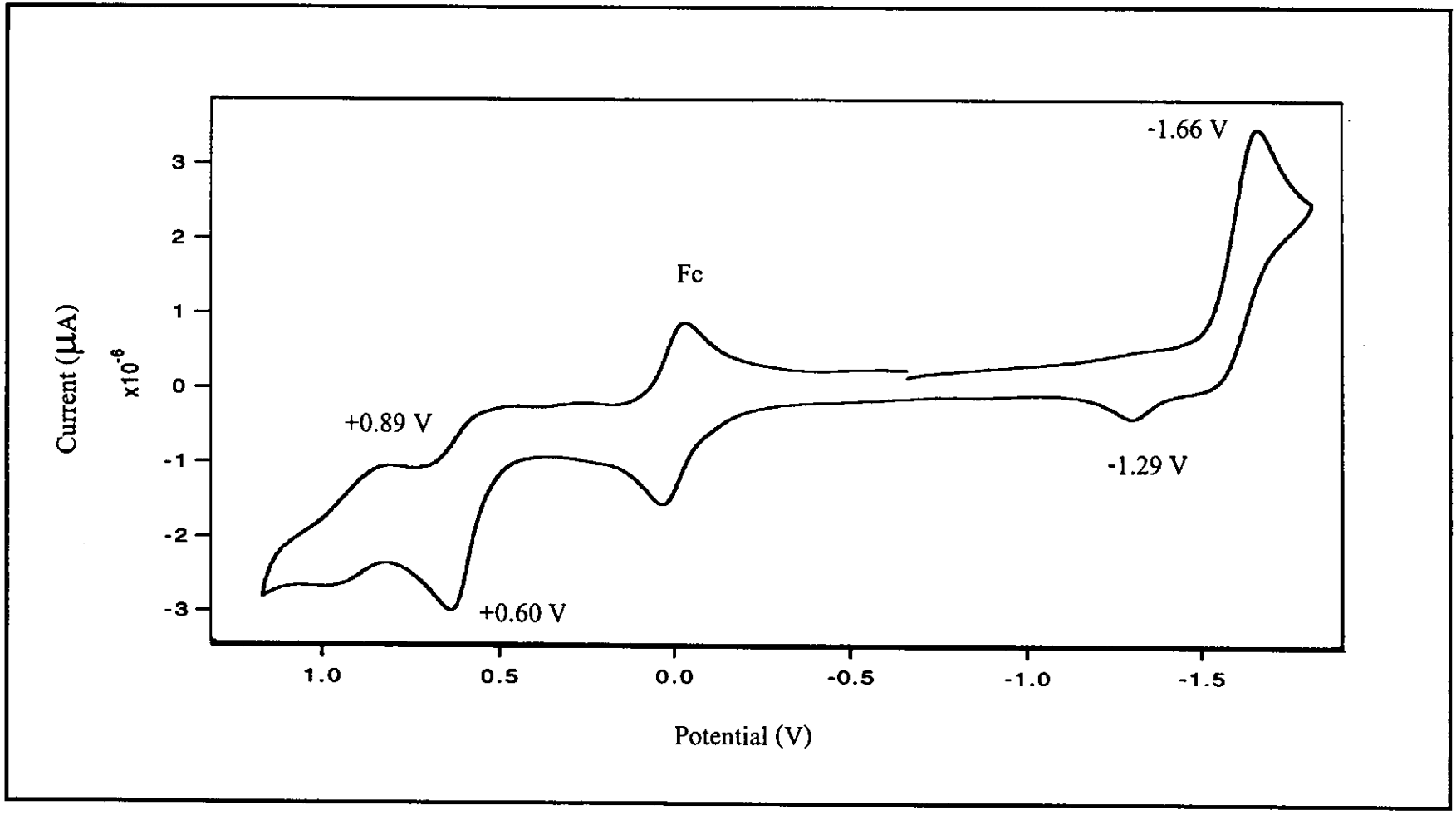

Figure 28 Cyclic voltammogram of deazpym in 0.1 M TBAH CH_3CN at scan rate 50 mV/s.

3.2.6 X-ray diffractometer

The X-ray crystallography is the most important technique to identify the geometries of the ligands. The single crystals of [protonated 2-(phenylazo)pyridine and protonated 2-(4-hydroxyphenylazo)pyridine (3:1)]tetrafluoroborated were grown by slowly diffusion of hexane into the ethanol solution. The crystallographic data are listed in Table 12 to 15. The crystal structure of [protonated 2-(phenylazo)pyridine and protonated 2-(4-hydroxyphenylazo)pyridine (3:1)]tetrafluoroborate is shown in Figure 29.

Table 12 Crystal and experimental data of [protonated 2-(phenylazo)pyridine and protonated 2-(4-hydroxyphenylazo)pyridine (3:1)]tetrafluoroborate

Formula	$(C_{11}H_{10}N_3O_{0.25})(BF_4)$
Formula weight	275.03
Crystal system	monoclinic
Space group	C_2/c
Z	8
Unit cell dimensions	$a = 29.875(4)$ Å, $\alpha = 90^\circ$
	$b = 5.930(1)$ Å, $\beta = 91.16(1)^\circ$
	$c = 13.743(2)$ Å, $\gamma = 90^\circ$
Volume	2434.2(6) $Å^3$
Density (calculated)	1.501 g/cm^3
Absorption coefficient	0.135 mm^{-1}
Temperature	293(2) K
Wavelength	0.71073 Å (Mo K_α)
Color	brown
R indices (all data)	$R = 0.074$ (on F), $R_w = 0.219$ (on I)
No. of reflection used	1472 ($I>2\sigma(I)$)
No. of parameter	181
Goodness-of-fit	1.04
Measurements	Siemens SMART CCD
Program system	NRCVAX
Structure determination	heavy atom methods (SHELXS-97)
Refinement	full matrix least-squares (SHELXS-97)

Table 13 Final coordinates and equivalent temperature facture ($Å^2$) for non-H atoms

Atom	x	y	z	U_{eq}
N(1)	0.1778(1)	0.2606(5)	0.3810(2)	0.056(1)
N(2)	0.1650(1)	0.0652(5)	0.3615(2)	0.056(1)
N(3)	0.0927(1)	0.1926(5)	0.4104(2)	0.060(1)
C(1)	0.2244(1)	0.2942(5)	0.3758(2)	0.050(1)
C(2)	0.2404(1)	0.5083(6)	0.4039(2)	0.064(1)
C(3)	0.2850(1)	0.5504(6)	0.4028(2)	0.069(1)
C(4)	0.3150(1)	0.3897(6)	0.3735(2)	0.064(1)
O(1)[#]	0.3514(3)	0.4792(17)	0.3846(6)	0.066(2)
C(5)	0.2990(1)	0.1816(6)	0.3440(2)	0.059(1)
C(6)	0.2542(1)	0.1332(5)	0.3444(2)	0.051(1)
C(7)	0.1182(1)	0.0368(5)	0.3672(2)	0.053(1)
C(8)	0.0480(1)	0.1680(7)	0.4147(3)	0.074(1)
C(9)	0.0273(1)	-0.0178(8)	0.3736(3)	0.076(1)
C(10)	0.0531(1)	-0.1786(7)	0.3305(3)	0.073(1)
C(11)	0.0989(1)	-0.1538(6)	0.3278(3)	0.064(1)
B(1)	0.4189(1)	0.8661(8)	0.3904(3)	0.066(1)
F(1)	0.3981(1)	0.8956(5)	0.3029(2)	0.113(1)
F(2)	0.3907(1)	0.9484(5)	0.4628(2)	0.114(1)
F(3)	0.4246(1)	0.6398(5)	0.4066(2)	0.113(1)
F(4)	0.4585(1)	0.9723(6)	0.3957(3)	0.142(1)

[#]Occupancy = 0.25, $U_{eq} = (1/3)\sum\sum U_{ij} a_i^* a_j^* (a_i a_j)$

Table 14 Non-hydrogen interatomic distances (Å)

Atom	Distance (Å)
N(1)-N(2)	1.248(4)
N(1)-C(1)	1.412(4)
N(2)-C(7)	1.411(4)
N(3)-C(7)	1.344(4)
N(3)-C(8)	1.346(4)
C(1)-C(6)	1.379(4)
C(1)-C(2)	1.408(5)
C(2)-C(3)	1.355(5)
C(3)-C(4)	1.374(5)
C(4)-O(1)	1.290(9)
C(4)-C(5)	1.382(5)
C(5)-C(6)	1.370(4)
C(7)-C(11)	1.375(5)
C(8)-C(9)	1.378(6)
C(9)-C(10)	1.369(5)
C(10)-C(11)	1.377(5)
B(1)-F(4)	1.339(5)
B(1)-F(1)	1.354(5)
B(1)-F(3)	1.370(5)
B(1)-F(2)	1.404(5)

Table 15 Non-hydrogen interatomic angle (°)

Atom	Angle (°)
N(2)-N(1)-C(1)	114.8(2)
N(1)-N(2)-C(7)	113.5(3)
C(7)-N(3)-C(8)	121.1(3)
C(6)-C(1)-C(2)	119.5(3)
C(6)-C(1)-N(1)	124.2(3)
C(2)-C(1)-N(1)	116.3(3)
C(3)-C(2)-C(1)	119.4(3)
C(2)-C(3)-C(4)	121.5(3)
O(1)-C(4)-C(3)	106.0(5)
O(1)-C(4)-C(5)	135.2(6)
C(3)-C(4)-C(5)	118.8(3)
C(6)-C(5)-C(4)	121.2(3)
C(5)-C(6)-C(1)	119.5(3)
N(3)-C(7)-C(11)	120.1(3)
N(3)-C(7)-N(2)	120.9(3)
C(11)-C(7)-N(2)	119.0(3)
N(3)-C(8)-C(9)	120.4(3)
C(10)-C(9)-C(8)	118.8(3)
C(9)-C(10)-C(11)	120.4(4)
C(7)-C(11)-C(10)	119.1(3)

Table 15 (continued)

Atom	Angle (°)
F(4)-B(1)-F(1)	112.1(4)
F(4)-B(1)-F(3)	110.3(3)
F(1)-B(1)-F(3)	108.9(3)
F(4)-B(1)-F(1)	112.1(4)
F(4)-B(1)-F(2)	109.8(3)
F(1)-B(1)-F(2)	108.2(3)
F(3)-B(1)-F(2)	107.4(4)

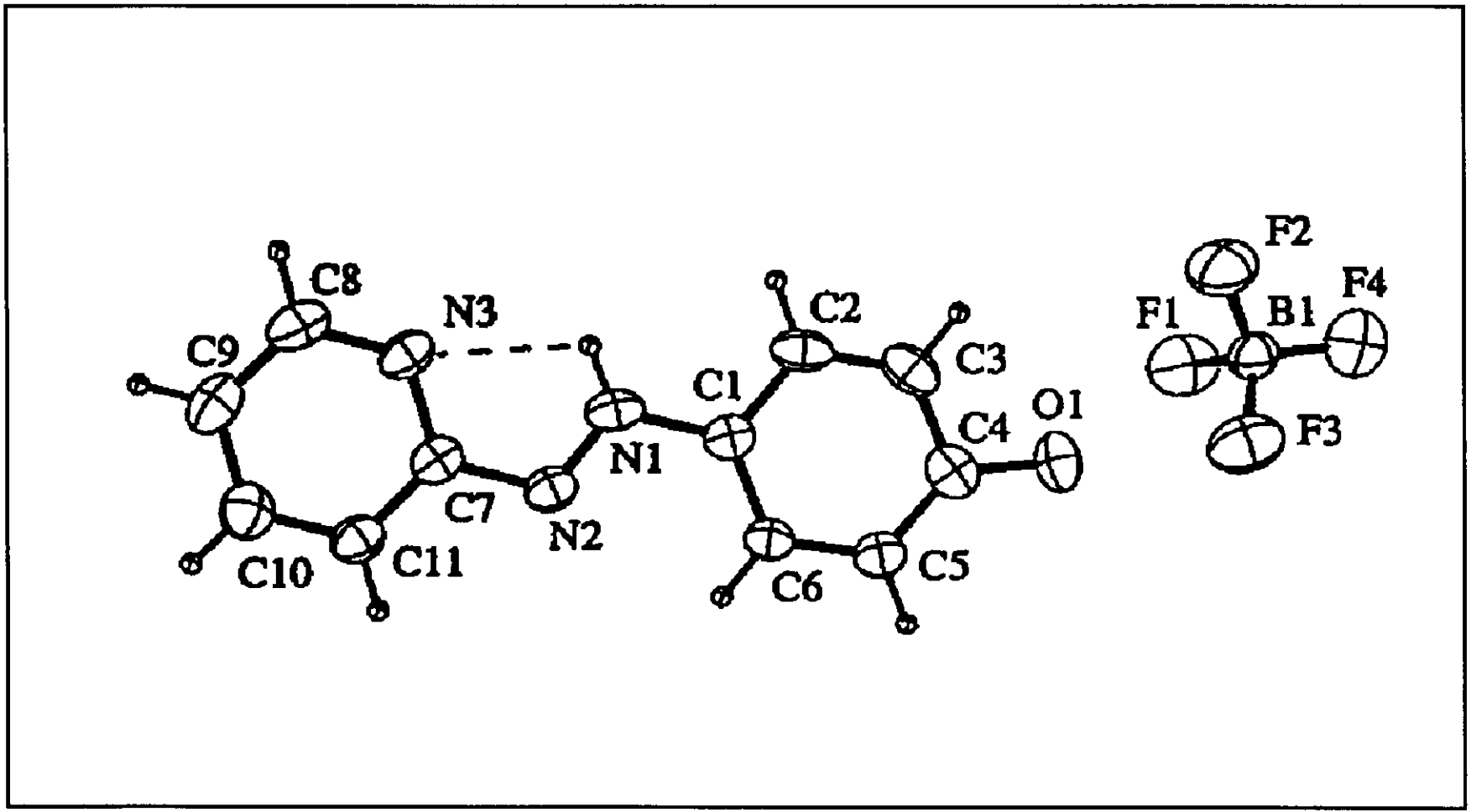

Figure 29 The structure of [protonated 2-(phenylazo)pyridine and protonated 2-(4-hydroxyphenylazo)pyridine (3:1)] tetrafluoroborate.

3.3 Preparation and characterization of the *cis*-$[Ru(phen)_2Cl_2]$ complex

cis-$[Ru(phen)_2Cl_2]$ complex was synthesized and used as starting material for synthesis the complexes of $[Ru(phen)_2L_2]^{2+}$ (L = azpy, dmazpy, deazpy, azpym and deazpym). The *cis*-$[Ru(phen)_2Cl_2]$ complex was prepared according to the similar literature method. (Sullivan, *et al.*, 1978) The structure of *cis*-$[Ru(phen)_2Cl_2]$ was characterized by ^1H NMR Spectroscopy in DMSO-d_6. The results are listed in Table 16. The ^1H NMR spectra of this complex is shown in Figure 30.

Table 16 ^1H NMR spectroscopic data of *cis*-$[Ru(phen)_2Cl_2]$

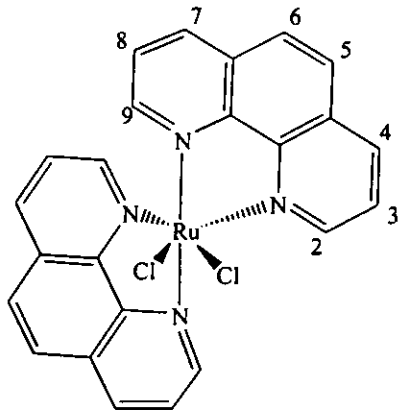

H-position	δ (ppm)	J-coupling (Hz)	Amount of H
4	10.68 (dd)	5.5, 1.5	2
2	8.38 (dd)	8.5, 1.5	2
3	8.03 (dd)	7.0, 2.0	2
5	8.01 (d)	8.0	2

Table 16 (continued)

H-position	δ (ppm)	J-coupling (Hz)	Amount of H
9	7.93 (dd)	8.0, 1.5	2
6	7.87 (d)	8.5	2
7	7.82 (dd)	5.5, 1.5	2
8	7.15 (d)	8.0	2

d = doublet, dd = doublet of doublet

The ^{1}H NMR results were used to confirm molecular structure. The complex of *cis*-[Ru(phen)$_2$Cl$_2$] had two phen ligands and it was equivalent. The H2 was next to nitrogen atom. The signals were doublet of doublet peaks at 8.38 ppm and splitted by H3 (J = 8.5 Hz) and H4 (J = 1.5 Hz). The H3 were located between H2 and H4. It appeared doublet of doublet peaks at 8.03 ppm by coupled with H2 (J = 7.0 Hz) and H4 (J = 2.0 Hz). The H4 had higher chemical shift value at 10.68 ppm by coupling with proton H2 (J = 1.5 Hz) and H3 (J = 5.5 Hz). The H5 and H6 signals were doublet peaks at 8.01 and 7.82 ppm. The H7 gave signals at by coupled with H8 (J = 5.5 Hz) and H9 (J = 1.5 Hz). The H8 were located between H7 and H9. The signals were also doublet peaks with J-coupling 8.0 Hz. The last proton, H9 was next to nitrogen atom. The H9 interacted with H8 (J = 8.0 Hz and H7 (J = 1.5 Hz) gave doublet of doublet peaks. The results of ^{1}H NMR could be demonstrated structure of *cis*-[Ru(phen)$_2$Cl$_2$].

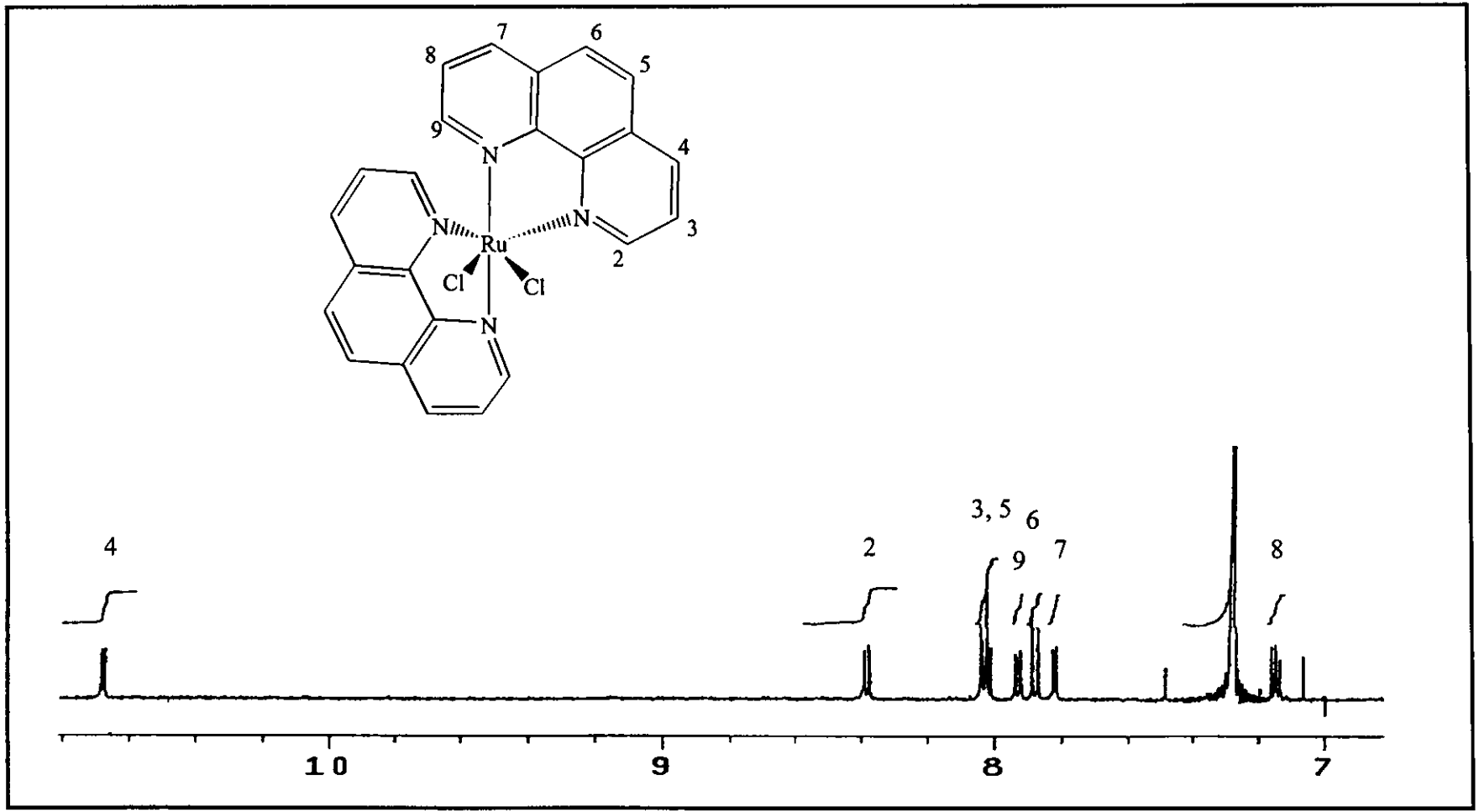

Figure 30 ^{1}H NMR spectrum of $[Ru(phen)_2Cl_2]$ in acetone-d_6

3.4 Preparation of the $[Ru(phen)_2L]^{2+}$ complexes

The reaction between *cis*-$[Ru(phen)_2Cl_2]$, ligands (azpy, dmazpy, deazpy, azpym and deazpym) and $AgNO_3$ in refluxing ethanol/water (3:1 v/v) solution. Then, these complexes were precipitated by BF_4^- or PF_6^- salts. The physical properties of all complexes are summarized in Table 17.

Table 17 The physical properties of complexes

Complex	Physical properties	
	Color	Melting point (^oC)
$[Ru(phen)_3](BF_4)_2$	Yellow-orange	355-356
$[Ru(phen)_2azpy](BF_4)_2$	Flushed red	315-316
$[Ru(phen)_2dmazpy](PF_6)_2$	Purple-Blue	315-316
$[Ru(phen)_2deazpy](PF_6)_2$	Blue	332-333
$[Ru(phen)_2azpym](PF_6)_2$	Red	301-302
$[Ru(phen)_2deazpym](PF_6)_2$	Green-blue	357-358

0.0020 g of complexes were tested their solubility in 10 mL of water, methanol, acetronitrile, acetone, ethanol, chloroform and dichlorometahne solvents. The symbol of solubility, +++ represented the completely soluble in 0.0020 g. of complexes in 10mL, ++ represented the moderately soluble of complexes in range 0.0006-0.0015 g. and + represented the partially soluble of those complexes less than 0.0005 g. The solubility of those complexes in some solvents is shown in Table 18.

Table 18 The solubility of complexes

Solvents	Solubility
Water	+
Methanol	++
Acetonitrile	+++
Acetone	+++
Ethanol	++
Chlorofrom	+
Dicholomethane	+++

+++ well soluble, ++ more soluble, + partially soluble

The solubility of complexes was useful for recrystallization. The suitable solvents may be selected from solvent in which complexes have different solubility.

3.5 Characterization of the $[Ru(phen)_2L]^{2+}$ complexes

Chemistry of $[Ru(phen)_2L]^{2+}$ complexes were characterized by using Elemental analysis, Electrospray mass spectrometry, Infrared spectroscopy, UV-Visible absorption spectroscopy, Nuclear magnetic Resonance spectroscopy and Cyclic Voltammetry techniques.

3.5.1 Elemental analysis

Elemental analysis confirms composition in complexes (%C, N and H). Results are given in Table 19.

Table 19 Elemental analysis data of $[Ru(phen)_2L]^{2+}$ (L = phen, azpy, dmazpy, deazpy, azpym and deazpym)

Complexes	%C		%N		%H	
	Calc.	Found	Calc.	Found	Calc.	Found
$[Ru(phen)_3](BF_4)_2$	53.04	51.55	10.31	10.39	2.96	3.06
$[Ru(phen)_2azpy](BF_4)_2$	51.37	50.83	11.98	12.31	3.08	3.53
$[Ru(phen)_2dmazpy](PF_6)_2$	45.46	45.55	11.46	10.94	3.09	3.14
$[Ru(phen)_2deazpy](PF_6)_2$	46.58	45.99	11.14	10.47	3.40	3.60
$[Ru(phen)_2azpym](PF_6)_2$	43.65	43.91	11.98	11.39	2.58	2.89
$[Ru(phen)_2deazpym](PF_6)_2$	45.34	44.00	12.52	12.48	3.30	2.91

3.5.2 The electrospray (ES) and the FAB mass spectrometry

The electrospray (ES) and FAB mass spectra of $[Ru(phen)_2L]^{2+}$ complexes, where L = phen, azpy, dmazpy, deazpy, azpym and deazpym were displayed in Figure 31 to 36. The important data of complexes with the corresponding relative abundance are shown in Table 20 and 21.

Table 20 Electrospray mass spectroscopic data of $[Ru(phen)_2L]^{2+}$ (L = azpy, dmazpy and deazpy)

$[Ru(phen)_2L]^{2+}$, L =	m/z	Stoichiometry	Equivalent species	Rel. Abun.
azpy	646.1	$[Ru(phen)_2azpy]^{2+}$	$[M-2BF_4]^+$	30
	322.8	$([Ru(phen)_2azpy]^{2+})^{2+}$	$([M-2BF_4]^+)^{2+}$	100
dmazpy	833.0	$[Ru(phen)_2dmazpy]^+(PF_6)$	$[M-PF_6]^+$	28
	646.4	$[Ru(phen)_2dmazpy]^{2+}$	$[M-2PF_6]^+$	68
	343.9	$([Ru(phen)_2dmazpy]^{2+})^{2+}$	$([M-2PF_6]^+)^{2+}$	100
deazpy	861.0	$[Ru(phen)_2deazpy]^+(PF_6)$	$[M-PF_6]^+$	53
	358.0	$([Ru(phen)_2deazpy]^{2+})^{2+}$	$([M-2PF_6]^+)^{2+}$	100

M = Molecular weight (MW) of each complex

MW of $[Ru(phen)_2azpy](BF_4)_2$ = 818.28 g/mol

MW of $[Ru(phen)_2dmazpy](PF_6)_2$ = 977.66 g/mol

MW of $[Ru(phen)_2deazpy](PF_6)_2$ = 1005.71 g/mol

Table 21 FAB mass spectroscopic data of $[Ru(phen)_2L]^{2+}$ (L = phen, azpym and deazpym)

$[Ru(phen)_2L]^{2+}$, L =	m/z	Stoichiometry	Equivalent species	Rel. Abun.
phen	729	$[Ru(phen)_3]^+(BF_4)$	$[M-BF_4]^+$	100
	641	$[Ru(phen)_3]^{2+}$	$[M-2BF_4]^+$	82

Table 21 (continued)

$[Ru(phen)_2L]^{2+}$, L =	m/z	Stoichiometry	Equivalent species	Rel. Abun.
azpym	791	$[Ru(phen)_2azpym]^+(PF_6)$	$[M\text{-}PF_6]^+$	52
	646	$[Ru(phen)_2azpym]^{2+}$	$[M\text{-}2PF_6]^+$	100
deazpym	862	$[Ru(phen)_2deazpym]^+(PF_6)$	$[M\text{-}PF_6]^+$	74
	717	$[Ru(phen)_2deazpym]^{2+}$	$[M\text{-}2PF_6]^+$	32
	689	$[Ru(phen)_2deazpym\text{-}C_2H4]^{2+}$	$[M\text{-}2PF_6\text{-}C_2H_4]^+$	100

M = Molecular weight (MW) of each comple

MW of $[Ru(phen)_3](BF_4)_2$ = 815.28 g/mol

MW of $[Ru(phen)_2azpym](PF_6)_2$ = 935.58 g/mol

Mw of $[Ru(phen)_2deazpym](PF_6)_2$ = 1006.69 g/mol

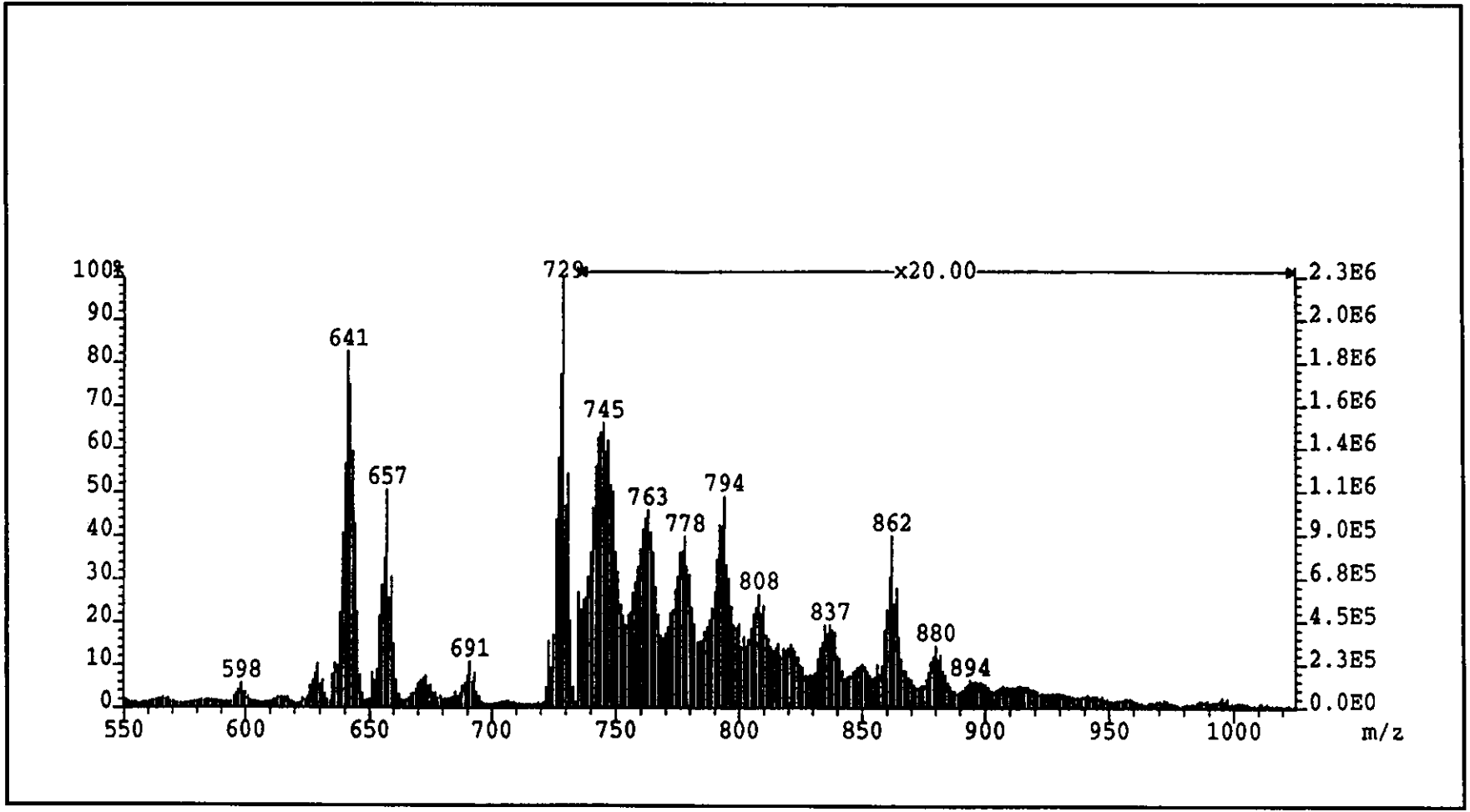

Figure 31 FAB mass spectrum of $[Ru(phen)_3](BF_4)_2$

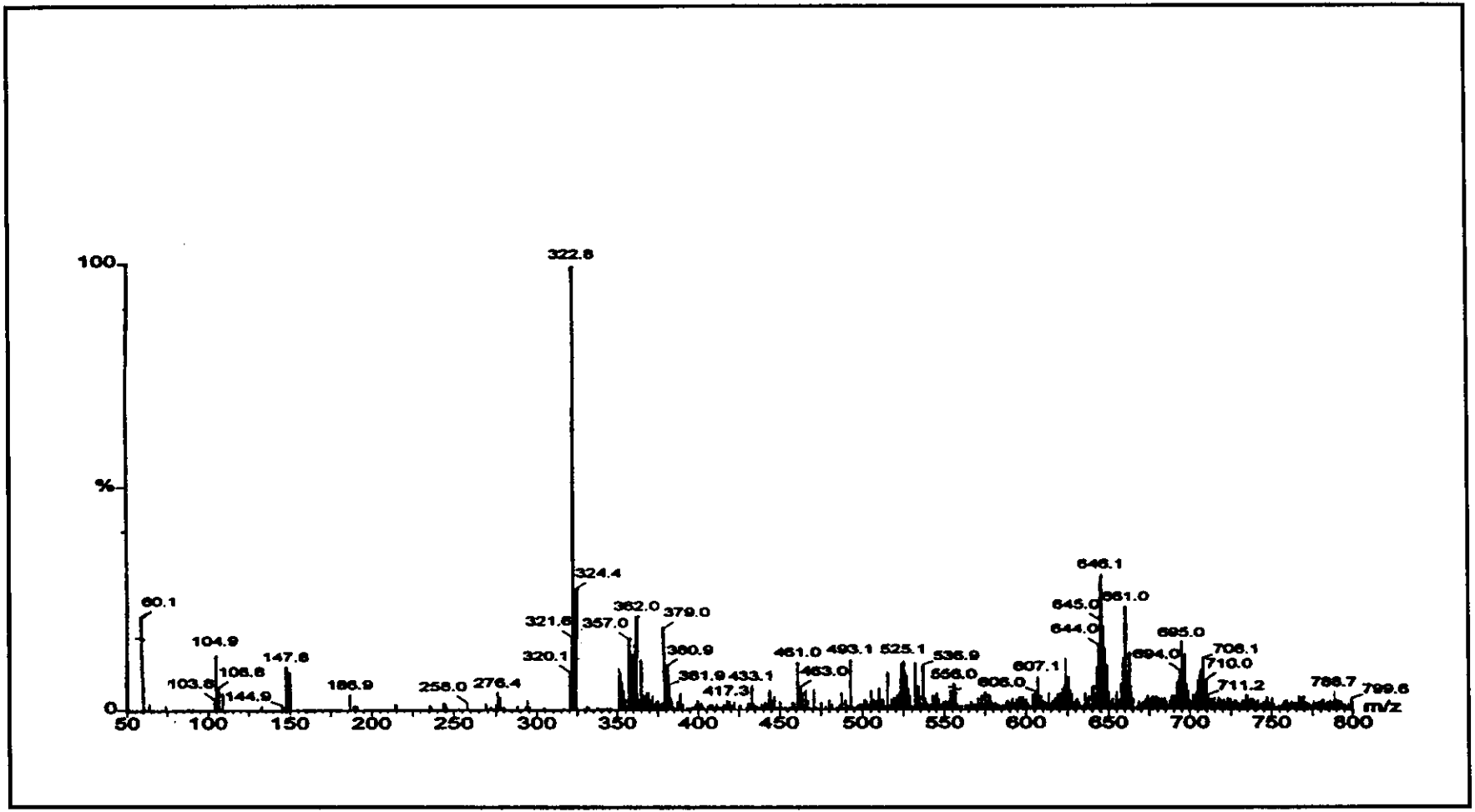

Figure 32 Electrospray mass spectrum of $[Ru(phen)_2azpy](BF_4)_2$.

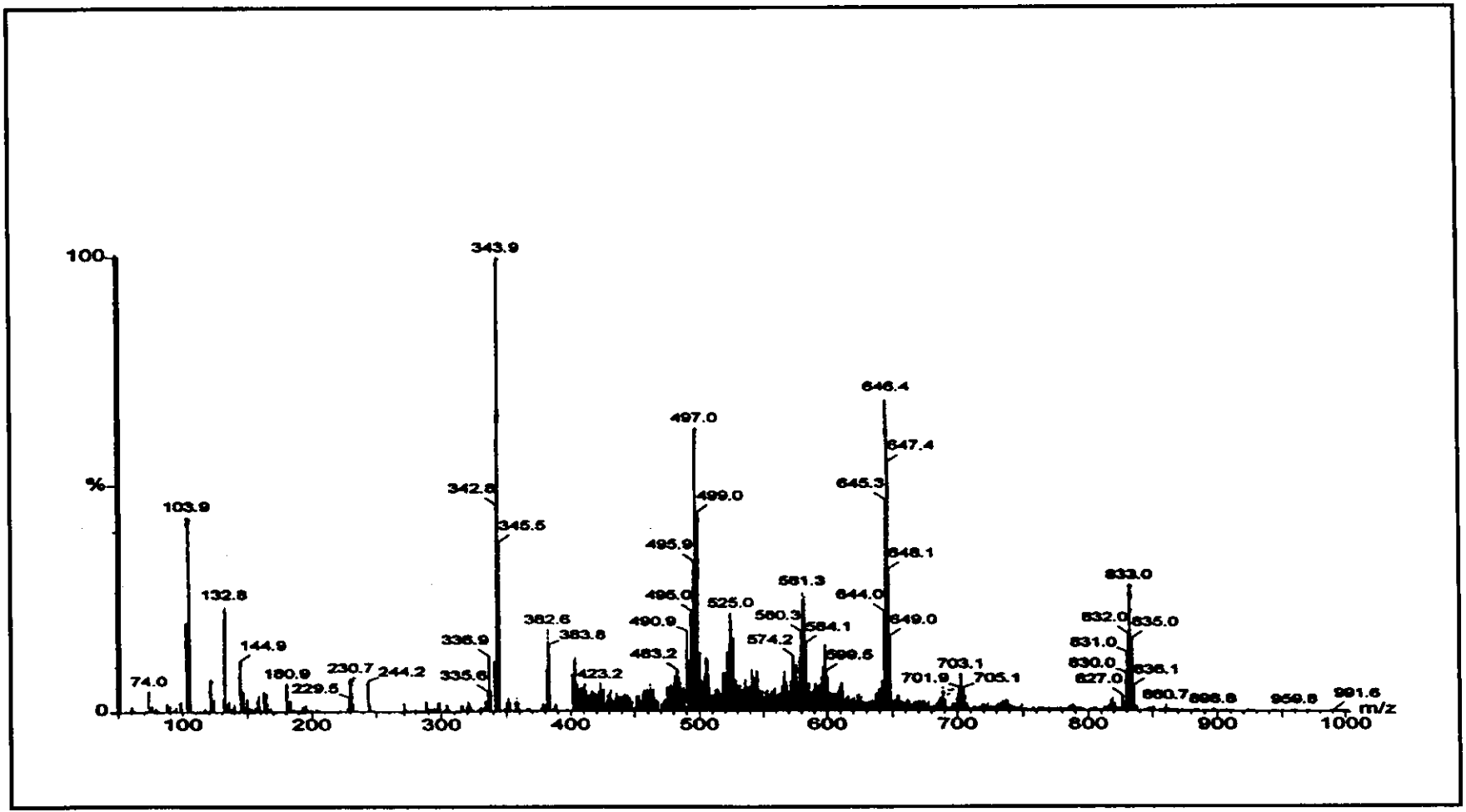

Figure 33 Electrospray mass spectrum of $[Ru(phen)_2dmazpy](PF_6)_2$.

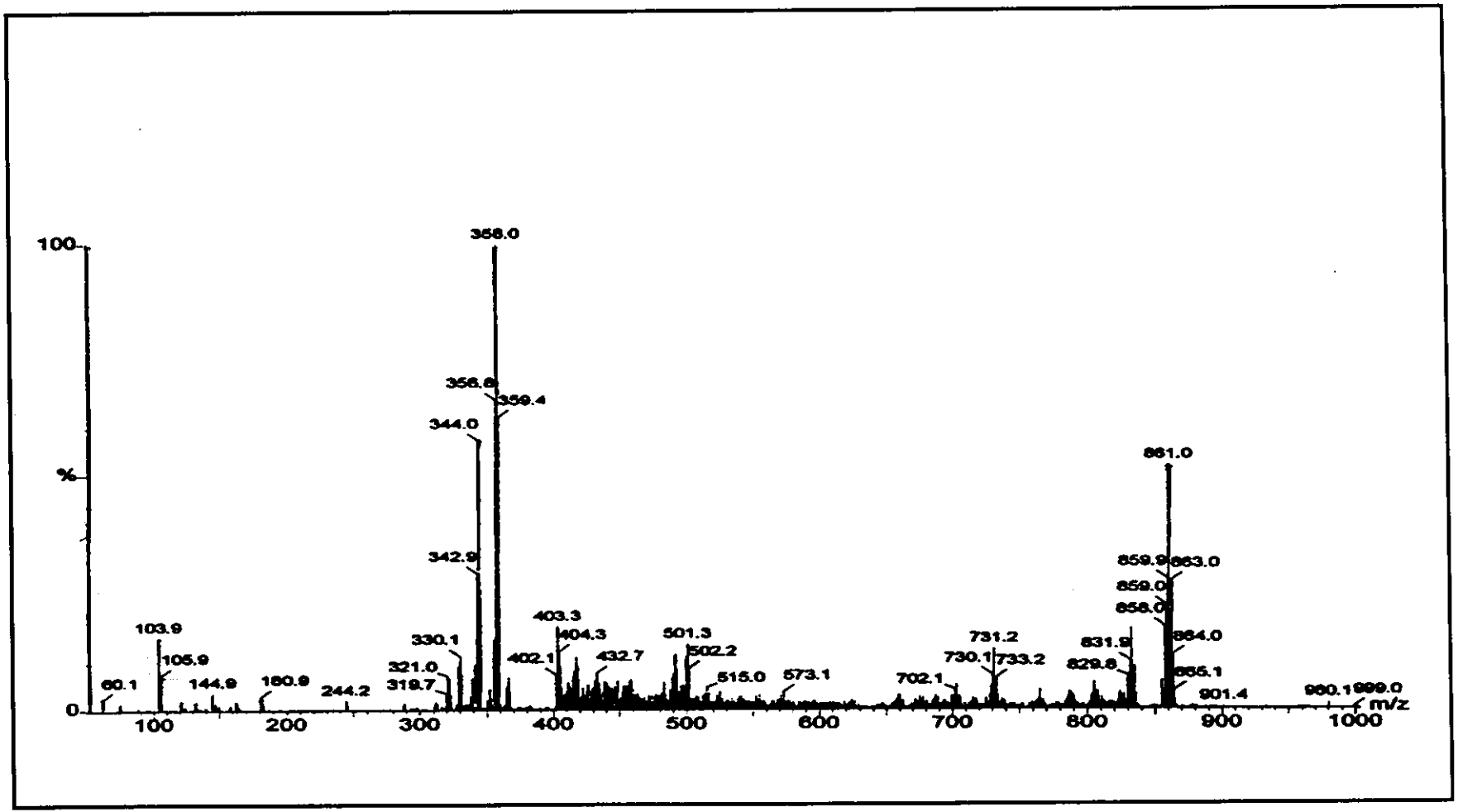

Figure 34 Electrospray mass spectrum of $[Ru(phen)_2deazpy](PF_6)_2$.

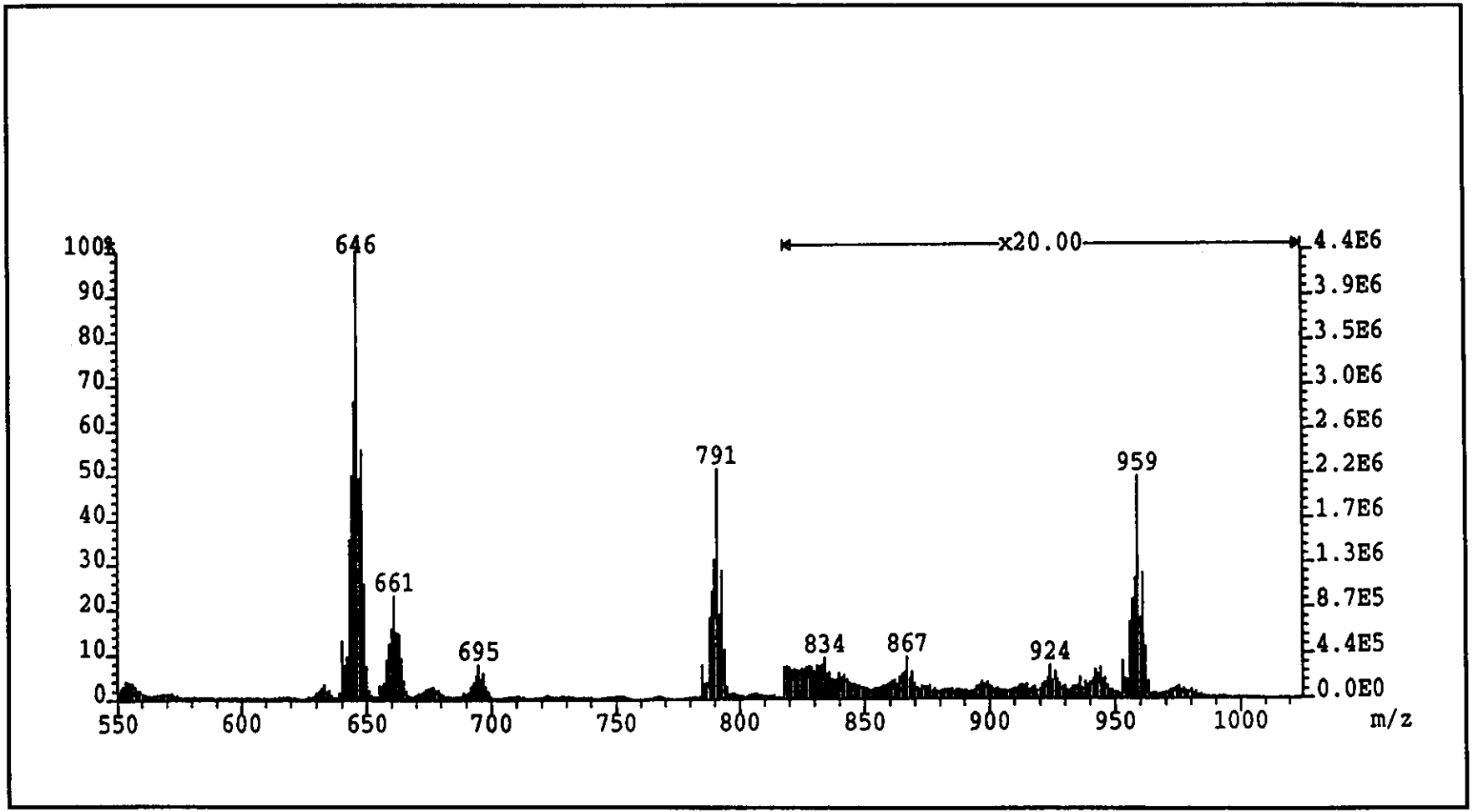

Figure 35 FAB mass spectrum of $[Ru(phen)_2azpym](PF_6)_2$.

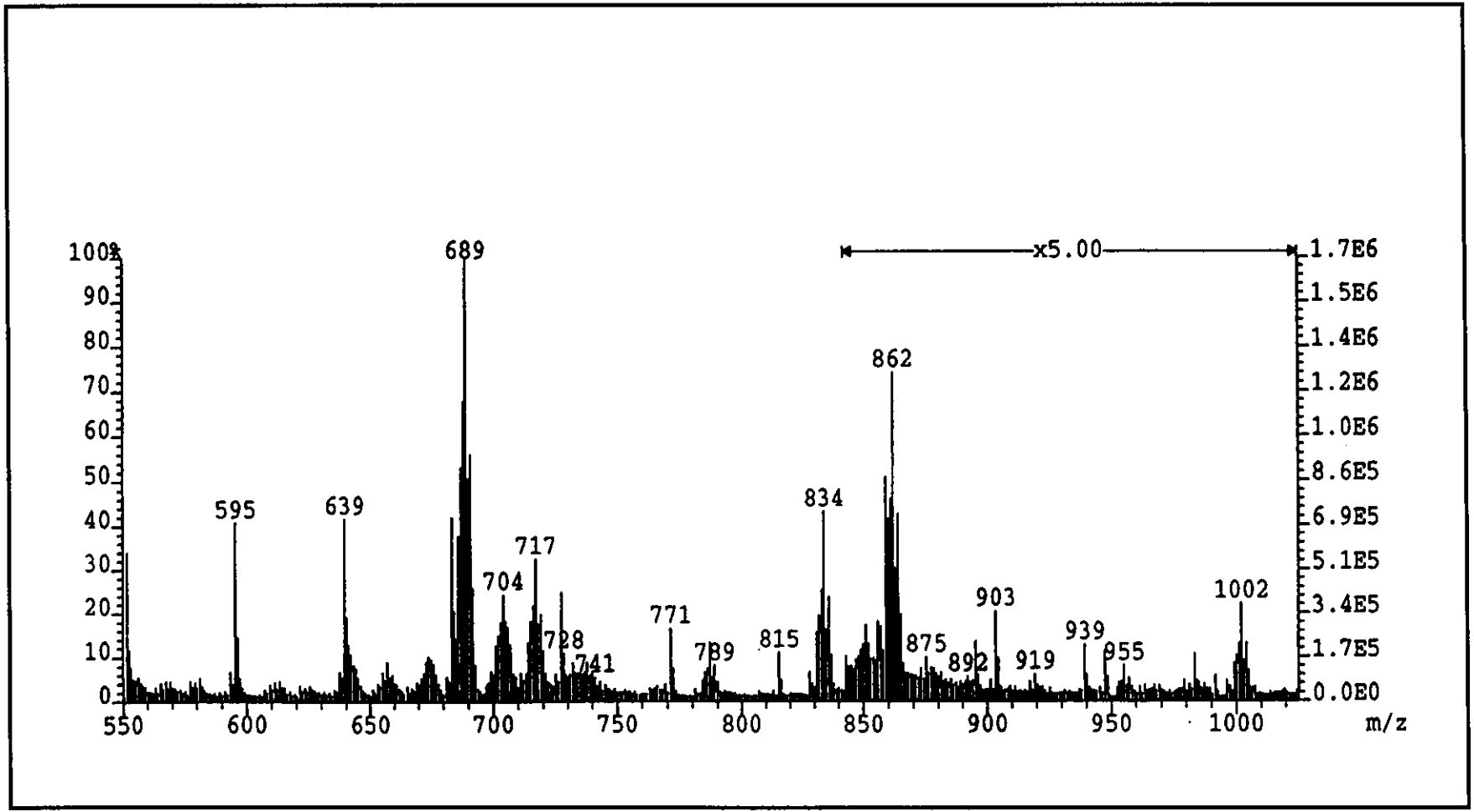

Figure 36 FAB mass spectrum of $[Ru(phen)_2deazpym](PF_6)_2$.

3.5.3 Infrared spectroscopy

The Infrared spectra of $[Ru(phen)_2L]^{2+}$ complexes, where L = phen, azpy, dmazpy, deazpy, azpym and deazpym in the range 1800-370 cm^{-1}. It can be used to give information about ligands coordinated to the ruthenium center. The infrared spectra of complexes are shown in Figure 37 to 42. The summaries of the infrared spectroscopic data are listed in Table 22.

Table 22 Infrared spectroscopic data of the $[Ru(phen)_2L]^{2+}$ complexes, where L = phen, azpy, dmazpy, deazpy, azpym and deazpym

Vibration modes	Frequencies (cm^{-1}) of $[Ru(phen)_2L]^{2+}$ (L = ligand in below)					
	phen	azpy	dmazpy	deazpy	azpym	deazpym
C=N	1599(m)	1600(m)	1596(s)	1593(s)	1584(s)	1595(s)
C=C	1424(s)	1514(m)	1523(m)	1515(w)	1546(m)	1594(w)
N=N	-	1304(s)	1294(s)	1293(s)	1300(s)	1260(s)
C-H bending of para disubstituted benzene	-	-	741(s)	721(s)	-	721(s)

s = strong, m = medium, w = weak

In general, characteristic peaks of all complexes were sharp peak of C=N stretching modes which were observed at frequencies in the range 1600-1500 cm^{-1}. The N=N (azo) stretching modes in complexes occurred in the spectral region 1400-

300 cm^{-1}. The N=N (azo) stretching modes in complexes were shifted to lower frequencies from free ligands.

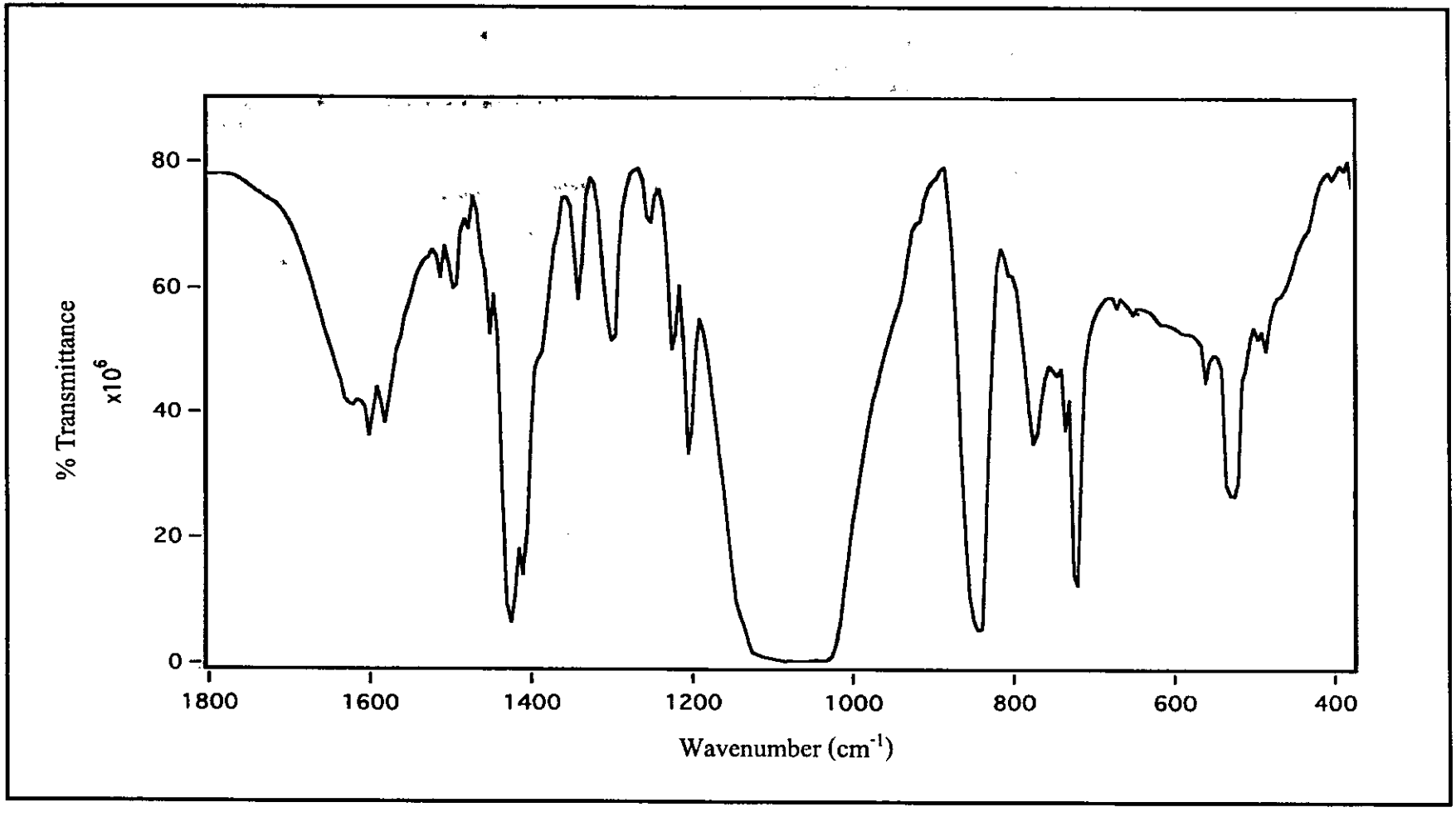

Figure 37 IR spectrum of $[Ru(phen)_3](BF_4)_2$.

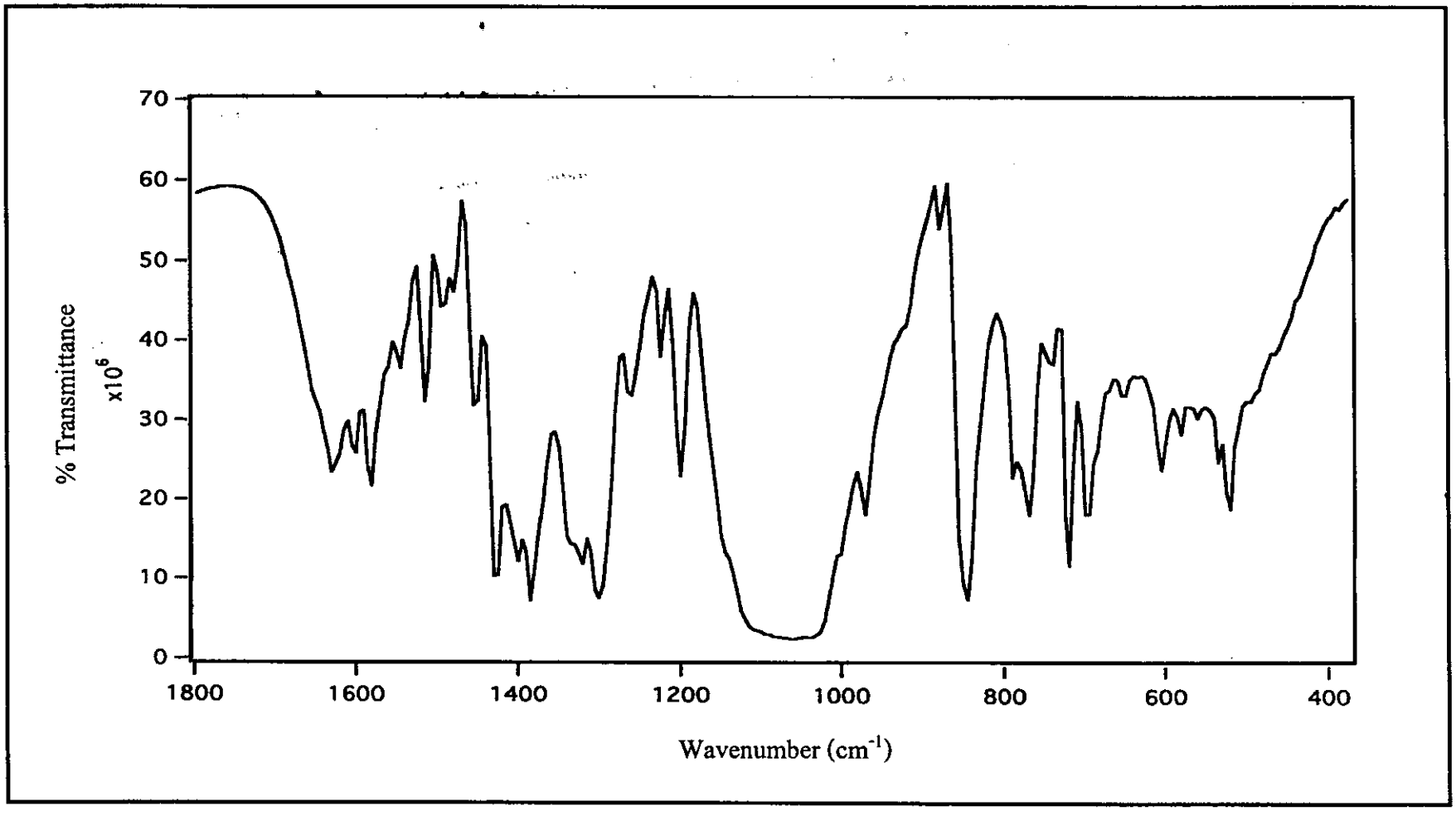

Figure 38 IR spectrum of $[Ru(phen)_2azpy](BF_4)_2$.

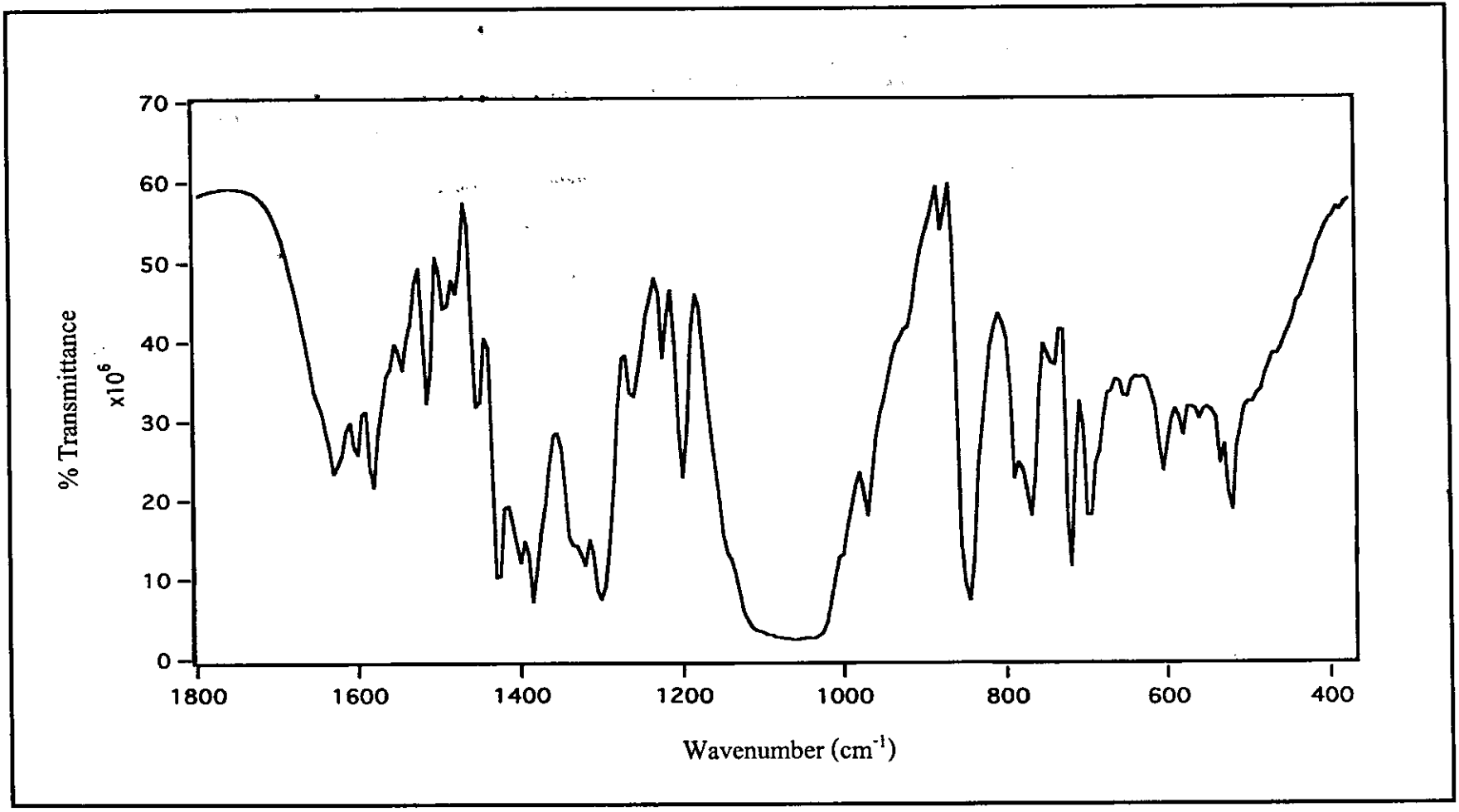

Figure 38 IR spectrum of $[Ru(phen)_2azpy](BF_4)_2$.

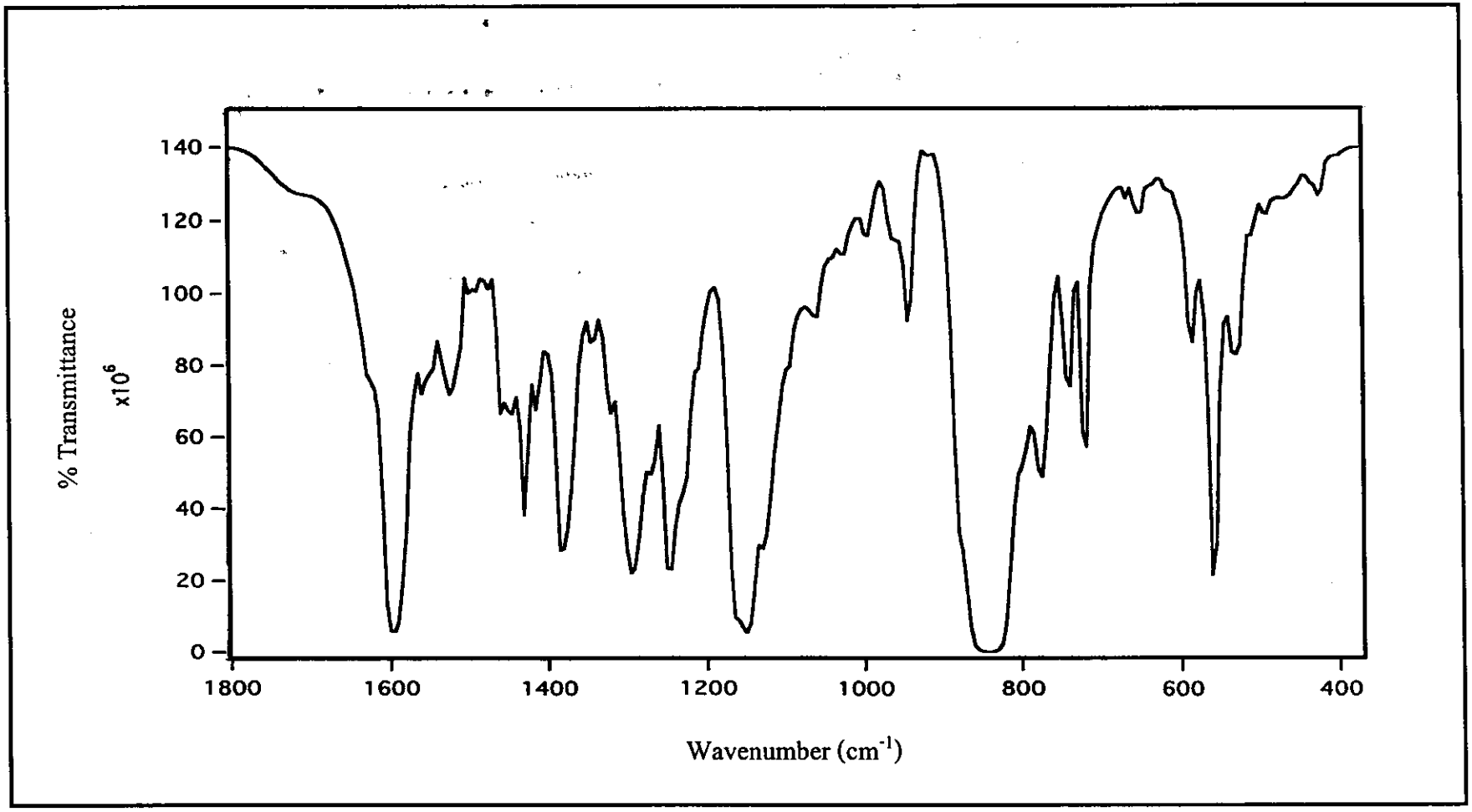

Figure 39 IR spectrum of $[Ru(phen)_2dmazpy](PF_6)_2$.

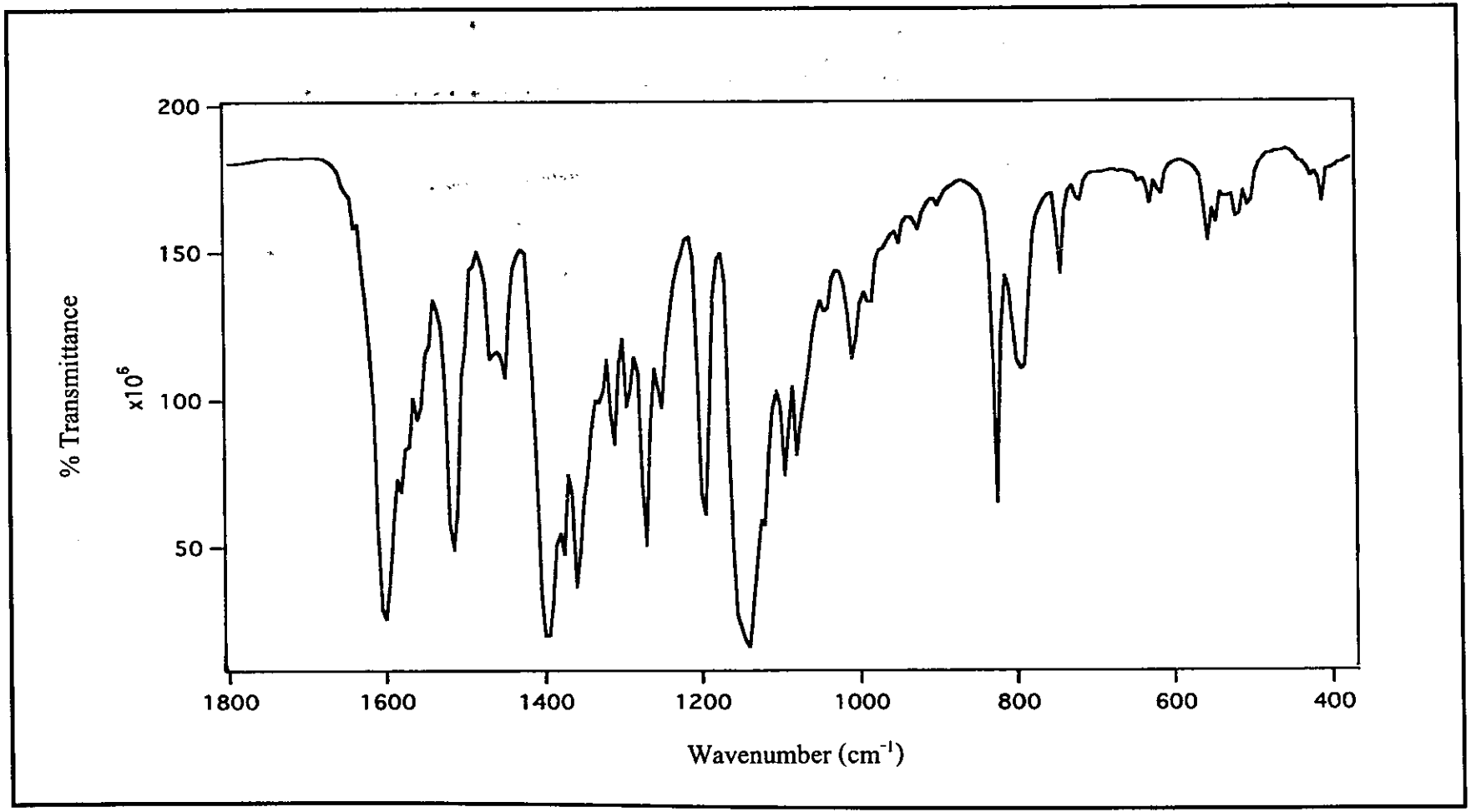

Figure 40 IR spectrum of $[Ru(phen)_2deazpy](PF_6)_2$.

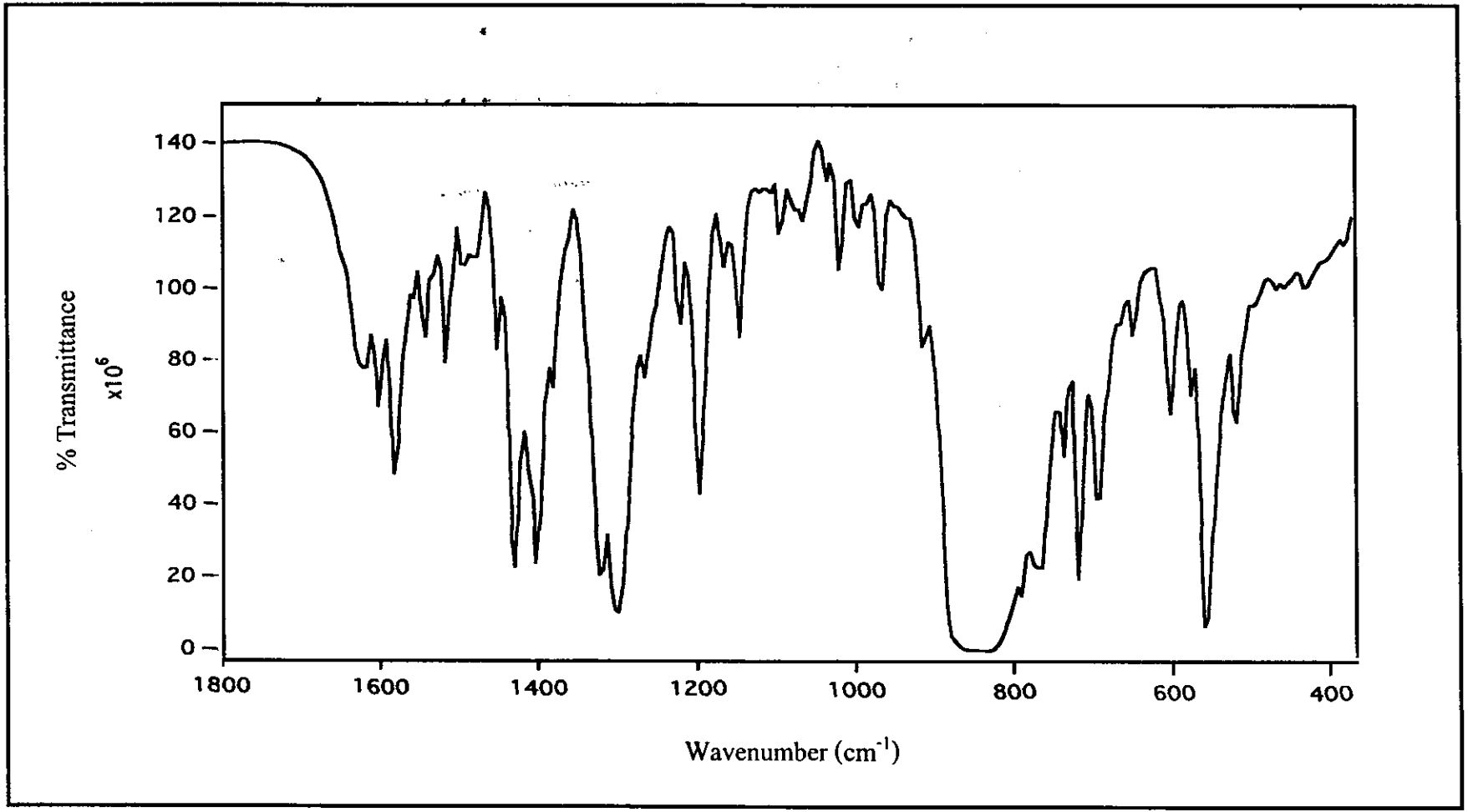

Figure 41 IR spectrum of $[Ru(phen)_2azpym](PF_6)_2$.

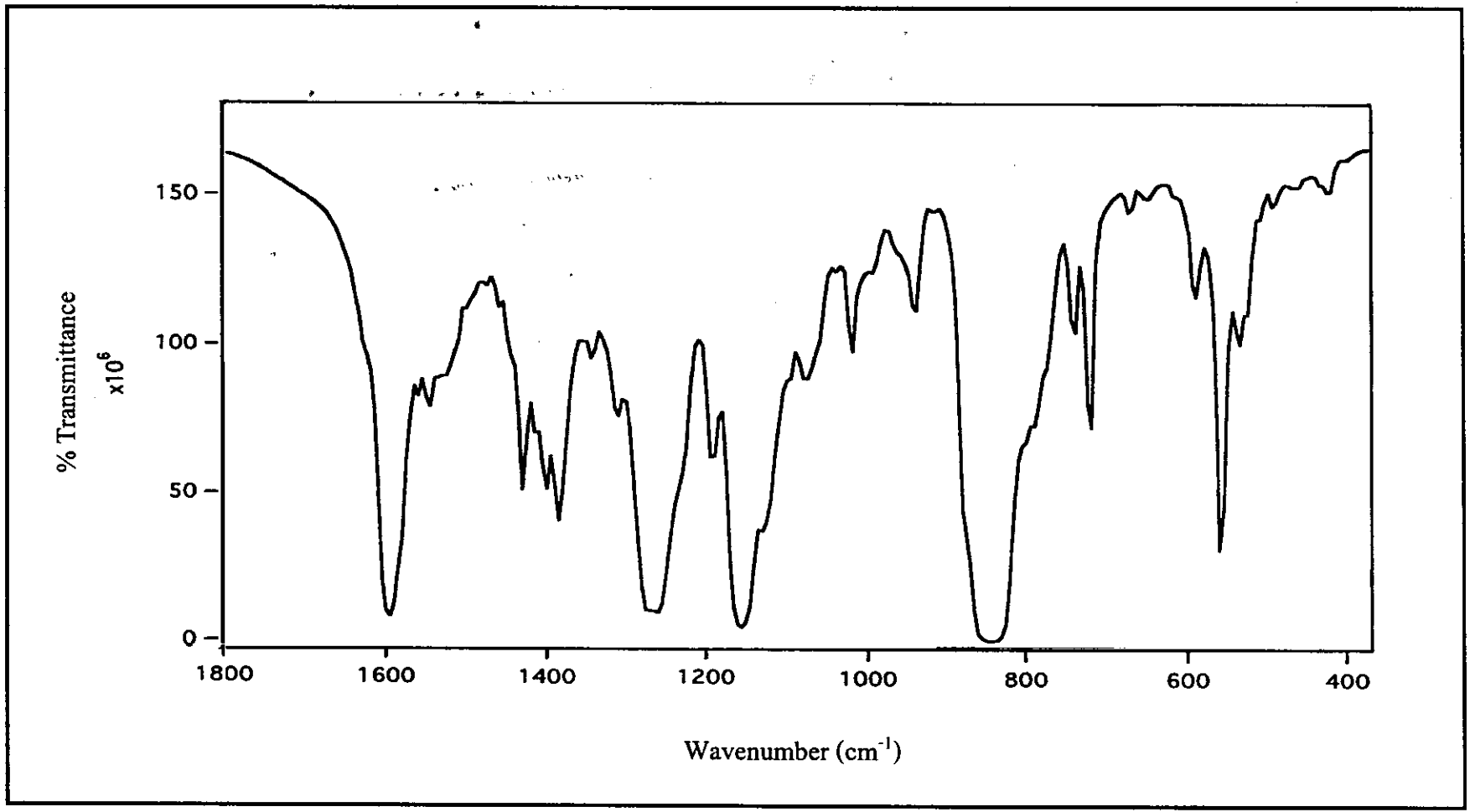

Figure 42 IR spectrum of $[Ru(phen)_2deazpym](PF_6)_2$.

3.5.4 UV-Visible absorption spectroscopy

The UV-Visible absorption spectra of $[Ru(phen)_2L]^{2+}$ complexes, where L = phen, azpy, dmazpy, deazpy, azpym and deazpym in acetronitrile solutions are shown in Figure 43 to 48. Electronic spectra of those complexes were recorded in five solvents; dimethyl sulfoxide (DMSO), acetronitrile (CH_3CN), acetone (CH_3COCH_3), ethanol (EtOH) and dichloromethane (CH_2Cl_2) which are listed in Table 23.

The absorption spectra of complexes were recorded in both ultraviolet region (200-400 nm) and visible region (400-800 nm). The intense bands in UV region belonged to the electronic transitions in phen and other ligand. In the visible region, each complex was shown intense bands, which referred to metal-to-ligand charge transfer (MLCT).

Table 23 UV-Visible absorption spectroscopic data of complexes

Complexes	λ_{max} nm,($\varepsilon^a X10^{-4} M^{-1}cm^{-1}$)				
	DMSO	CH_3CN	CH_3COCH_3	EtOH	CH_2Cl_2
$[Ru(phen)_3]^{2+}$	450 (8.9)	264 (sh) 446 (1.0)	446 (8.9)	266 (sh) 446 (0.9)	266 (sh) 448 (9.6)
$[Ru(phen)_2\ azpy]^{2+}$	328 (2.0) 500 (0.8)	224 (6.3) 264 (6.2) 328 (2.1) 496 (0.9)	328 (2.3) 496 (0.9)	224 (5.7) 264 (5.7) 332 (1.9) 496 (0.8)	264 (6.1) 340 (1.9) 500 (0.9)

Table 23 (continued)

Complexes	λ_{max} nm,(ε^{a}X10^{-4} M^{-1}cm^{-1})				
	DMSO	CH_3CN	CH_3COCH_3	EtOH	CH_2Cl_2
$[Ru(phen)_2dmazpy]^{2+}$	369 (1.4) 509 (2.5) 588 (2.9)	220 (6.8) 262 (8.1) 364 (1.1) 502 (2.3) 577 (2.7)	367 (1.0) 503 (2.2) 581 (2.6)	220 (6.3) 263 (7.6) 367 (1.2) 504 (2.3) 583 (3.1)	264 (9.3) 369 (1.1) 506 (2.3) 590 (3.2)
$[Ru(phen)_2$ deazpy$]^{2+}$	368 (1.3) 510 (2.3) 594 (3.1)	220 (7.2) 262 (8.3) 365 (1.3) 505 (2.4) 587 (3.2)	367 (1.2) 505 (2.3) 588 (3.1)	222 (6.9) 263 (7.6) 367 (1.2) 504 (2.3) 583 (3.1)	264 (9.9) 369 (1.3) 509 (2.2) 599 (3.9)
$[Ru(phen)_2azpym]^{2+}$	334 (2.2) 496 (0.8)	226 (5.9) 262 (5.6) 334 (1.9) 494 (7.4)	338 (2.8) 494 (6.9)	226 (5.7) 264 (5.7) 334 (1.9) 494 (6.8)	264 (5.8) 338 (1.9) 498 (0.7)
$[Ru(phen)_2deazpym]^{2+}$	378 (1.2) 510 (1.3) 623 (2.3)	222 (sh) 266 (23) 379 (1.2) 505 (1.3) 616 (2.5)	379 (0.6) 505 (0.6) 614 (1.6)	224 (sh) 266 (11) 380 (1.2) 507 (1.3) 619 (2.5)	266 (10) 380 (1.4) 507 (1.3) 616 (2.7)

[a]Molar Extinction coefficient

sh = shoulder

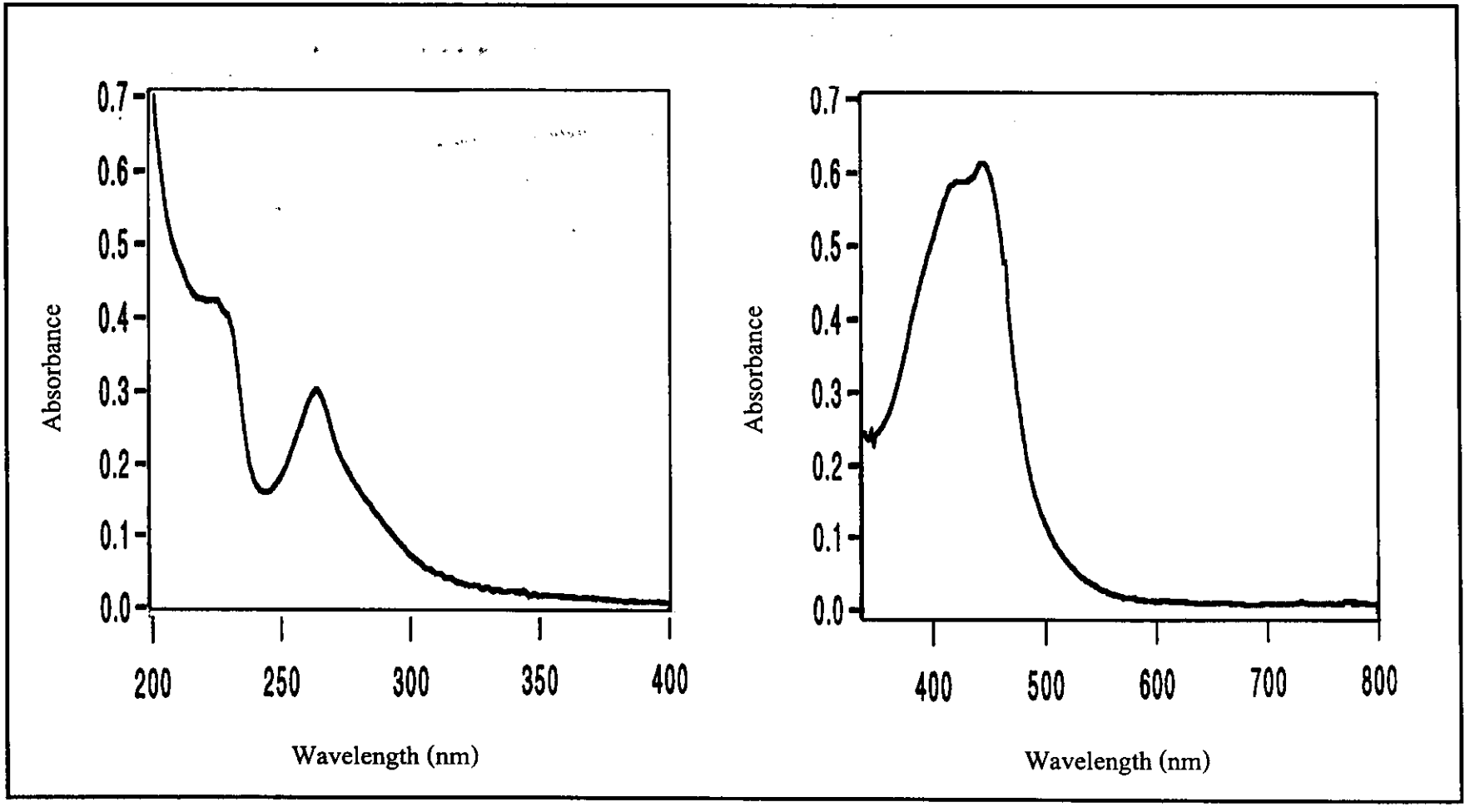

Figure 43 UV-Visible absorption spectrum of $[Ru(phen)_3](BF_4)_2$ in CH_3CN.

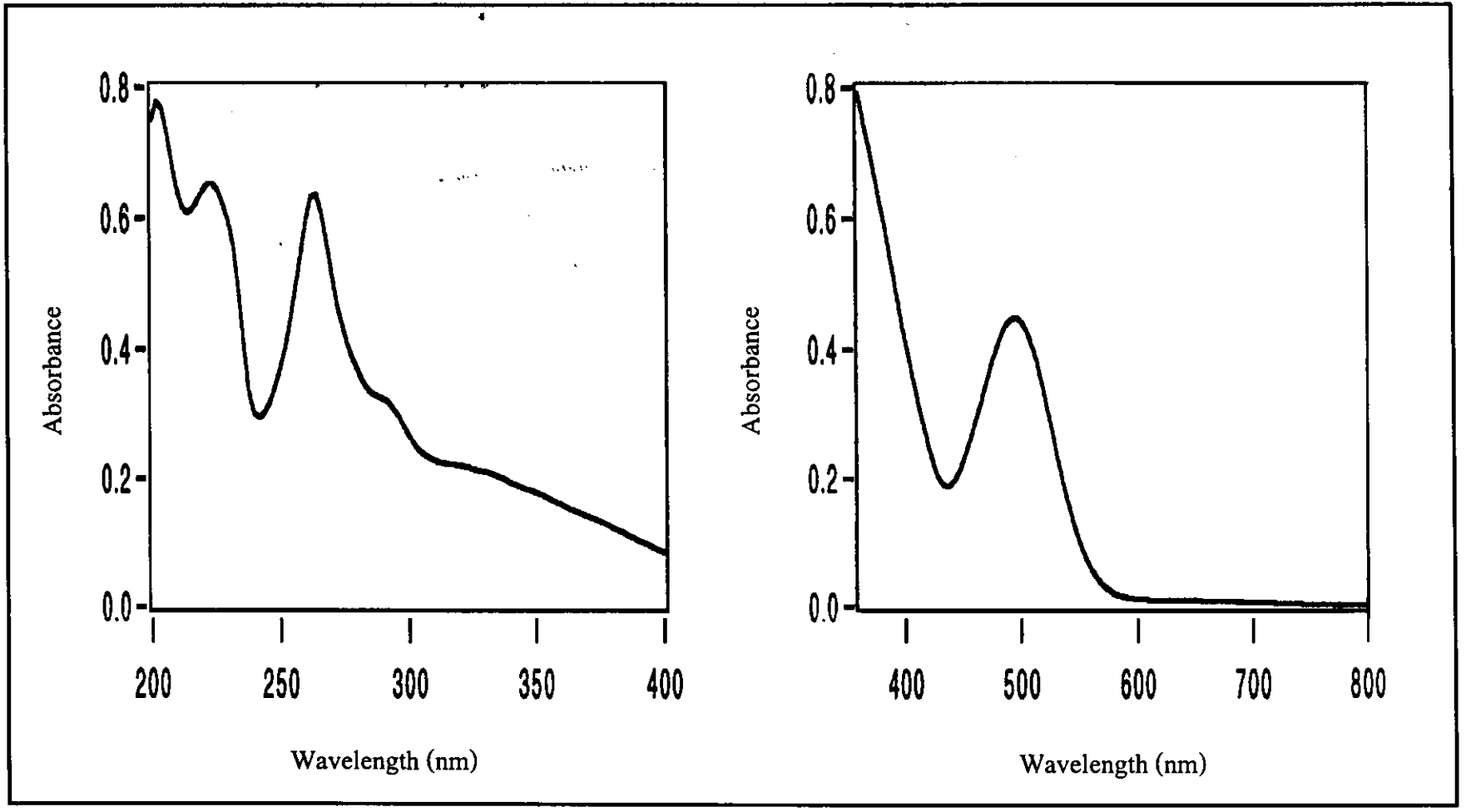

Figure 44 UV-Visible absorption spectrum of $[Ru(phen)_2azpy](BF_4)_2$ in CH_3CN.

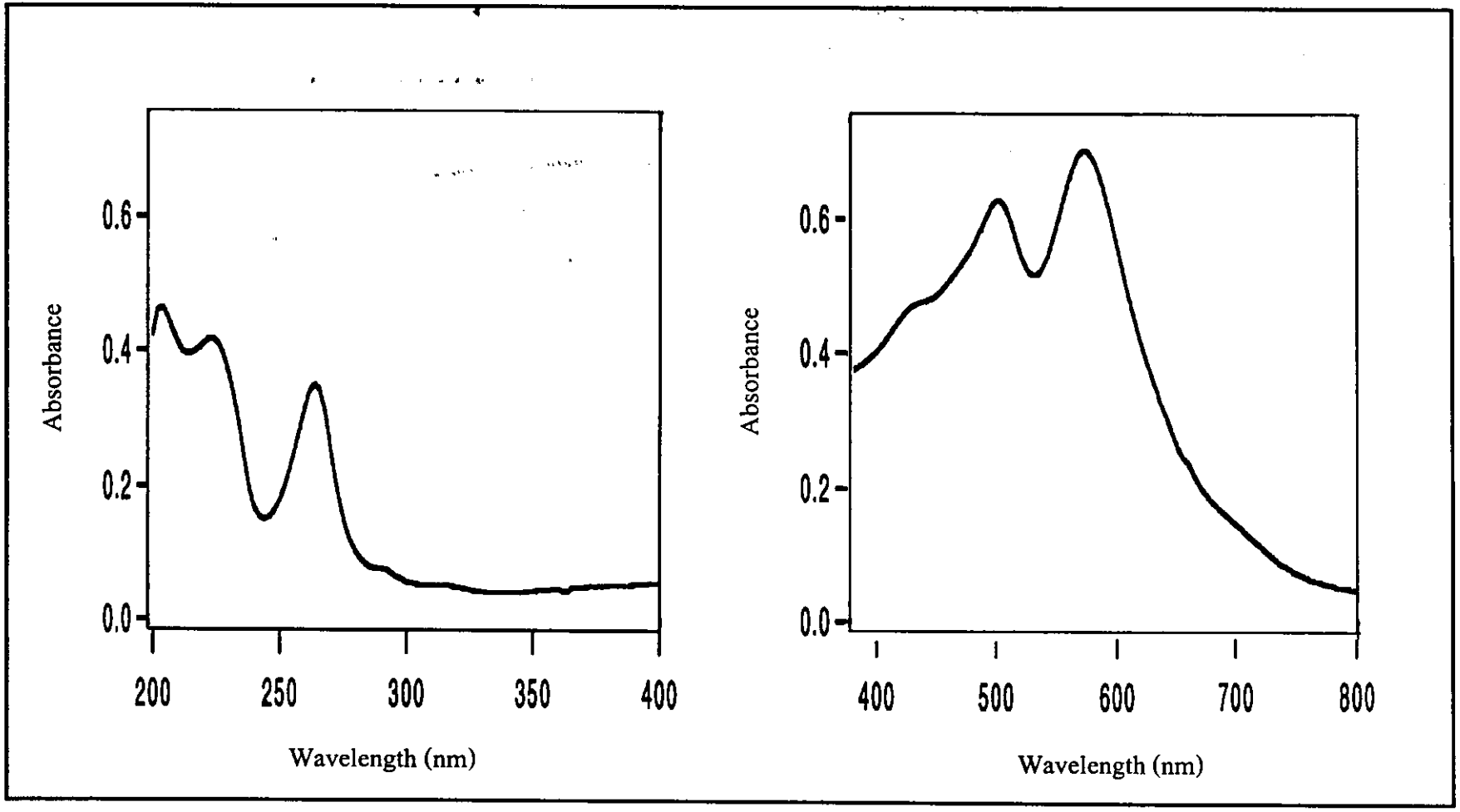

Figure 45 UV-Visible absorption spectrum of $[Ru(phen)_2dmazpy](PF_6)_2$ in CH_3CN.

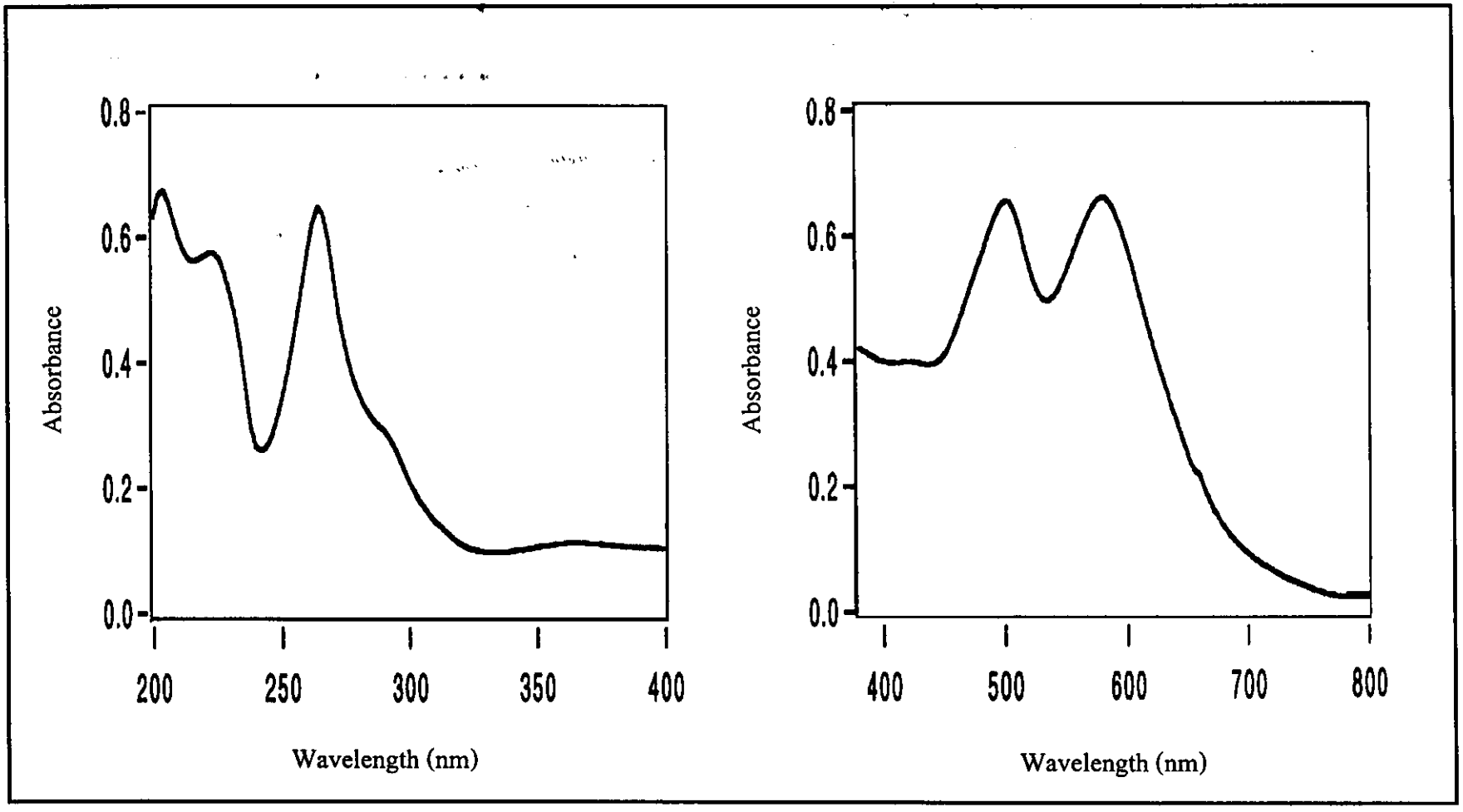

Figure 46 UV-Visible absorption spectrum of $[Ru(phen)_2deazpy](PF_6)_2$ in CH_3CN.

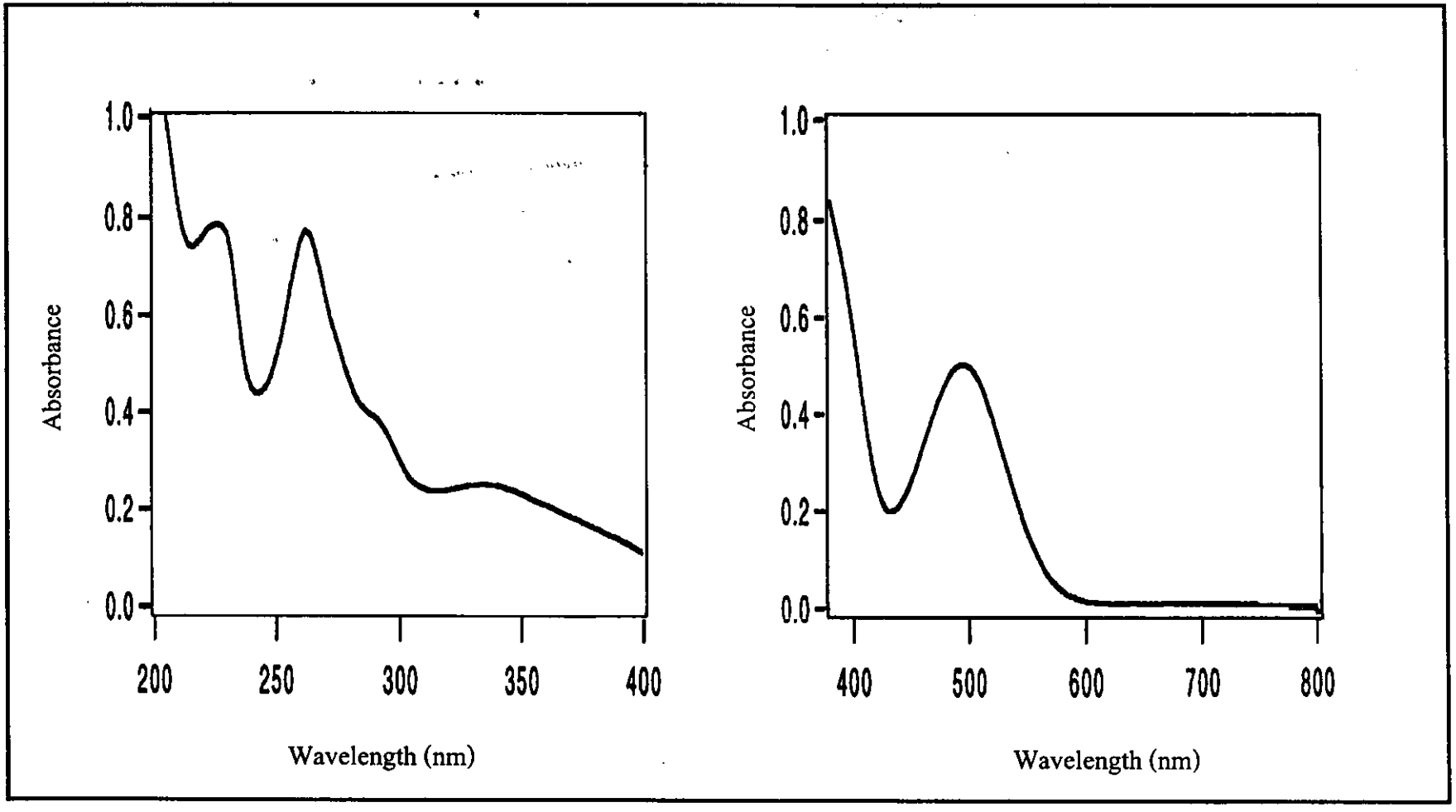

Figure 47 UV-Visible absorption spectrum of $[Ru(phen)_2azpym](PF_6)_2$ in CH_3CN.

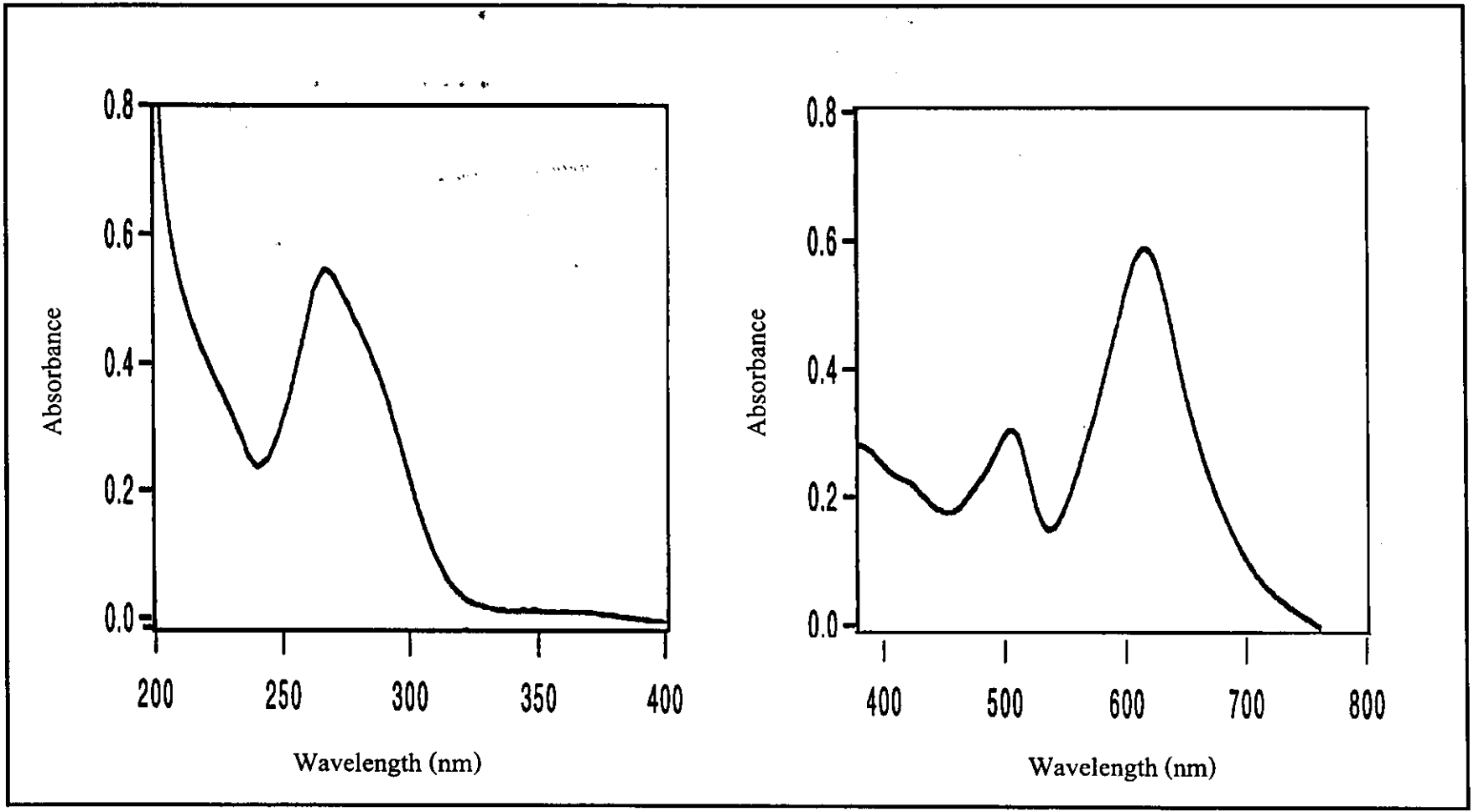

Figure 48 UV-Visible absorption spectrum of $[Ru(phen)_2deazpym](PF_6)_2$ in CH_3CN.

3.5.5 Nuclear magnetic resonance spectroscopy

Nuclear magnetic resonance spectroscopy is an important technique to determine molecular structure because the different protons in the molecular structure showed the different chemical shifts. In this work, the structure of $[Ru(phen)_2L](PF_6)_2$ complexes (L = azpy, dmazpy, deazpy, azpym and deazpym) was explained by using 1D and 2D NMR spectroscopic techniques.

In $[Ru(phen)_2L](PF_6)_2$ complexes, there were many protons which were close location. Thus, the positions of protons were determined from ^1H-^1H COSY spectra. The ^1H-^1H COSY spectra could be described as coupling in each proton. The chemical shifts (δ) were reported in part per million (ppm) and *J*-couplings were reported in hertz (Hz). The tetramethylsilane (TMS, $(CH_3)_4Si$) solution was used as an internal standard. The aromatic protons in each ligand exhibited complex multiplets in the region 9.4-6.0 ppm and the substituent groups appear in range 3.5-1.0 ppm in the ^1H NMR spectra of compounds. The NMR spectroscopic data of each complexes are given in Table 24-29 (Figure 49 to 60).

Table 24 ^{1}H NMR spectroscopic data of $[Ru(phen)_3](BF_4)_2$

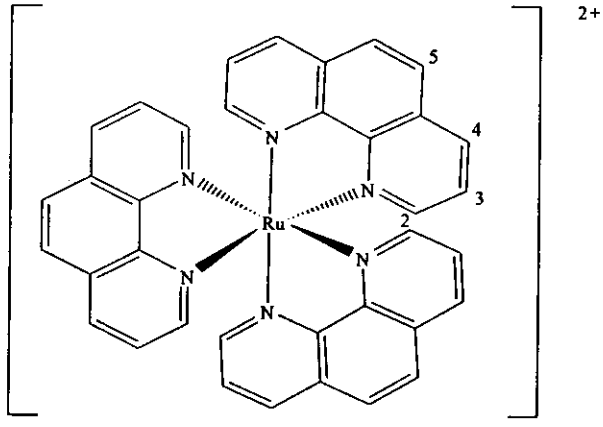

H-position	δ (ppm)	J-coupling (Hz)	Amount of H
4	8.79 (dd)	8.0, 1.5	6
5	8.42 (s)	-	6
2	8.39 (dd)	5.0, 1.5	6
3	7.81 (dd)	8.0, 5.0	6

s = singlet and dd = doublet of doublet

The ^{1}H NMR spectroscopic data of $[Ru(phen)_3](BF_4)_2$ has four group of protons, which were equivalent proton. The H4 appeared at the lowest field. In contrast, the H3 occurred at the highest field. The H5 did not interact with another proton, thus it was shown singlet peak. The H2 was located next to nitrogen atom and the signal was also doublet peaks (J = 5.0, 1.5 Hz).

Table 25 ^{1}H NMR spectroscopic data of $[Ru(phen)_2azpy](BF_4)_2$

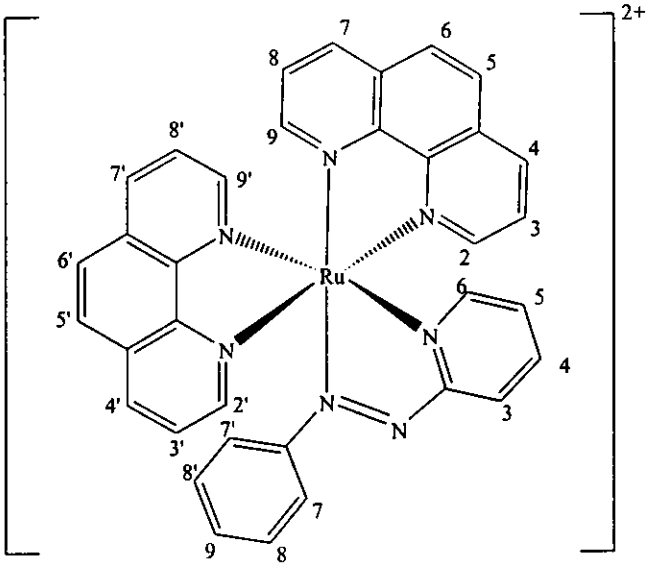

H-position	δ (ppm)	J-coupling (Hz)	Amount of H
3 (azpy)	9.02 (ddd)	8.0, 1.0, 1.0	1
4	9.01 (dd)	8.5, 1.0	1
4'	8.99 (dd)	8.5, 1.0	1
2	8.95 (dd)	5.0, 1.0	1
7	8.91 (dd)	8.0, 1.5	1
7'	8.65 (dd)	8.0, 1.5	1
5	8.51 (d)	9.0	1
6	8.48 (d)	9.0	1
4 (azpy)	8.41 (td)	8.0, 1.5	1
5'	8.34 (d)	9.0	1
9	8.26 (dd)	5.0, 1.5	1

Table 25 (continued)

H-position	δ (ppm)	J-coupling (Hz)	Amount of H
2'	8.24 (dd)	5.0, 1.5	1
6'	8.24 (dd)	9.0	1
9'	8.22 (dd)	6.5, 2.0	1
6 (azpy)	8.18 (dd)	6.0, 1.0	1
3	8.13 (dd)	8.5, 5.0	1
3'	8.10 (dd)	8.5, 5.0	1
8	7.86 (dd)	8.0, 5.5	1
5 (azpy)	7.71 (dd)	6.5, 2.0	1
8'	7.69 (dd)	8.5, 5.5	1
9 (azpy)	7.17 (dt)	7.5, 1.0	1
7, 7' (azpy)	7.10 (dd)	8.5, 1.0	2
8, 8' (azpy)	7.01 (dd)	9.0, 2.0	2

d = doublet, s = singlet, dd = doublet of doublet, dt = doublet of triplet, td = triplet of doublet and ddd = doublet of doublet of doublet

Table 26 ^{1}H NMR spectroscopic data of $[Ru(phen)_2dmazpy](PF_6)_2$

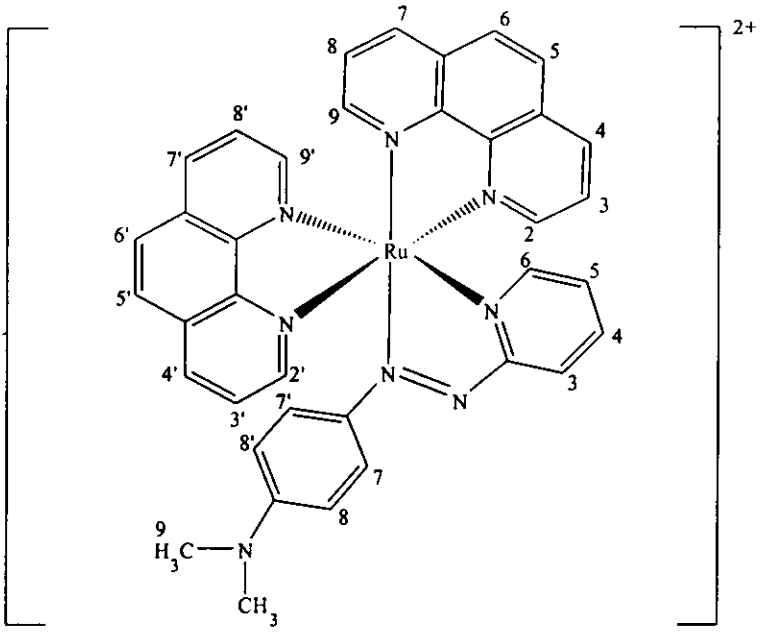

H-position	δ (ppm)	J-coupling (Hz)	Amount of H
4	8.96 (dd)	8, 1.5	1
4'	8.94 (dd)	9, 1.5	1
2	8.85 (dd)	5, 1.5	1
7	8.83 (dd)	8, 1.5	1
7'	8.75 (dd)	8, 1.5	1
3 (azpy)	8.72 (ddd)	8, 1.5, 1	1
5	8.48 (d)	8.5	1
6	8.44 (d)	9	1
5'	8.38 (d)	8.5	1
6'	8.32 (d)	9.0	1
9'	8.27 (dd)	5, 1.5	1

Table 26 (continued)

H-position	δ (ppm)	J-coupling (Hz)	Amount of H
4 (azpy)	8.24 (ddd)	8.0, 7.5, 2.0	1
2'	8.13 (dd)	5.0, 1.5	1
3	8.10 (dd)	8.5, 5.0	1
9	8.09 (dd)	5.0, 1.0	1
3'	8.05 (dd)	8.5, 5.0	1
6 (azpy)	7.93 (dd)	5.0, 1.5, 1.0	1
8	7.78 (dd)	8.0, 5.5	1
8'	7.73 (dd)	8.0, 5.5	1
3 (azpy)	7.43 (ddd)	6.0, 7.5, 1.5	1
7, 7' (azpy)	7.39 (d)	9.5	2
8, 8' (azpy)	6.36 (d)	7.5	2
9 (azpy)	2.97 (s)	-	6

d = doublet, s = singlet, dd = doublet of doublet and ddd = doublet of doublet of doublet,

Table 27 ^{1}H NMR spectroscopic data of $[Ru(phen)_2deazpy](PF_6)_2$

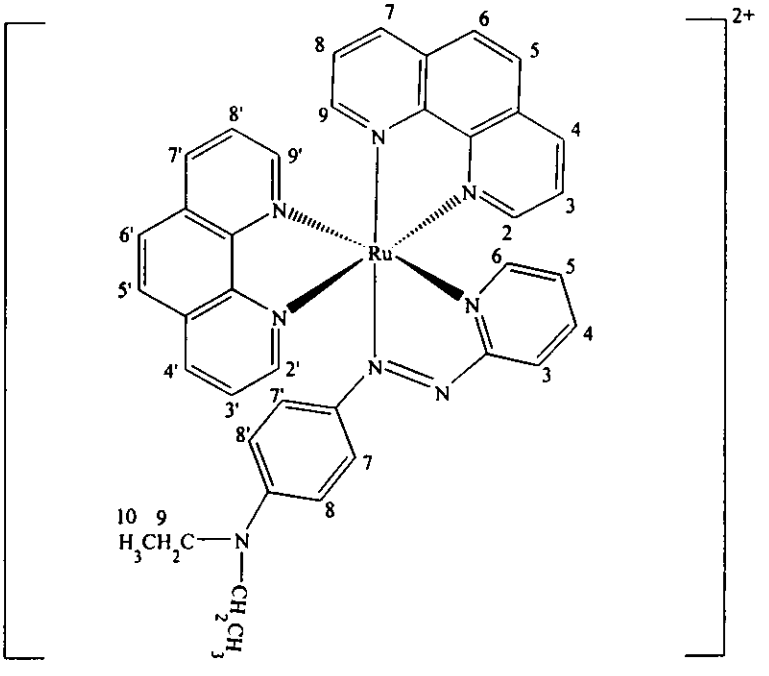

H-position	δ (ppm)	J-coupling (Hz)	Amount of H
4	8.97 (dd)	8.0, 1.5	1
4'	8.95 (dd)	8.0, 1.5	1
2	8.87 (dd)	5.0, 2.0	1
7	8.85 (dd)	8.0, 1.0	1
7'	8.75 (dd)	8.0, 1.0	1
3 (azpy)	8.69 (d)	8.0	1
5	8.49 (d)	9.0	1
6	8.45 (d)	9.0	1
5'	8.38 (d)	9.0	1
6'	8.33 (d)	9.0	1

Table 27 (continued)

H-position	δ (ppm)	J-coupling (Hz)	Amount of H
9'	8.28 (dd)	5.0, 1.5	1
4 (azpy)	8.24 (ddd)	8.0, 8.0, 1.5	1
2'	8.14 (dd)	7.0, 1.0	1
9	8.12 (dd)	5.0, 1.0	1
3	8.11 (dd)	8.0, 5.0	1
3'	8.06 (dd)	8.0, 5.0	1
6 (azpy)	7.91 (d)	5.0	1
8	7.81 (dd)	8.0, 5.0	1
8'	7.74 (dd)	8.0, 5.0	1
5 (azpy)	7.41 (dd)	6.0, 1.5	1
7 (azpy)	7.37 (d)	9.0	1
7' (azpy)	7.33 (d)	9.0	1
8 (azpy)	6.35 (d)	9.0	1
8' (azpy)	6.25 (d)	9.0	1
9 (azpy)	3.39 (q)	7.0	4
10 (azpy)	1.11	7.0	6

d = doublet, q = quartet, t = triplet, dd = doublet of doublet and ddd = doublet of doublet of doublet,

Table 28 ^{1}H NMR spectroscopic data of $[Ru(phen)_2azpym](PF_6)_2$

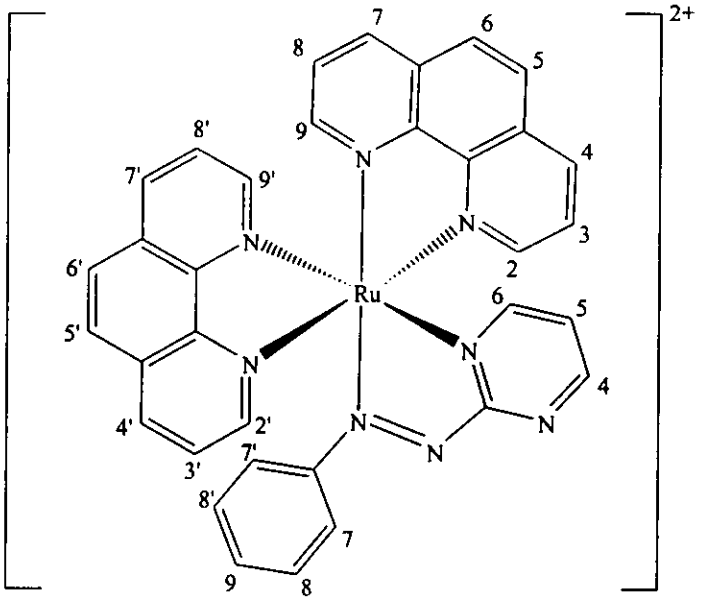

H-position	δ (ppm)	J-coupling (Hz)	Amount of H
4 (azpy)	9.31 (dd)	5.0, 2.0	1
4	9.03 (dd)	6.0, 1.5	1
4'	9.02 (dd)	6.0, 1.5	1
2	8.98 (dd)	5.0, 1.5	1
7	8.91 (dd)	8.5, 1.5	1
7'	8.66 (dd)	8.0, 1.5	1
6 (azpy)	8.57 (dd)	6.0, 2.0	1
5	8.51 (d)	9.0	1
6	8.48 (d)	9.0	1

Table 28 (continued)

H-position	δ (ppm)	J-coupling (Hz)	Amount of H
4 (azpy)	8.57 (dd)	6.0, 2.0	1
5'	8.51 (d)	9.0	1
6'	8.48 (d)	9.0	1
2'	8.39 (dd)	5.0, 1.5	1
5'	8.35 (d)	8.5	1
6'	8.23 (d)	9.0	1
9	8.22 (dd)	5.0, 1.5	1
9'	8.17 (dd)	5.5, 1.0	1
3	8.16 (dd)	9.0, 5.5	1
3'	8.11 (dd)	8.0, 5.5	1
8	7.85 (dd)	8.0, 5.5	1
8'	7.69 (dd)	8.0, 5.5	1
5 (azpy)	7.68 (dd)	6.0, 5.0	1
9 (azpy)	7.21 (ddt)	7.0, 7.0, 1.0	1
7, 7' (azpy)	7.13 (ddd)	8.0, 3.0, 2.0	2
8, 8' (azpy)	7.02 (ddt)	7.0, 7.0, 1.0	2

d = doublet, dd = doublet of doublet, ddd = doublet of doublet of doublet and ddt = doublet of doublet of triplet

Table 29 ^{1}H NMR spectroscopic data of $[Ru(phen)_2deazpym](PF_6)_2$

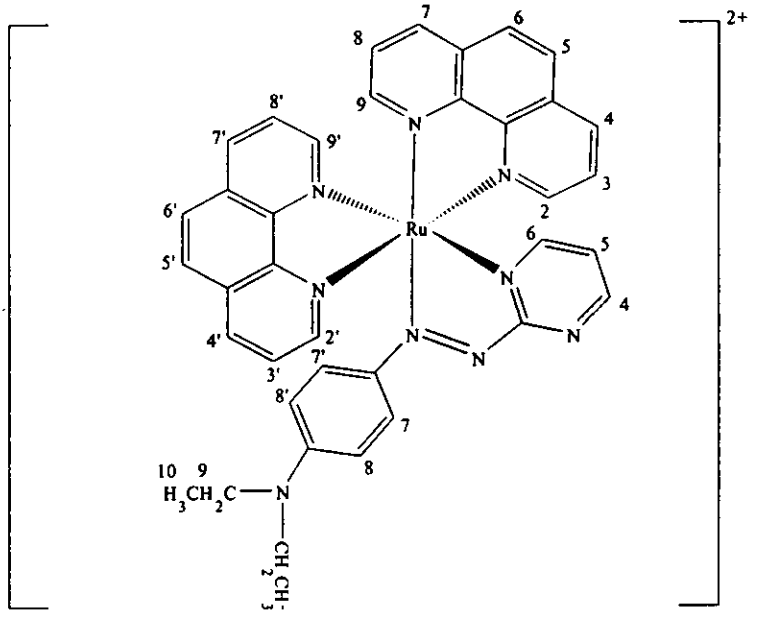

H-position	δ (ppm)	J-coupling (Hz)	Amount of H
4 (azpy)	9.11 (dd)	4.5, 2.0	1
4	8.98 (dd)	8.0, 1.5	1
4'	8.97 (dd)	8.0, 1.5	1
3	8.88 (dd)	9.0, 5.0	1
7	8.83 (dd)	8.0, 1.5	1
7'	8.79 (dd)	8.0, 1.5	1
5	8.48 (d)	9.0	1
6	8.44 (d)	9.5	1
5'	8.41 (d)	9.0	1
9'	8.40 (dd)	5.0, 1.5	1
6'	8.35 (d)	9.0	1

Table 29 (continued)

H-position	δ (ppm)	J-coupling (Hz)	Amount of H
2'	8.33 (dd)	5.0, 1.5	1
6 (azpy)	8.25 (d)	9.0	1
2	8.11 (dd)	5.0, 1.0	1
3'	8.08 (dd)	8.5, 5	1
9	8.05 (dd)	5.5, 1.5	1
8'	7.81 (dd)	8.0, 5.5	1
8	7.77 (dd)	8.0, 5.5	1
7 (azpy)	7.53 (d)	9.5	1
7' (azpy)	7.53 (d)	9.5	1
5 (azpy)	7.30 (dd)	6.0, 4.5	1
8 (azpy)	6.44 (d)	9.5	1
8' (azpy)	6.43 (d)	9.5	1
9 (azpy)	3.45 (q)	7.5	4
10 (azpy)	1.09 (t)	7.5	6

d = doublet, q = quartet, t = triplet, dd = doublet of doublet and ddd = doublet of doublet of doublet

These results of complexes had shown many resonances. In $[Ru(phen)_2L]^{2+}$, where L = azpy, azpym and deazpym complex, the proton on their ligands appeared at the low field than phen in each complex (9.02; H3 (azpy), 9.31; H4 (azpym) and 9.11; H4 (deazpym)), because azpy, azpym and deazpym ligands gave many electrons to metal. Electron densities of azpy, azpym and deazpym decreased, then their had

chemical shift at lowest field. The other complexes, the proton on phen ligand appeared at the low field than the third ligands (dmazpy and deazpy). Because of the properties of varying ligands and the effect of different stereochemistry. Electron densities of dmazpy and deazpy increased when compared with phen. The chemical shifts of phen appeared at lowest field (8.96; H4 and 8.97; H4, respectively).

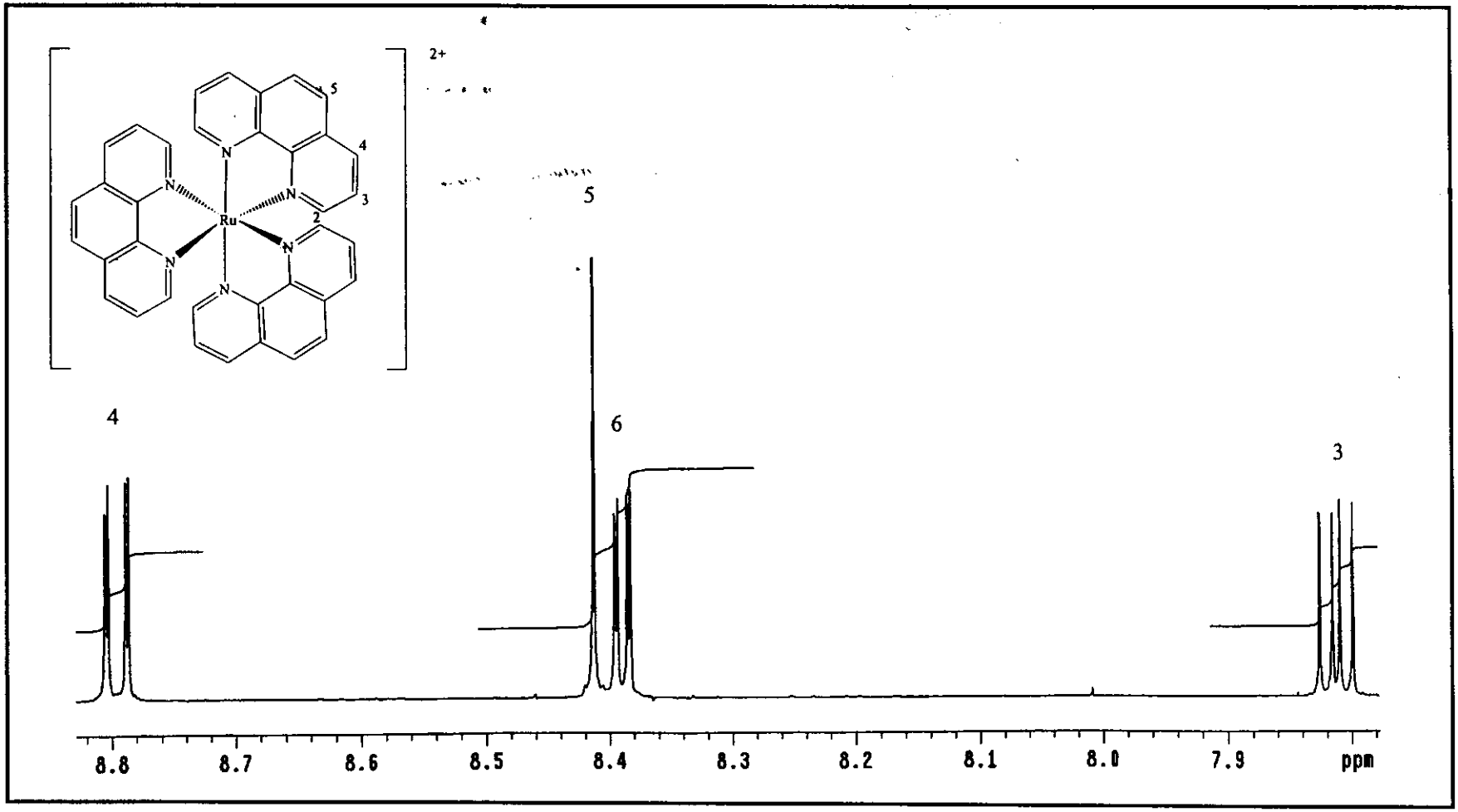

Figure 49 ^{1}H NMR spectrum of $[Ru(phen)_3](BF_4)_2$ in acetone-d_6

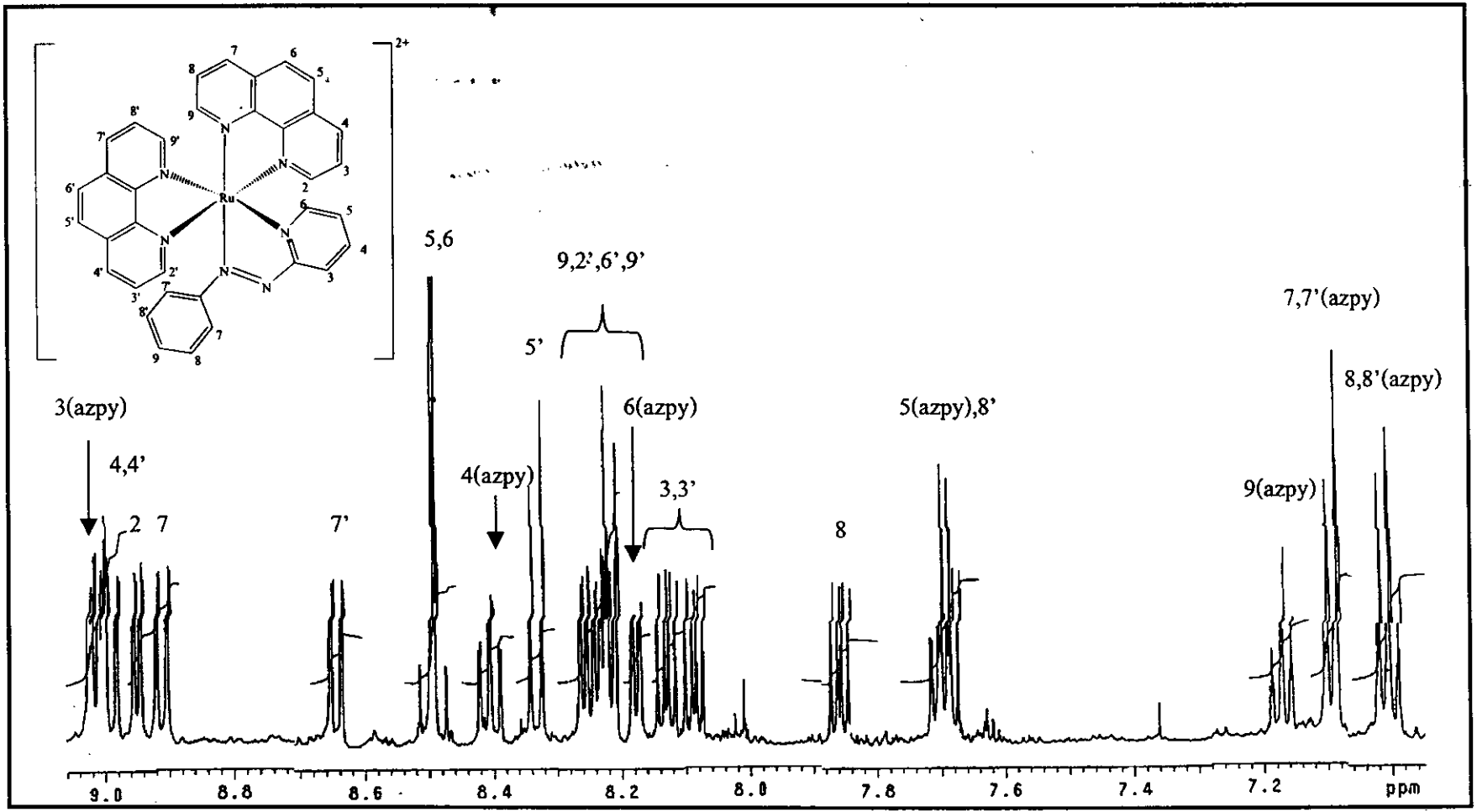

Figure 50 ^{1}H NMR spectrum of $[Ru(phen)_2azpy](BF_4)_2$ in acetone-d_6

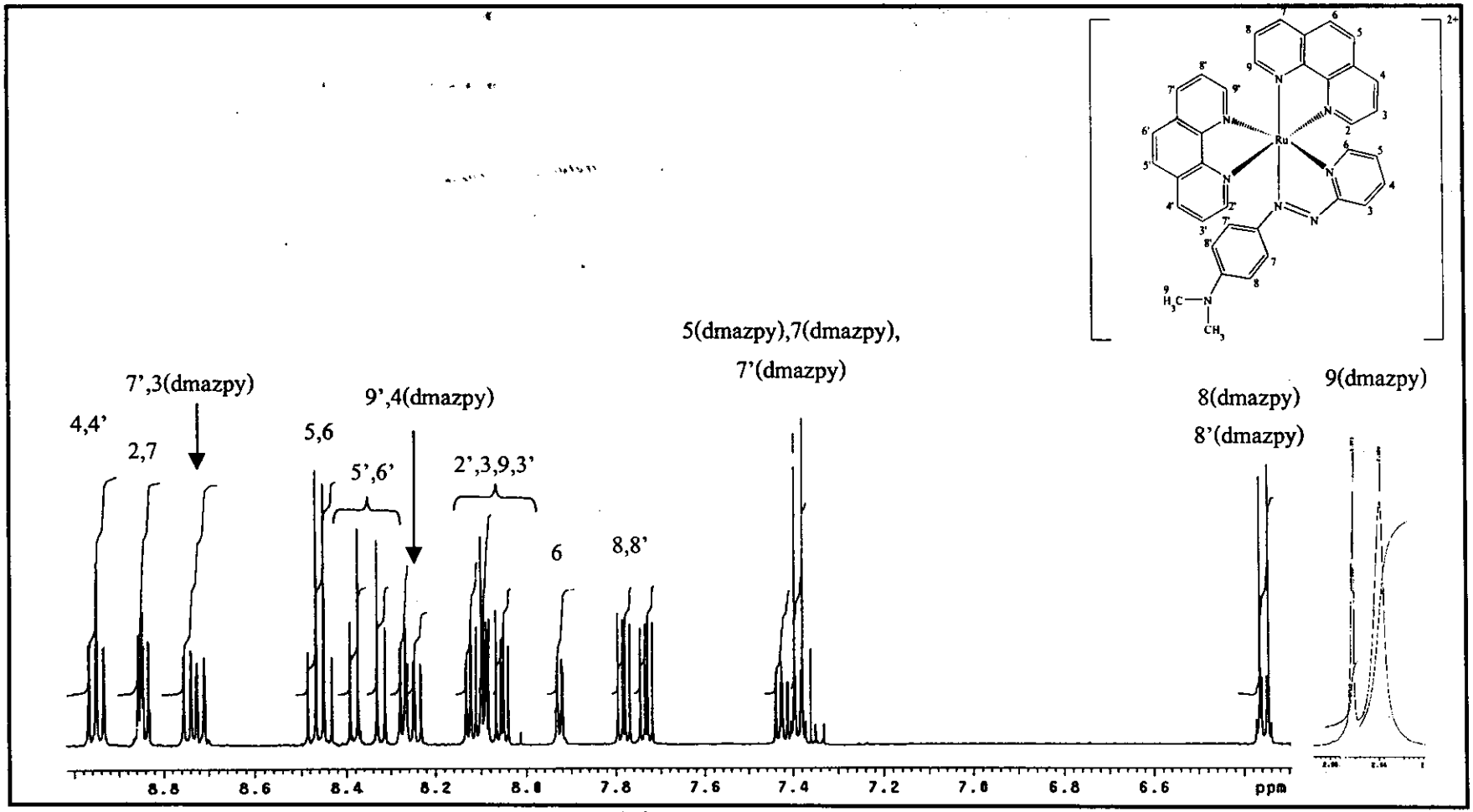

Figure 51 ^{1}H NMR spectrum of [Ru(phen)$_2$dmazpy](PF$_6$)$_2$ in acetone-d_6.

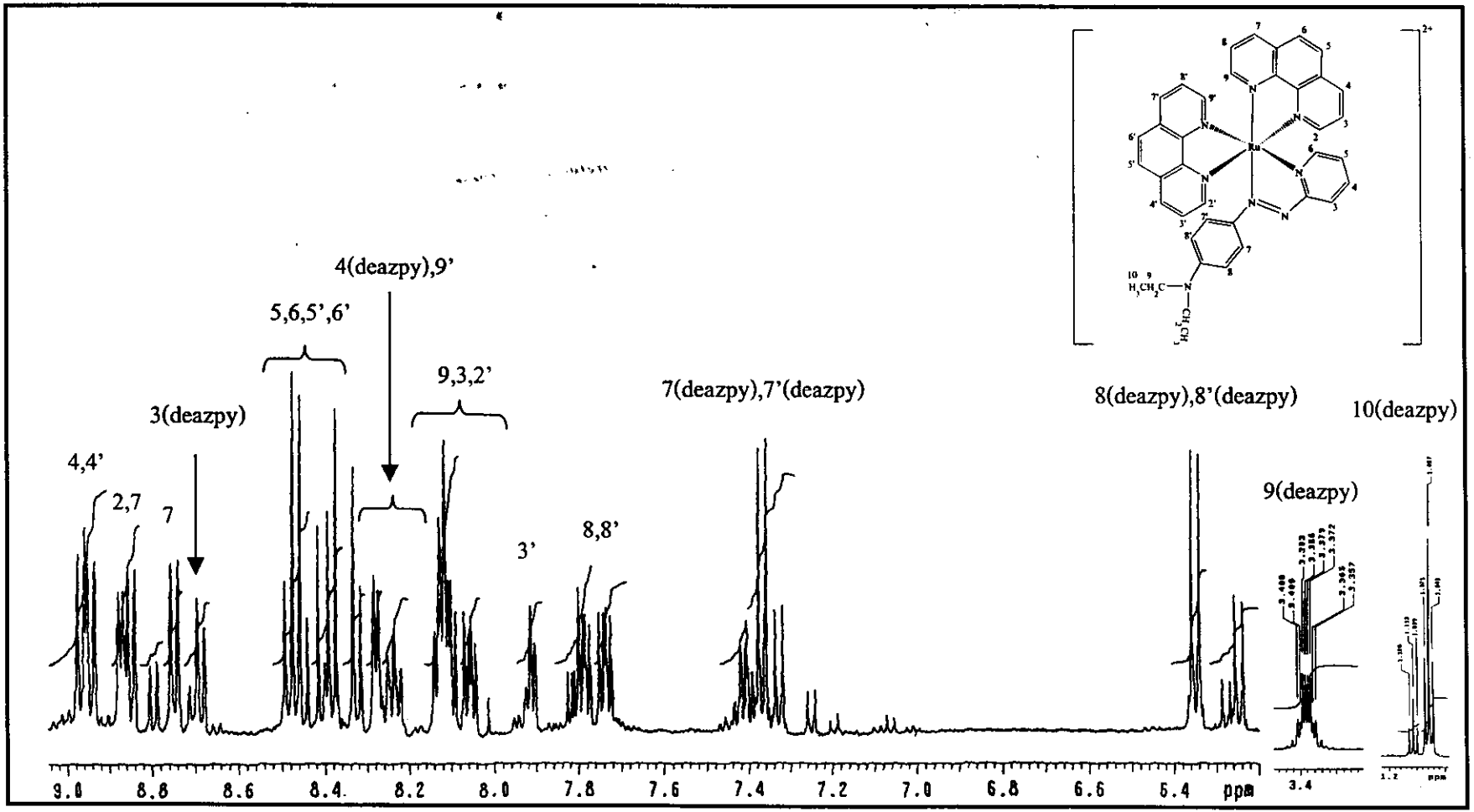

Figure 52 ^{1}H NMR spectrum of [Ru(phen)$_2$deazpy](PF$_6$)$_2$ in acetone-d_6

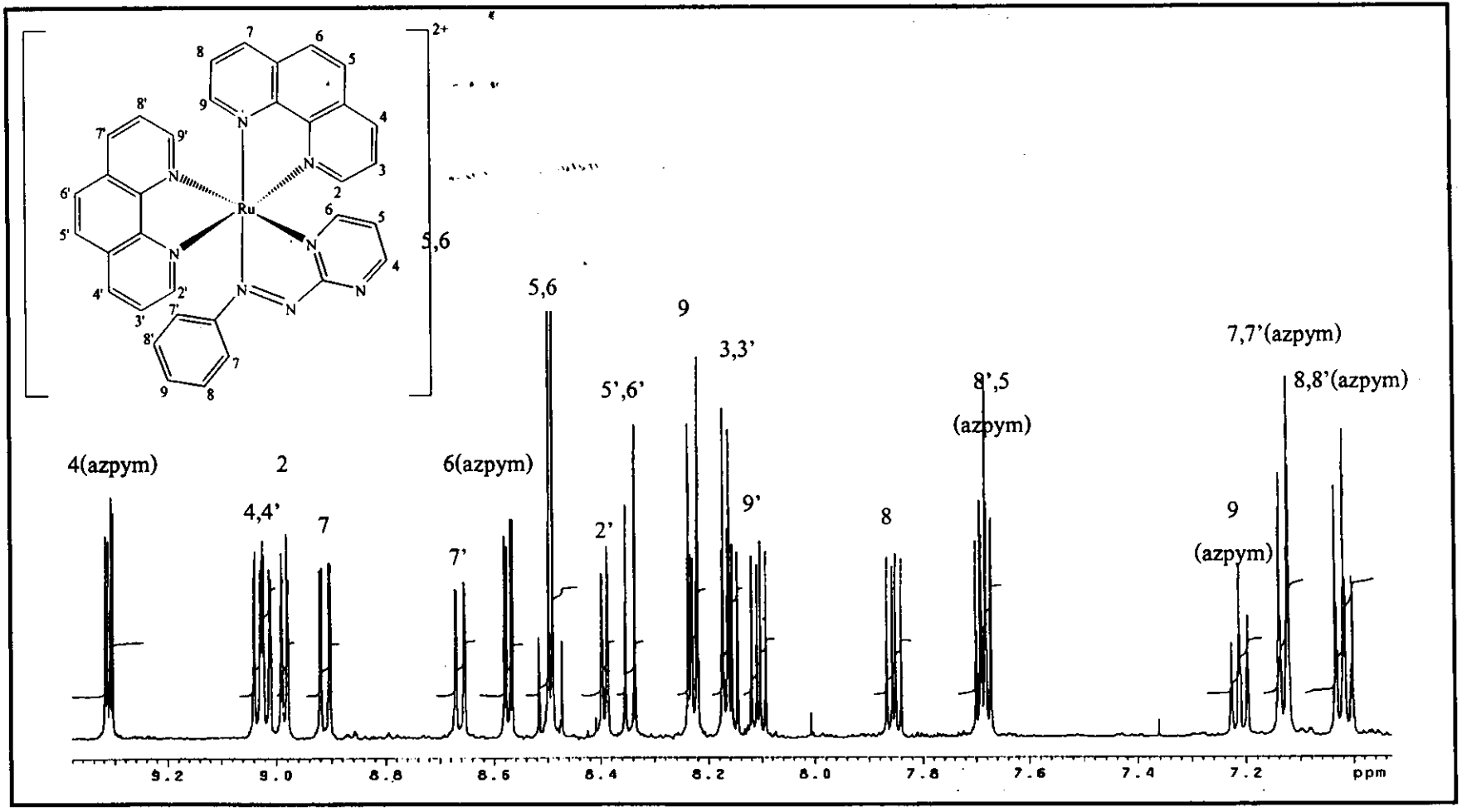

Figure 53 ^{1}H NMR spectrum of $[Ru(phen)_2azpym](PF_6)_2$ in acetone-d_6

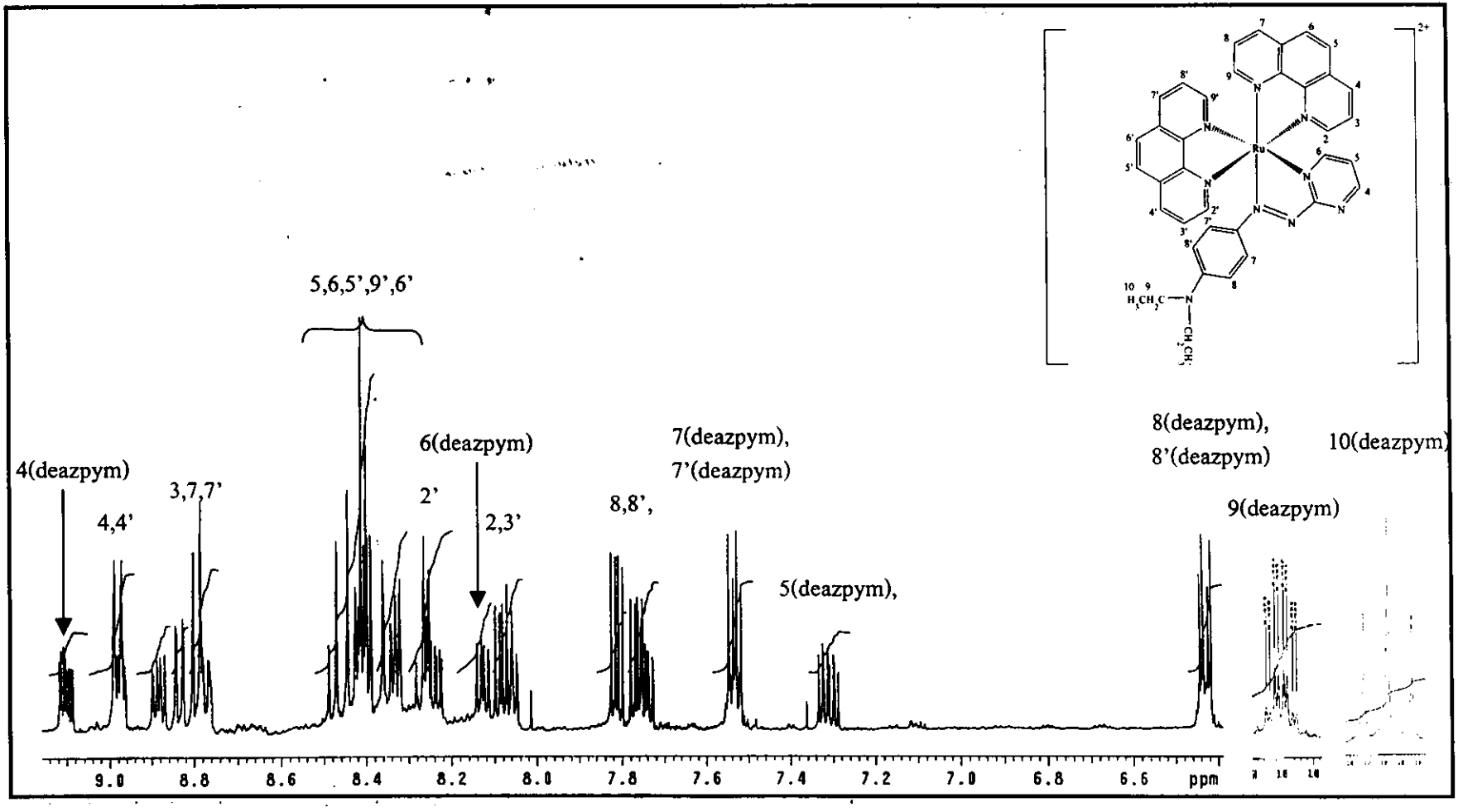

Figure 54 ^{1}H NMR spectrum of $[Ru(phen)_2deazpym](PF_6)_2$ in acetone-d_6.

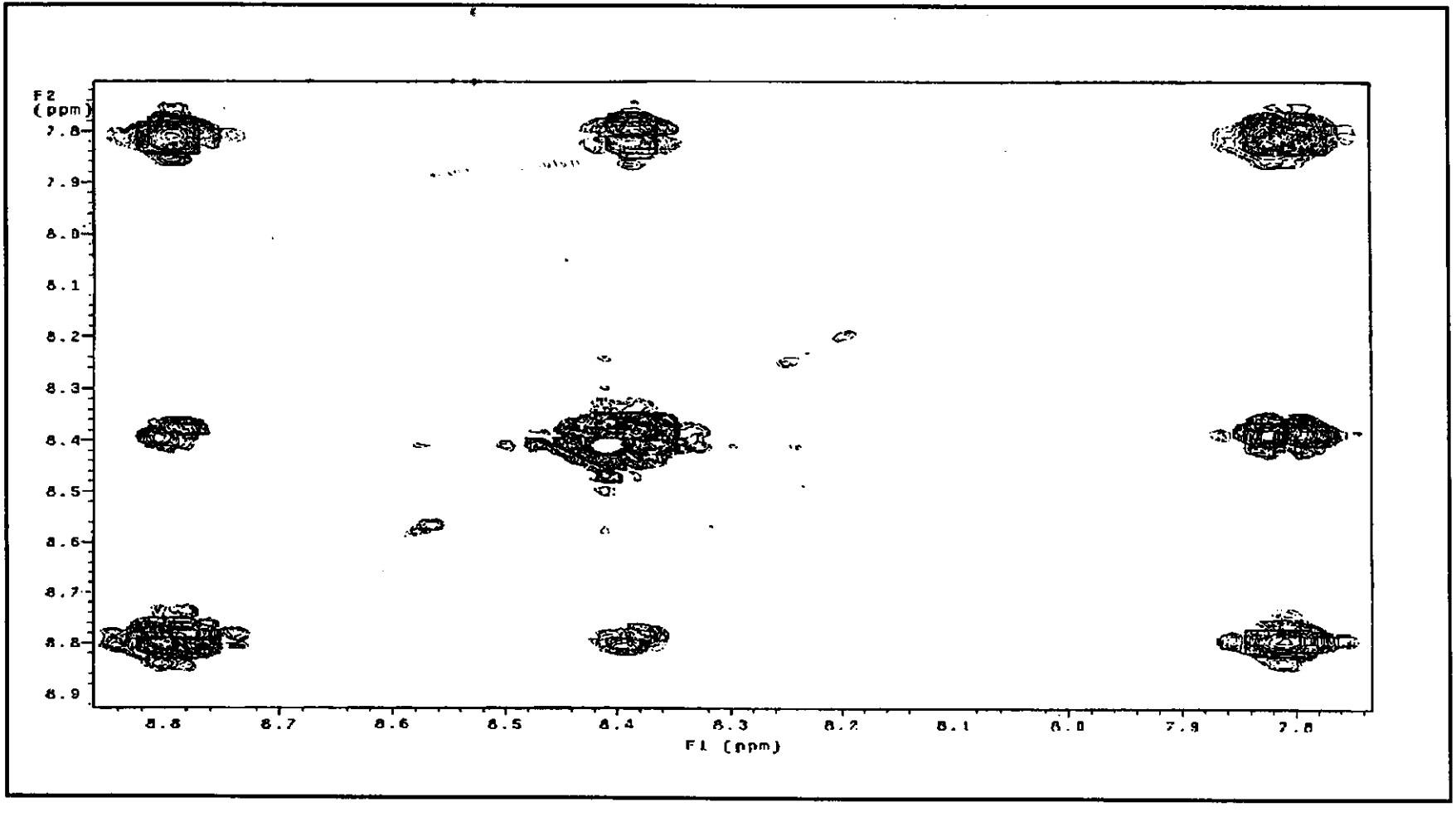

Figure 55 ^{1}H NMR spectrum of $[Ru(phen)_3](BF_4)_2$ in acetone-d_6

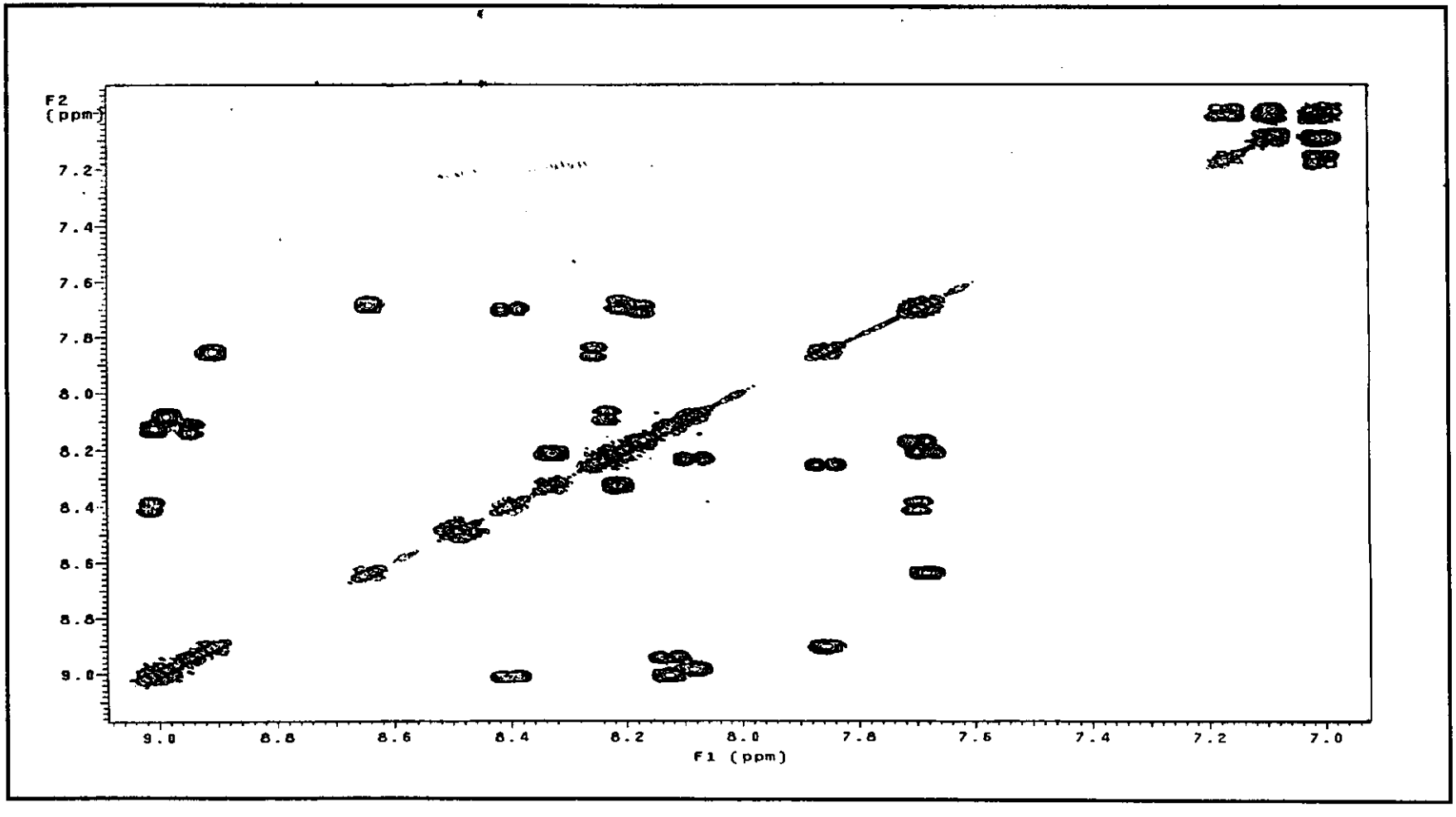

Figure 56 ^{1}H NMR spectrum of $[Ru(phen)_2azpy](BF_4)_2$ in acetone-d_6

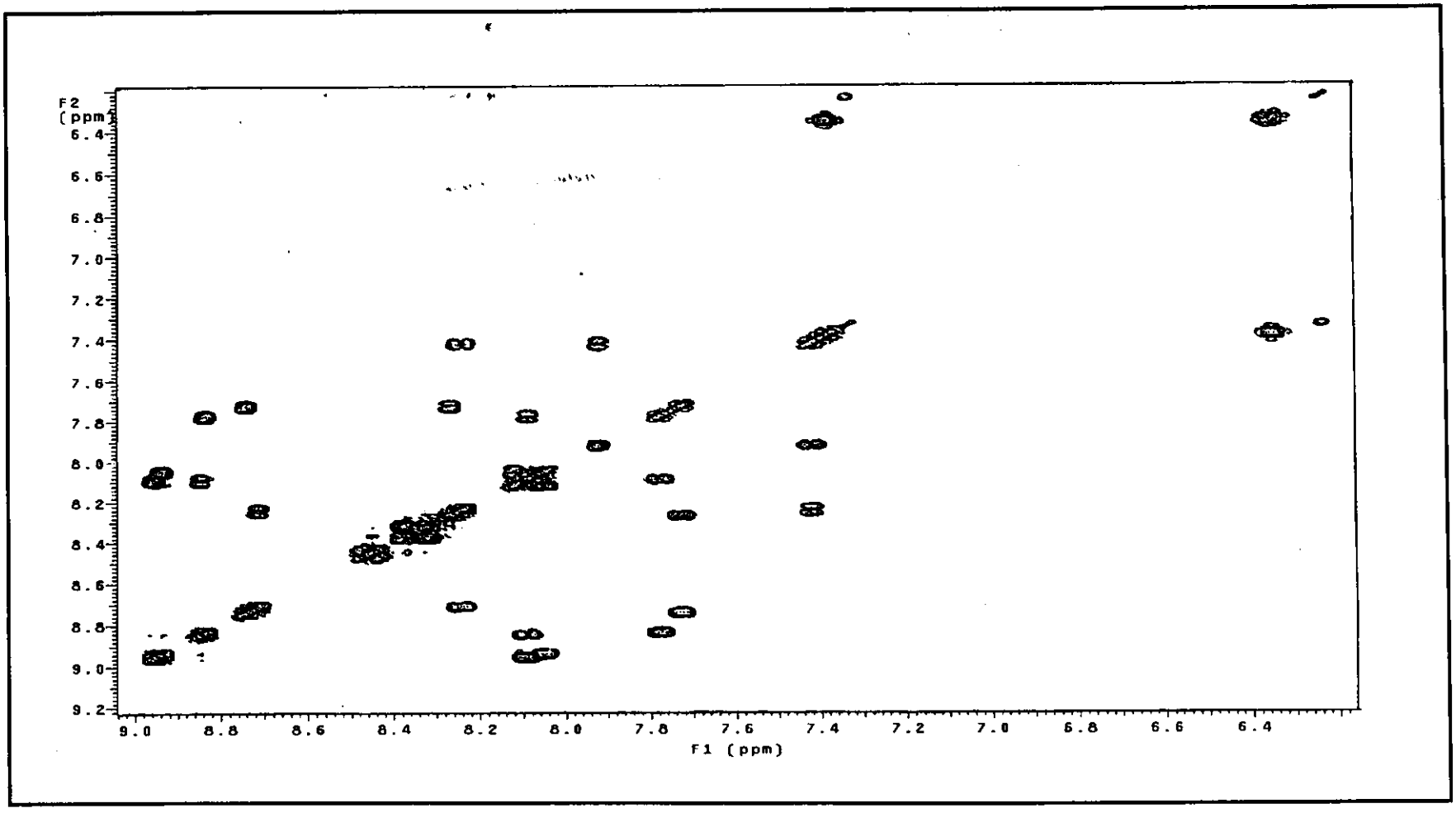

Figure 57 ^{1}H NMR spectrum of $[Ru(phen)_2dmazpy](PF_6)_2$ in acetone-d_6

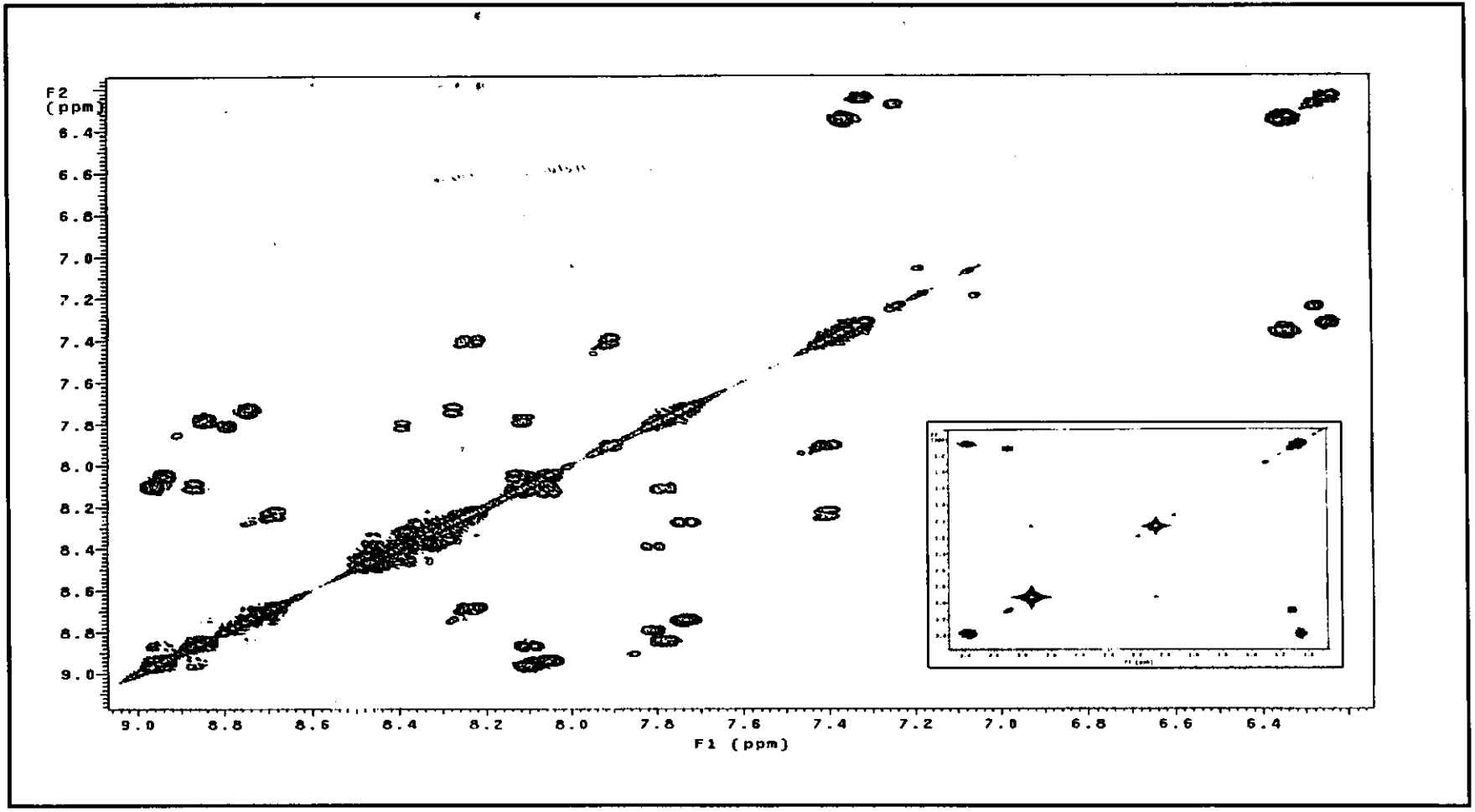

Figure 58 ^{1}H NMR spectrum of $[Ru(phen)_2deazpy](PF_6)_2$ in acetone-d_6

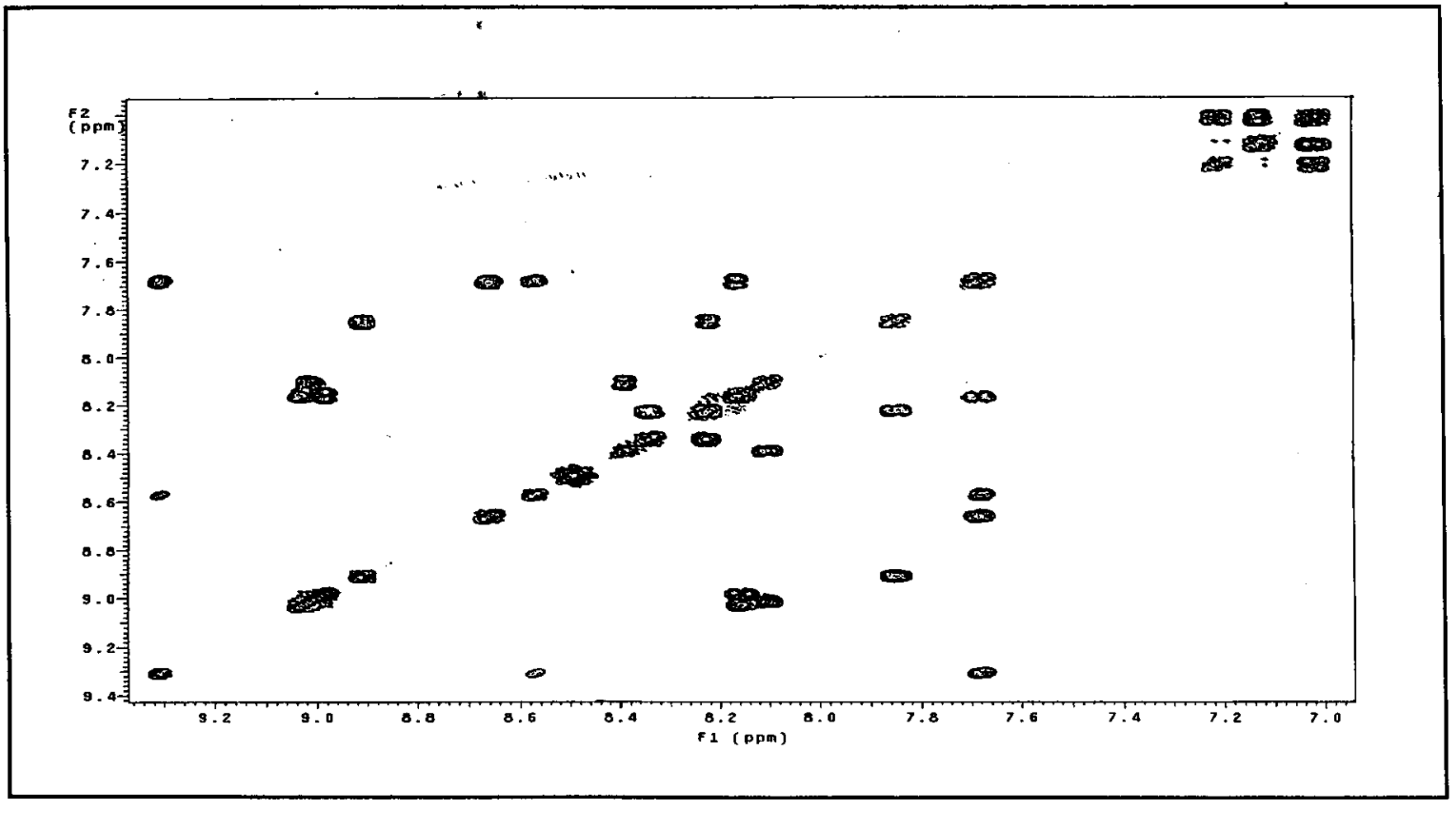

Figure 59 ^{1}H NMR spectrum of $[Ru(phen)_2azpym](PF_6)_2$ in acetone-d_6

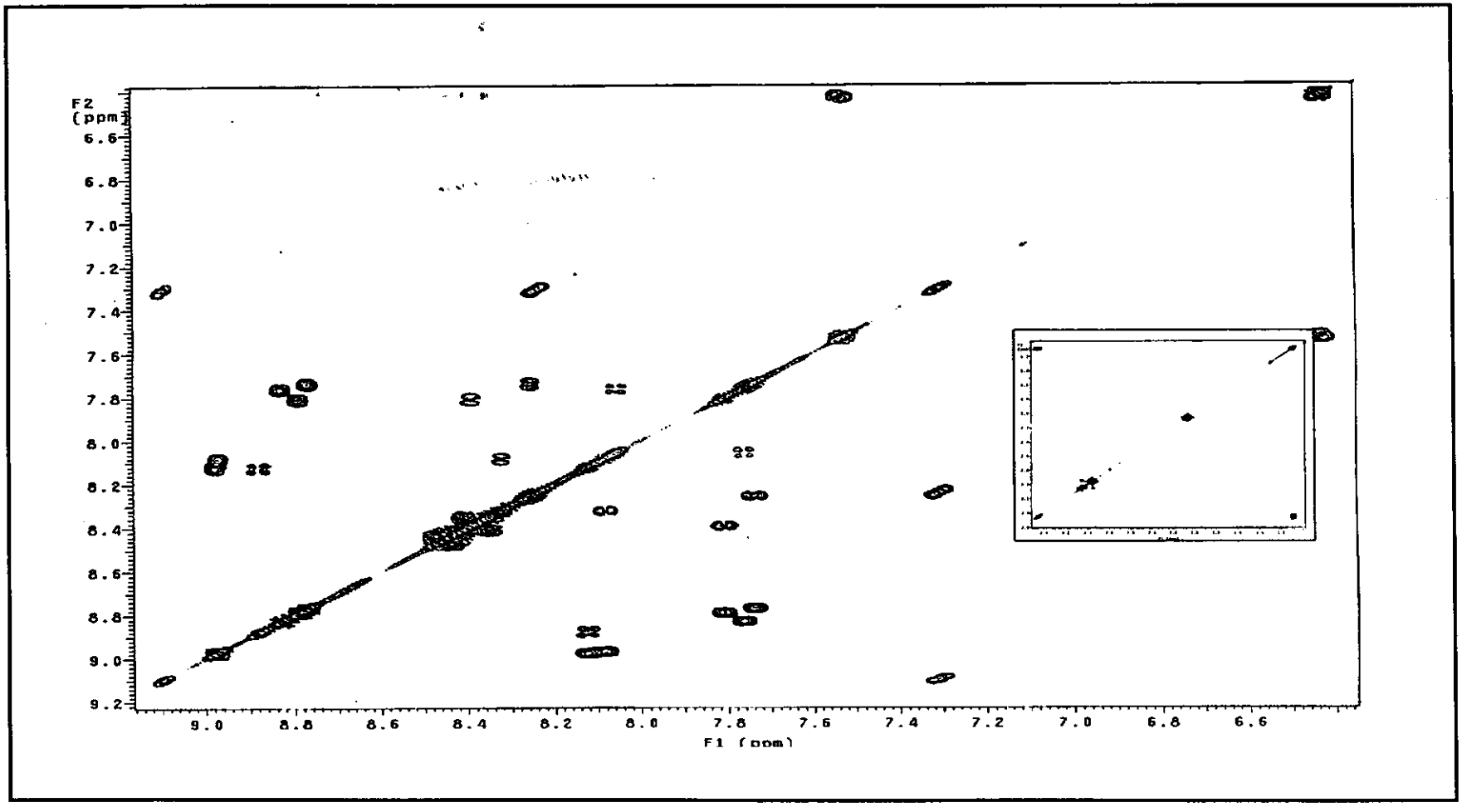

Figure 60 ^{1}H NMR spectrum of $[Ru(phen)_2dezpym](PF_6)_2$ in acetone-d_6

3.5.6 Cyclic voltammetry

Cyclic voltammetry is a technique to study the redox processes in free ligands and complexes. The cyclic voltammograms of $[Ru(phen)_2L]^{2+}$, where L = phen, azpy, dmazpy, deazpy, azpym and deazpym complex are shown in Figure 61 to 66, respectively. The cyclic voltammetric data are summarized in Table 34.

Table 30 Cyclic voltammetric data of $[Ru(phen)_2L]^{2+}$ complex, where L = phen, azpy, dmazpy, deazpy, azpym and deazpym in 0.1 M TBAH acetronitrile solution at scan rate 50 mV/s (ferrocene as an internal standard, ΔE_p = 70 mV)

$[Ru(phen)_2L]^{2+}$, L =	Oxidation range		Reduction range			
			$E_{1/2}$, V (ΔE_p, mV)			
	$E_{1/2}$, V (ΔE_p, mV)	Ru(II/III), V (ΔE_p, mV)	I	II	III	IV
phen	-	+0.89(75)	-1.80 (155)	-1.89[b]	-	-
azpy	+1.38(63)	-	-0.88 (80)	-1.61 (75)	-2.05 (65)	-2.33 (125)
dmazpy	n	+0.85	-1.01 (70)	-1.76 (70)	-2.04 (70)	-2.27 (100)
deazpy	n	+0.70(75)	-0.93 (68)	-1.77 (74)	-2.03 (80)	-2.27 (130)

E_{pa} = anodic peak and n = cannot be observed

Table 30 (continued)

$[Ru(phen)_2L]^{2+}$, L =	Oxidation range		Reduction range			
			$E_{1/2}$, V (ΔE_p, mV)			
	$E_{1/2}$, V (ΔE_p, mV)	Ru(II/III), V (ΔE_p, mV)	I	II	III	IV
azpym	n	-	-0.69 (70)	-1.45 (85)	-2.01 (65)	-2.25 (175)
deazpym	n	+0.75(60)	-0.88 (53)	-1.63 (60)	-2.01 (60)	-2.26 (120)

E_{pa} = anodic peak and n = cannot be observed

Reduction range

The complexes were studied in the range 0.0-2.4 V. The cyclic voltammogram of $[Ru(phen)_3]^{2+}$ complexes were shown one couple at -1.72 V and Ep_c value at -1.89 V , whereas the $[Ru(phen)_2L]^{2+}$ complexes, where L = azpy, dmazpy, deazpy, azpym and deazpym ligands gave similar patterns but the potential value in each peak was shifted. There were four couples in reduction range. The two couples of the third ligands (azpy, dmazpy, deazpy, azpym and deazpym) were reversible couples. Whereas other couples of phen ligands, this one couple was reversible couple and the last couple was quasi-reversible couple.

Oxidation range

All complexes were studied in the range 0.0-1.6 V. The couple V belonged to the substituent character of the third ligands, which occurred spontaneously. This couple was reversible couple. The Ru(II/III) couple appeared in the phen and azpy complexes but other complexes are not observed. Because the Ru(II/III) couple of dmazpy, deazpy, azpym and deazpym complexes located in beside area. The Ru(II/III) couple of $[Ru(phen)_3]^{2+}$ and $[Ru(phen)_2azpy]^{2+}$ were reversible couple (+0.89(75) and +1.38(63) V).

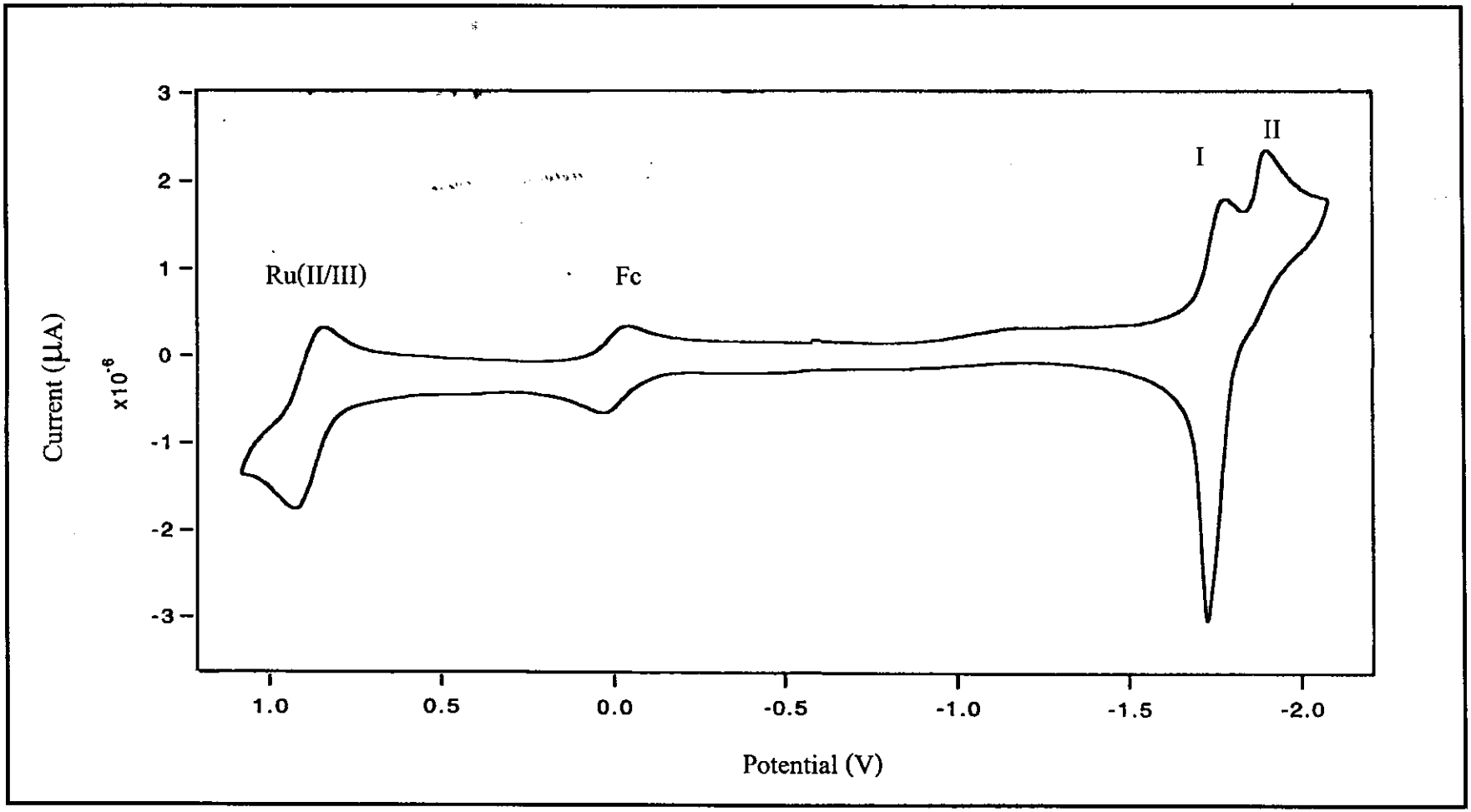

Figure 61 Cyclic voltammogram of $[Ru(phen)_3](BF_4)_2$ in 0.1 M TBAH CH_3CN at scan rate 50 mV/s.

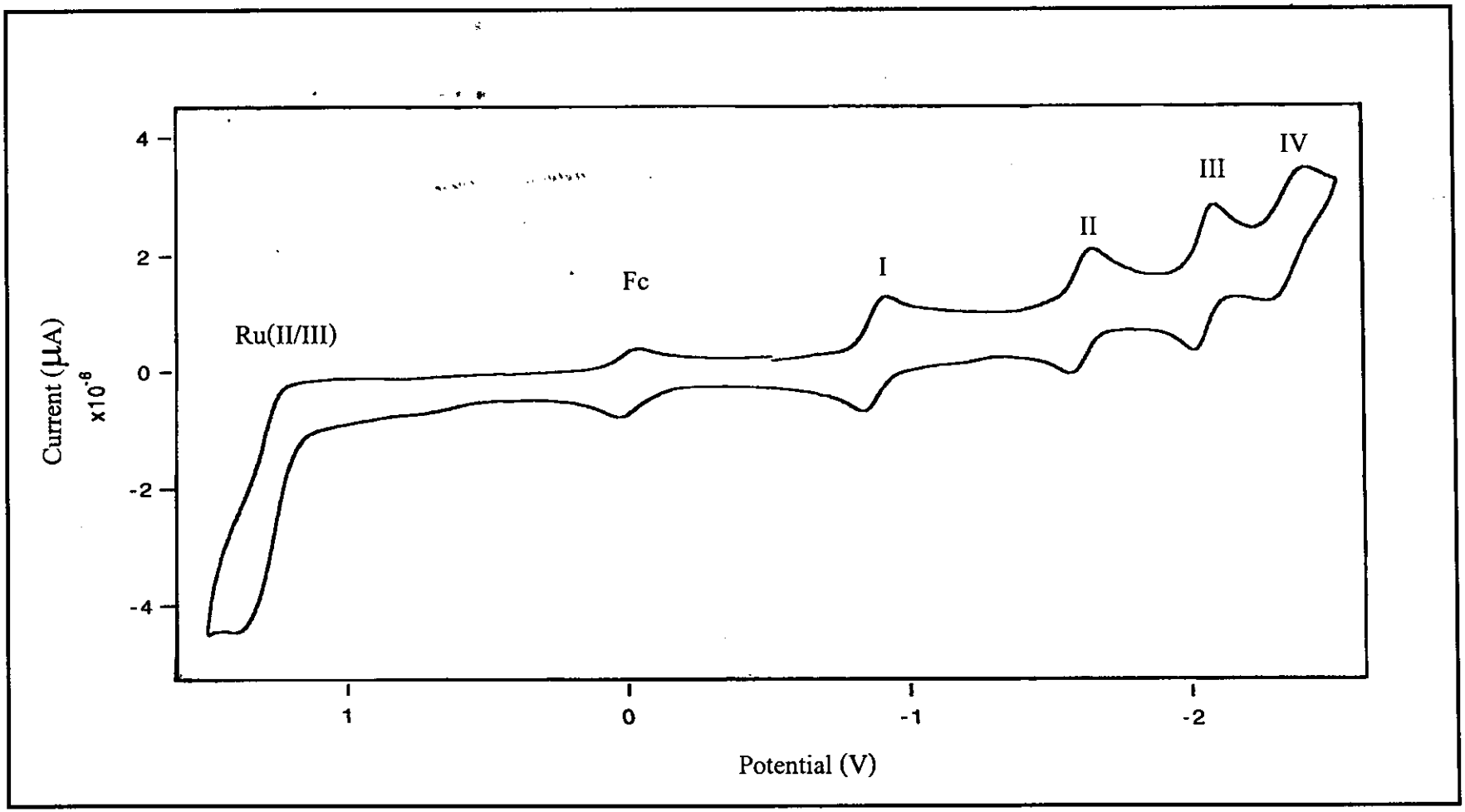

Figure 62 Cyclic voltammogram of $[Ru(phen)_2azpy](BF_4)_2$ in 0.1 M TBAH CH_3CN at scan rate 50 mV/s.

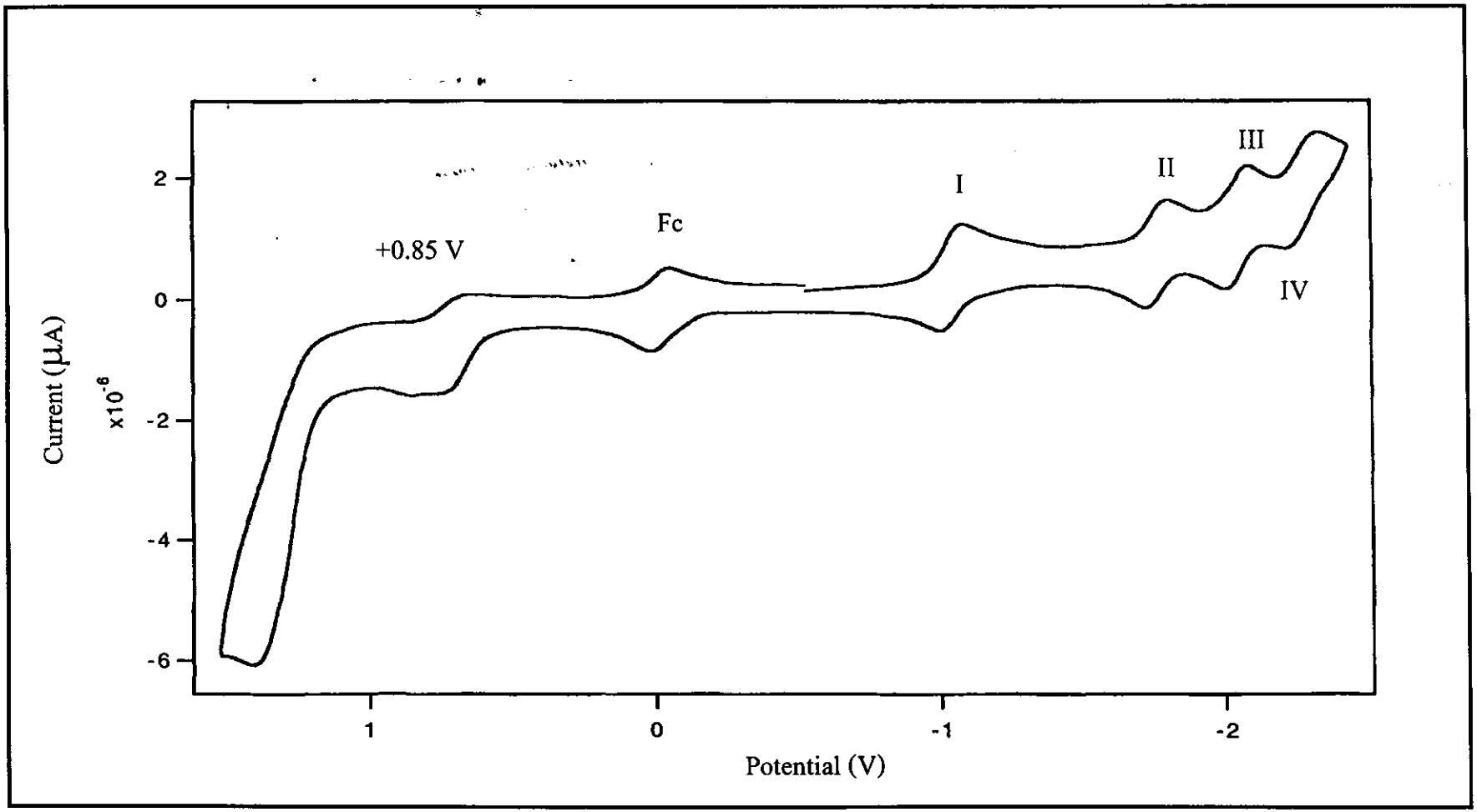

Figure 63 Cyclic voltammogram of $[Ru(phen)_2dmazpy](PF_6)_2$ in 0.1 M TBAH CH_3CN at scan rate 50 mV/s.

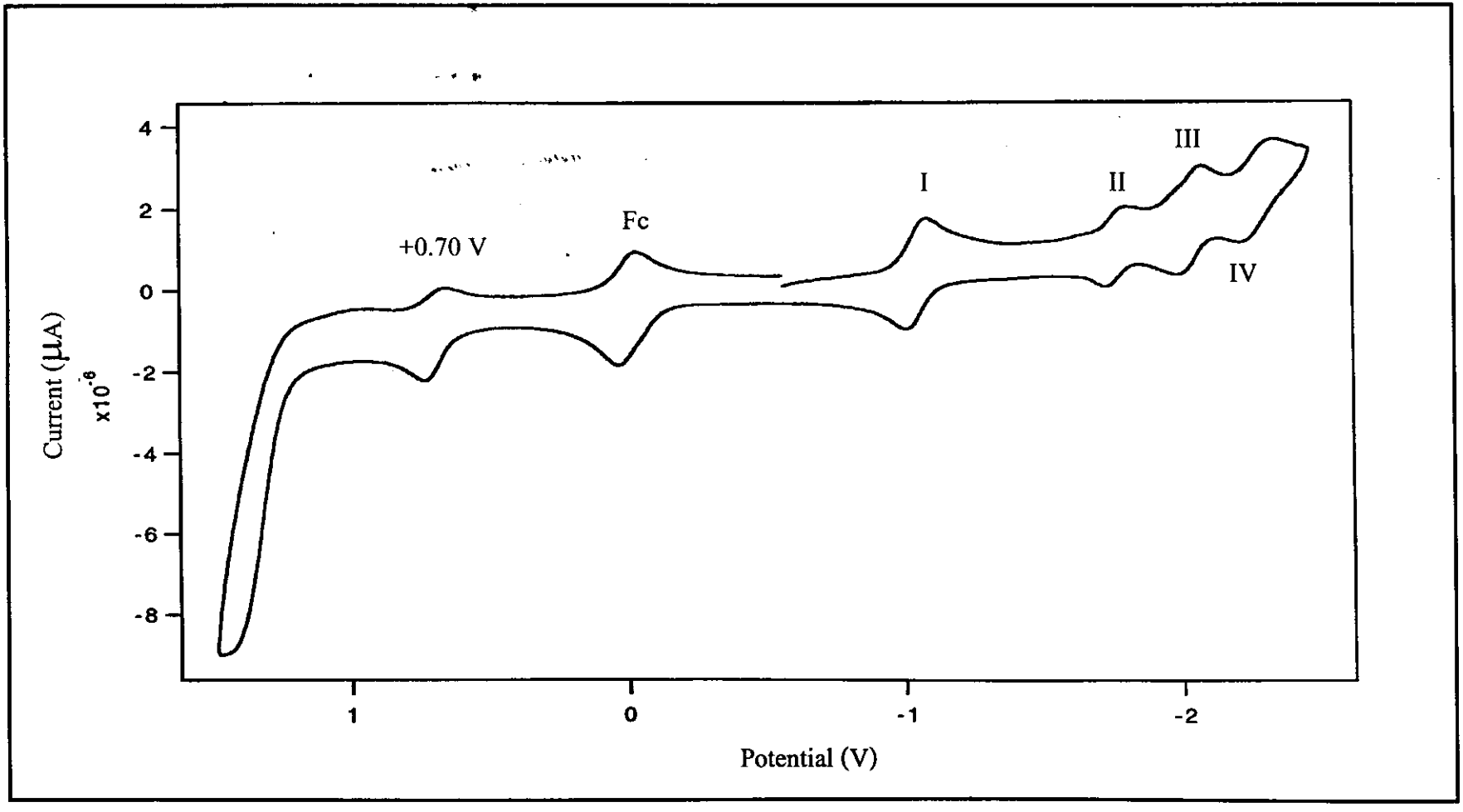

Figure 64 Cyclic voltammogram of $[Ru(phen)_2deazpy](PF_6)_2$ in 0.1 M TBAH CH_3CN at scan rate 50 mV/s.

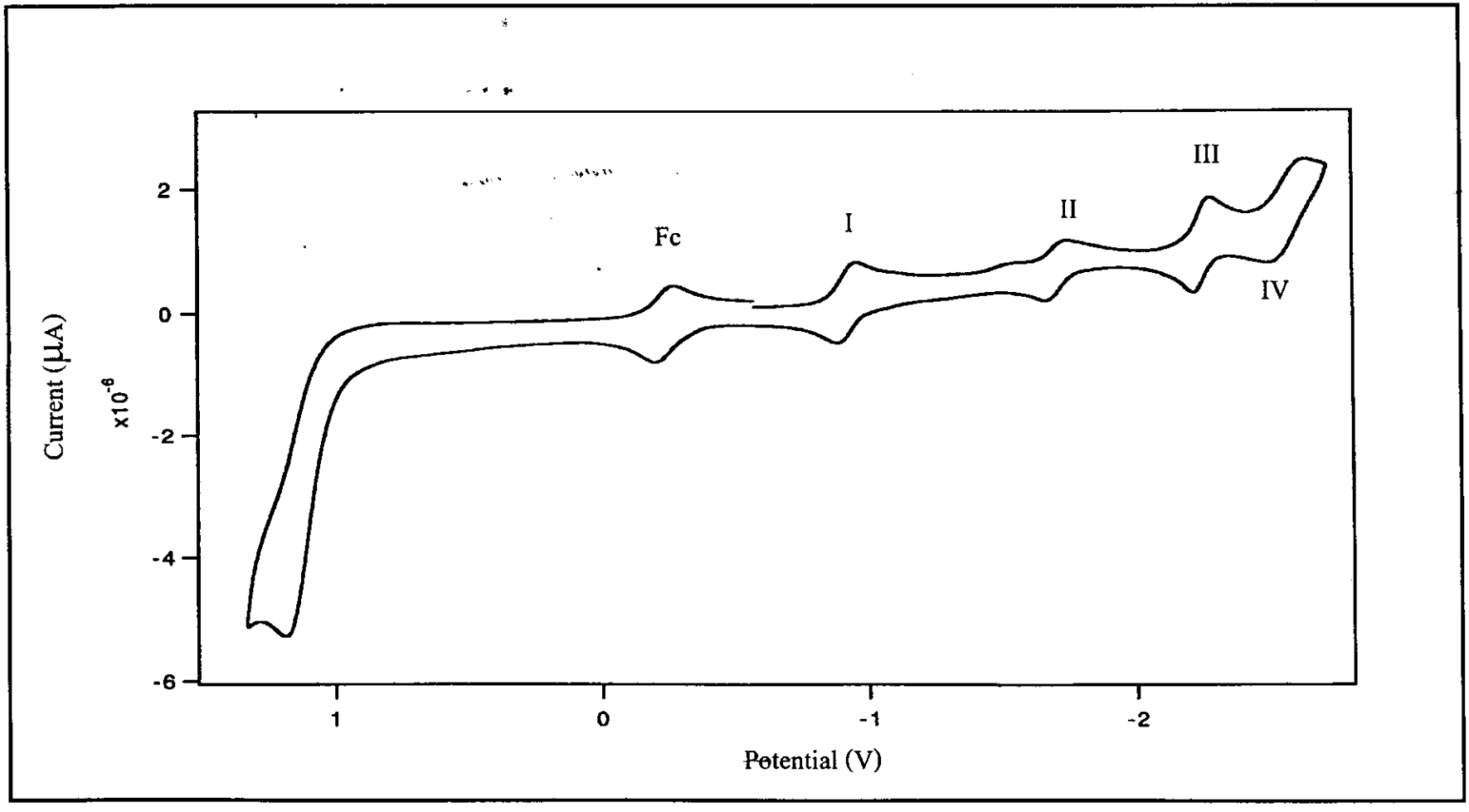

Figure 65 Cyclic voltammogram of $[Ru(phen)_2azpym](PF_6)_2$ in 0.1 M TBAH CH_3CN at scan rate 50 mV/s.

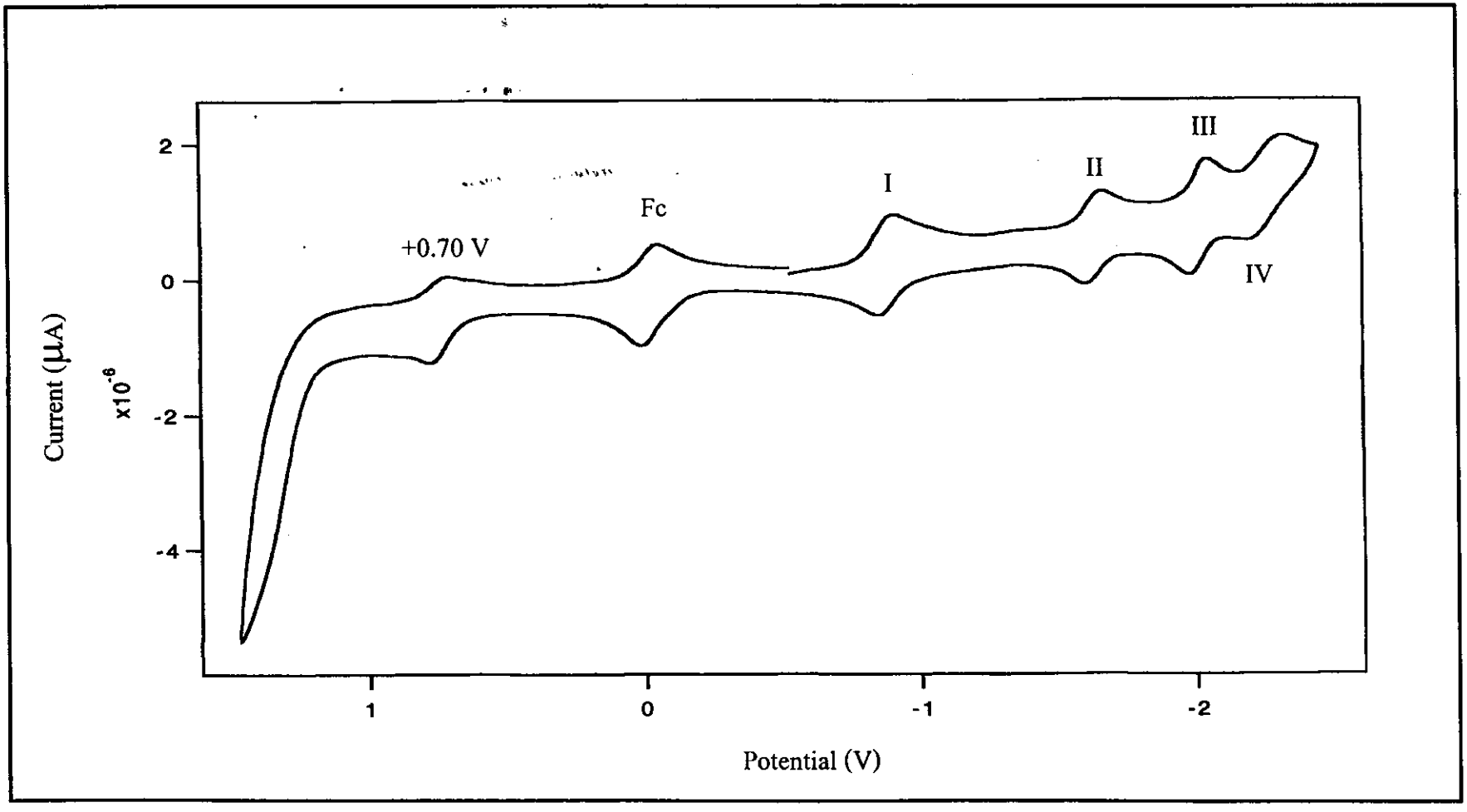

Figure 66 Cyclic voltammogram of $[Ru(phen)_2deazpym](PF_6)_2$ in 0.1 M TBAH CH_3CN at scan rate 50 mV/s.